Molycorp 4

Geochemistry of the Red River Stream System Before and After Open-Pit Mining, Questa Area, Taos County, New Mexico

Final Report prepared for the

New Mexico Office of the Natural Resources Trustee

B.D. Allen[1], A.R. Groffman[2], M.C. Molles, Jr.[3], R.Y. Anderson[2], and L.J. Crossey[2]

[1]NM Bureau of Mines and Mineral Resources, NM Tech
[2]Department of Earth and Planetary Sciences, UNM
[3]Biology Department, UNM

October, 1999

2-76

Geochemistry of the Red River Stream System Before and After Open-Pit Mining, Questa Area, Taos County, New Mexico

Final Report prepared for the

New Mexico Office of the Natural Resources Trustee

B.D. Allen[1], A.R. Groffman[2], M.C. Molles, Jr.[3], R.Y. Anderson[2], and L.J. Crossey[2]

[1]NM Bureau of Mines and Mineral Resources, NM Tech
[2]Department of Earth and Planetary Sciences, UNM
[3]Biology Department, UNM

October, 1999

Geochemistry of the Red River Stream System Before and After Open-Pit Mining, Questa Area, Taos County, New Mexico

EXECUTIVE SUMMARY

Previous geochemical and biologic investigations in the Red River watershed have not clearly defined the degree to which mining operations at the Molycorp open-pit mine may be responsible for increased metal loading or impairment of the Red River. Estimates of the effects of mining operations and mine dumps are complicated by the effects of weathering on natural exposures of mineralized bedrock, which occur in the same watershed and also generate acidic waters that enhance the mobility of metals and influence the stream environment.

This investigation has approached this problem by measuring and comparing the effects of weathering and metal transport on the stream system at key sites along the stream in areas of both natural mineralization and mine dumps. The research included the sampling and analysis of both stream water and stream sediments during a 1-year period of field study. The geochemical results are in general agreement with those of previous investigations, which indicate a significant increase in metal loading in reaches of the stream that are adjacent to and downstream from the mine dumps. Adjacent to areas of natural exposures of mineralized rocks (scars), concentrations of trace metals in stream waters during baseflow conditions increase measurably above upstream, background levels. For example, concentrations of dissolved zinc in winter-month (1997-98) water samples increased from < 2 ug/L in upstream, non-mineralized area of the watershed, to ~50 ug/L downstream from scar areas. In reaches below the mine dumps, metal loading can increase by nearly an order of magnitude above concentrations found downstream from scar areas.

This study was also able to compare metal loadings before and after open-pit mining operations by collecting and analyzing samples in impoundments that pre-date the mine dumps. Metal concentrations in pond sediments in the scar areas upstream from the mine remain unchanged since creation of the pond. In a pond below the mine dumps the metal concentrations are initially low, except for molybdenum, and somewhat more concentrated in trace metals than in the upstream pond deposits. However, after the mid-1980s there occurs a significant increase in some metals (e.g. 5-fold increase in zinc), accompanied by the accumulation of white, gelatinous layers enriched in aluminum. A lag of decades between initiation of open-pit operations and higher metal loading in the lower pond suggests a finite reaction time for the weathering and transport of metals and a delayed response in stream impairment.

This study also compared patterns in the distributions of metals in the stream system and invertebrate fauna living within the stream sediments. A census of hyporheic invertebrates indicates changes in population and diversity that are consistent with upstream and downstream changes in metal concentration, with reduced sub-bottom fauna in the reach below the mine dumps.

Hydrologic investigations will be needed to determine the specific pathways for metal transport. Continuous monitoring of the stream system will help determine the long-term response and will assist in quantifying the impacts of acid drainage from waste-rock dumps and restoring and preserving the Red River ecosystem.

Geochemistry of the Red River Stream System Before and After Open-Pit Mining, Questa Area, Taos County, New Mexico

CONTENTS

TABLES

FIGURES

Geochemistry of the Red River Stream System Before and After Open-Pit Mining, Questa Area, Taos County, New Mexico

INTRODUCTION

Open-pit mining operations at the Molycorp molybdenum mine, beginning in the mid 1960s, led to the excavation of over 300 million tons of rock which was deposited in waste dumps adjacent to the Red River. Concern over the potential for these rocks to generate acidic waters, resulting in impairment of water supplies and aquatic habitats, led to investigations of the Red River aimed at documenting geochemical and biologic conditions in the stream (e.g. USDHEW, 1966; USEPA, 1971; Jacobi and Smolka, 1984, 1986; Smolka and Tague, 1987, 1989; Smolka, 1993).

Today, numerous acidic seeps discharge near the stream below the mine property, and during winter months the stream below the mine is visibly clouded by a white chemical precipitate, enriched in aluminum, that in places armors the stream bed. Comparatively high concentrations of trace metals are commonly measured in stream waters below the mine near Questa (e.g. Smolka and Tague, 1989). Biologic surveys indicate downstream decreases in the abundance and number of taxa in communities of benthic organisms, with the strongest decrease occurring below the mine property near Questa (e.g. Smolka and Tague, 1989; Smolka, 1993). Populations of trout are also severely impaired in the reach of the stream below the mine (Smolka and Tague, 1989). Relationships between mining activities, decreased water quality, and impairment of habitat downstream from the mine have remained vague, however, due largely to occurrences of natural exposures of mineralized rock in the drainage.

This study was designed to clarify the effects of open-pit mining on the river system by examining geochemical conditions in stream reaches affected by natural mineralization, as well as areas of mine-related seepage. Water and stream sediment were collected along the Red River to document spatial patterns in the distribution of geochemical constituents in the vicinity of the open-pit mine. As part of this effort, metal-oxide crusts and cements, alluvium associated with natural exposures of altered bedrock, and wood in trees rooted near the Red River were analyzed. Accumulations of sediment that pre-date open-pit mining activities were studied to characterize temporal changes that may have occurred since excavation of the open-pit mine. Samples of organisms living beneath the stream bed of the Red River were collected to provide census information for this sensitive biologic community. This report summarizes the results of these investigations, provides analytical data, evaluates geochemical and biological responses, and suggests means for further clarifying the effects of mine waste on the Red River system.

ACKNOWLEDGMENTS

The investigation was funded by the Office of the Natural Resources Trustee, a State agency charged with investigating environmental impacts in New Mexico, and was conducted by researchers from the Department of Earth and Planetary Sciences, University of New Mexico (UNM), the Biology Department, UNM, and the New Mexico Bureau of Mines and Mineral Resources, a division of New Mexico Tech. Laura Hagan, Mike Henderson, and David Johnson assisted in the field. Laboratory work was supervised by John Husler and Charles Shearer. Chris Adcock and Sheila Hutcherson assisted in the lab. We are grateful to Ron Thibedeau of the U.S. Forest Service, Questa Ranger District, for authorizing field work on USFS land.

STUDY AREA

Physiographic, geologic, and hydrologic aspects of the Red River watershed, as well as historical accounts of mining activities at the Molycorp mine, are presented in other reports (Kent, 1995; SRK, 1995; Slifer, 1996). Those discussions and accounts are briefly summarized here. The Red River drains 290 km^2 within the Sangre de Cristo Mountains of northern New Mexico, including some of the highest peaks in the state (Fig. 1). The stream flows north from Wheeler Peak, turns west near the town of Red River and flows through a canyon until leaving the mountains near Questa. To the west of the mountains the stream has cut through a sequence of basalt flows and unconsolidated sediments, and is again confined to a narrow canyon by the time it reaches the Rio Grande.

Mean annual discharge by the Red River at the U.S. Geological Survey (USGS) gage near Questa (Fig. 1) was 56 cfs prior to 1966 (USGS, 1988). Since then, Molycorp has periodically diverted water upstream from the gage for use in mining operations, and the mean annual discharge near Questa is somewhat less. Instantaneous discharge during the period of record has ranged from less than 2.5 cfs during freezeup to over 750 cfs during spring runoff.

Results of flow surveys along the Red River, conducted by the USGS in October, 1965 and October, 1988, are summarized by Smolka and Tague (1989) and indicate that the Red River is a gaining stream over much of its course. Contributions of groundwater to the Red River, as measured between the stream gage near Questa and the abandoned gage upstream from the town of Red River (Zwergle Dam, Fig. 1) were 9.0 cfs in 1965, and 9.9 cfs in 1988. During the 1988 survey the stream gained about 4 cfs from groundwater as it flowed through the reach below the open-pit mine.

After turning west near the town of Red River, the stream flows along the southern margin of a major, Tertiary-age volcanic center (Lipman and Reed, 1989).

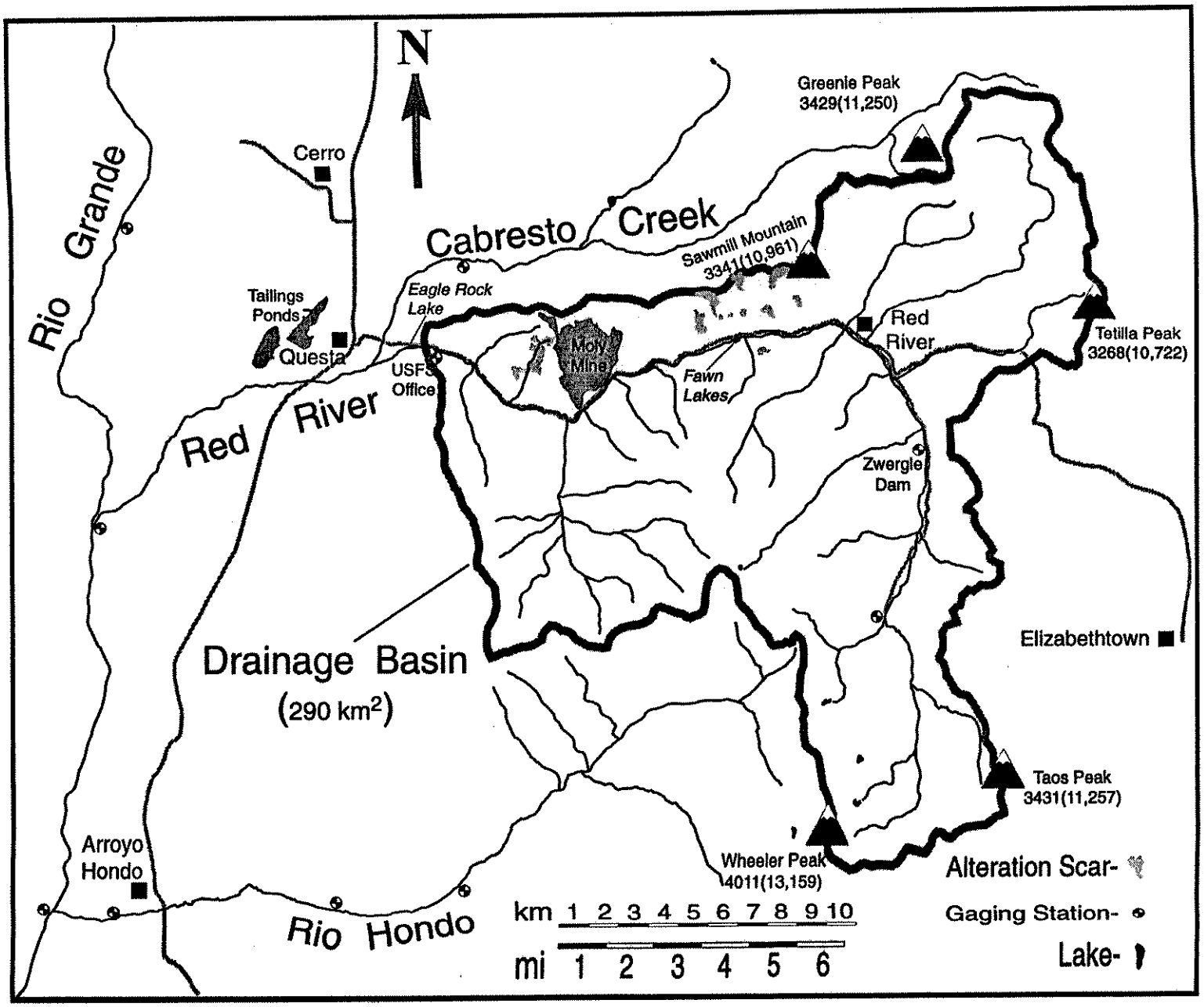

Figure 1. Location map of Red River drainage basin.

Associated with this center are extrusive rocks of intermediate to silicic composition, complex structures related to caldera collapse and subsequent opening of the Rio Grande rift to the west, numerous intrusive rock bodies, and zones of altered and mineralized rocks. Propylitic alteration of quartz latites, andesites, and other rock types (Lipman and Reed, 1989) along the margin of the caldera has produced a zone of sulfide-enriched rocks (up to a few percent pyrite) to the north of the river. More intense alteration of rocks occurred in the vicinity of faults, breccia zones, and intrusive contacts (Roberts et al., 1990). Weathering of natural exposures of these altered rocks has produced extensive, non-vegetated hillslopes that are susceptible to rapid rates of erosion. These so-called "alteration scars" stand out as brightly colored areas on the north side of the canyon between Questa and the town of Red River (Figs. 1, 2). Scar areas occur in other areas, not shown in Fig. 1, that drain into the Red River (e.g. Bitter Creek drainage), and also occur on the mine property, where alteration led not only to widespread pyritization, but also to economically important concentrations of molybdenite.

Early mining operations at the molybdenum mine resulted in the excavation of tens of kilometers of underground working by the 1950s (Schilling, 1956). These underground workings were located within and beneath the site presently occupied by the open-pit mine. During the early underground period of mining activity, initial processing of ore was conducted at a mill located close to the Red River on the southeastern end of the mine property, and waste from milling operations was dumped nearby. In the mid 1960s the mine was converted to an open-pit operation. Open-pit mining continued until the early 1980s. During this period an estimated 328 million tons of waste rock was produced and dumped in drainages around the periphery of the open-pit mine, within the pit itself, and along the Red River in the reach between Columbine Creek and the mill (Fig. 2; SRK, 1995). A new mill was constructed on the old mill site, and a pipeline was built to convey flotation wastes to settling ponds constructed near Questa (Fig. 1). Efforts were made to prevent surface runoff and sediments eroded from the waste-rock dumps from reaching the Red River, and some runoff and seepage from the waste dumps was re-routed to underground workings, pumped, and piped to the tailings ponds near Questa.

After the early 1980s open-pit operations were abandoned and new underground workings were developed on the mine property. Mining stopped in 1992 and the underground workings were allowed to fill with water to an elevation of 7600 ft (SRK, 1995). In 1994, mine dewatering began again (SRK, 1995). The current status of mine dewatering is unknown.

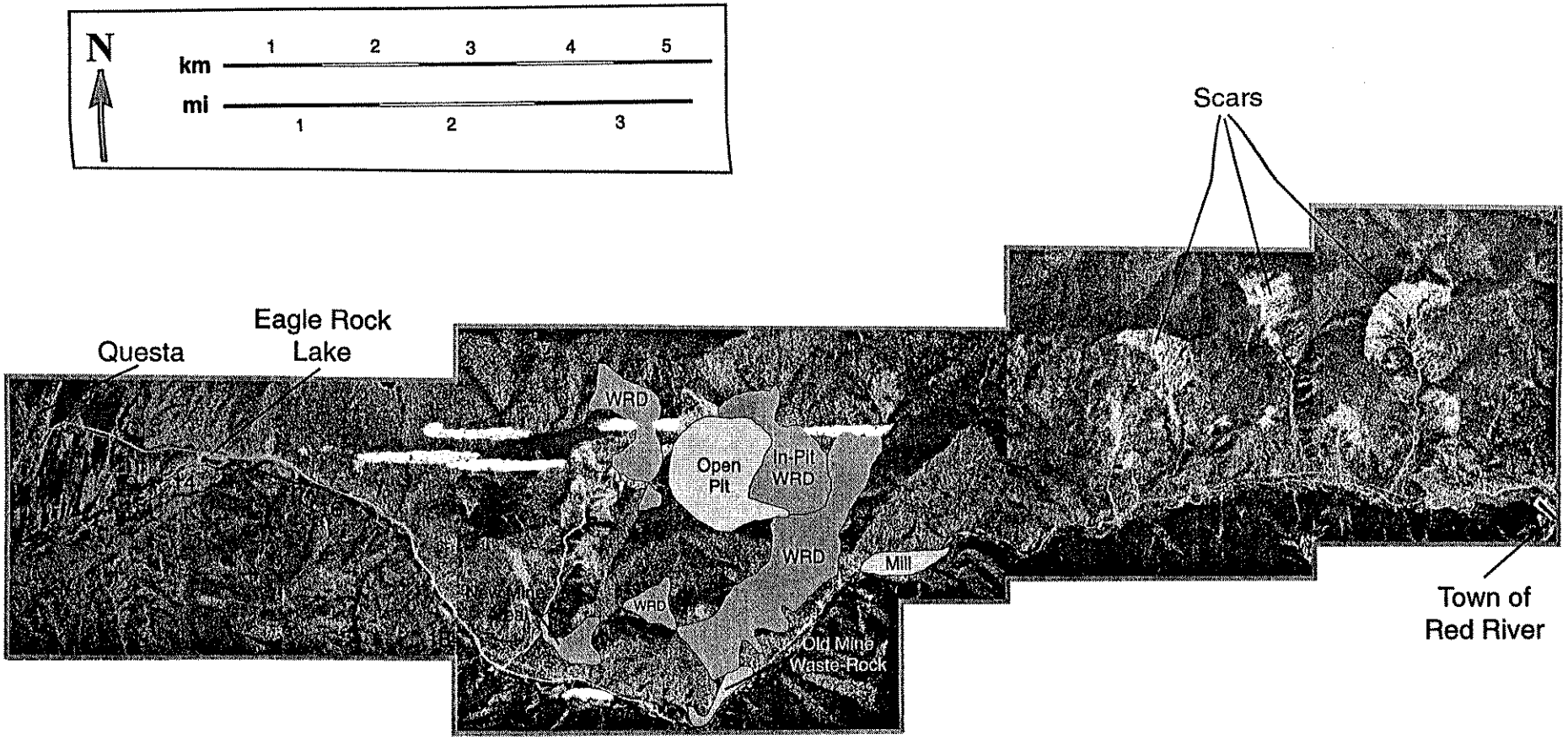

Figure 2 . Middle reach of Red River, showing distribution of natural scar areas (light-colored areas), waste-rock dumps (WRD), and river distance in kilometers. Mining-related features from SRK (1995).

SAMPLING PROGRAM

Seven stations were established along a 23 km reach of the Red River, upstream from the town of Questa, and a program of sampling was initiated (Fig. 3, Table 1). This program included the periodic collection of water and stream-sediment samples over a complete annual cycle. These same stations were used as locations for collecting samples of hyporheic invertebrates. Samples were also collected from coatings and cements in the area of seeps and from sediments beneath fluvial terraces. Other collections included cores and sediment-trap samples from Fawn Lakes and Eagle Rock Lake, and tree wood from localities along the stream channel. Specific details about these collecting localities are provided in this section, and the rationale for selecting these sites and designing the sampling program is included in the interpretation of results.

Water Samples

Water samples were collected over a 1-year period and analyzed for a number of field parameters (pH, alkalinity, temperature, Eh, dissolved oxygen, electrical conductivity, and temperature) and dissolved constituents (major anions and cations, Al, Fe, Mn, Cd, Co, Cu, Ni, and Zn). Sample localities are shown in Figure 3. Filtered water samples were collected on a monthly basis at three localities on the Red River, corresponding to reaches downstream from the mine (locality 01), upstream from the mine (locality 02), and at the mouth of a scar-area drainage (Hottentot Canyon) downstream from the town of Red River (locality 03). Water-quality samples collected at locality 01 reflect contributions that may be attributed to seepage from the mine-waste dumps and from natural exposures of sulfide-mineralized rock. Samples from upstream localities 02 and 01 provide information about expected contributions from natural scar areas.

Water samples were collected quarterly from 3 additional localities to provide concentration data from areas unaffected by scar- or mine-derived seepage (localities S10, above the town of Red River, and S3, Columbine Creek), as well as data from the Red River about midway through the mine property (locality S2). Unfiltered water samples were also collected quarterly to measure total concentrations of selected metals. Brief descriptions of each location and water-sampling intervals are described in Table 1.

Water samples were collected from the stream using a peristaltic pump. Prior to sampling, water was pumped through a YSI flow-through cell fitted with probes for approximately 20 minutes or until pH and electrical conductivity stabilized. After stabilization, the pump outlet tube was disconnected from the flow-through cell and samples were collected. Filtered samples were collected using in-line filtration through a

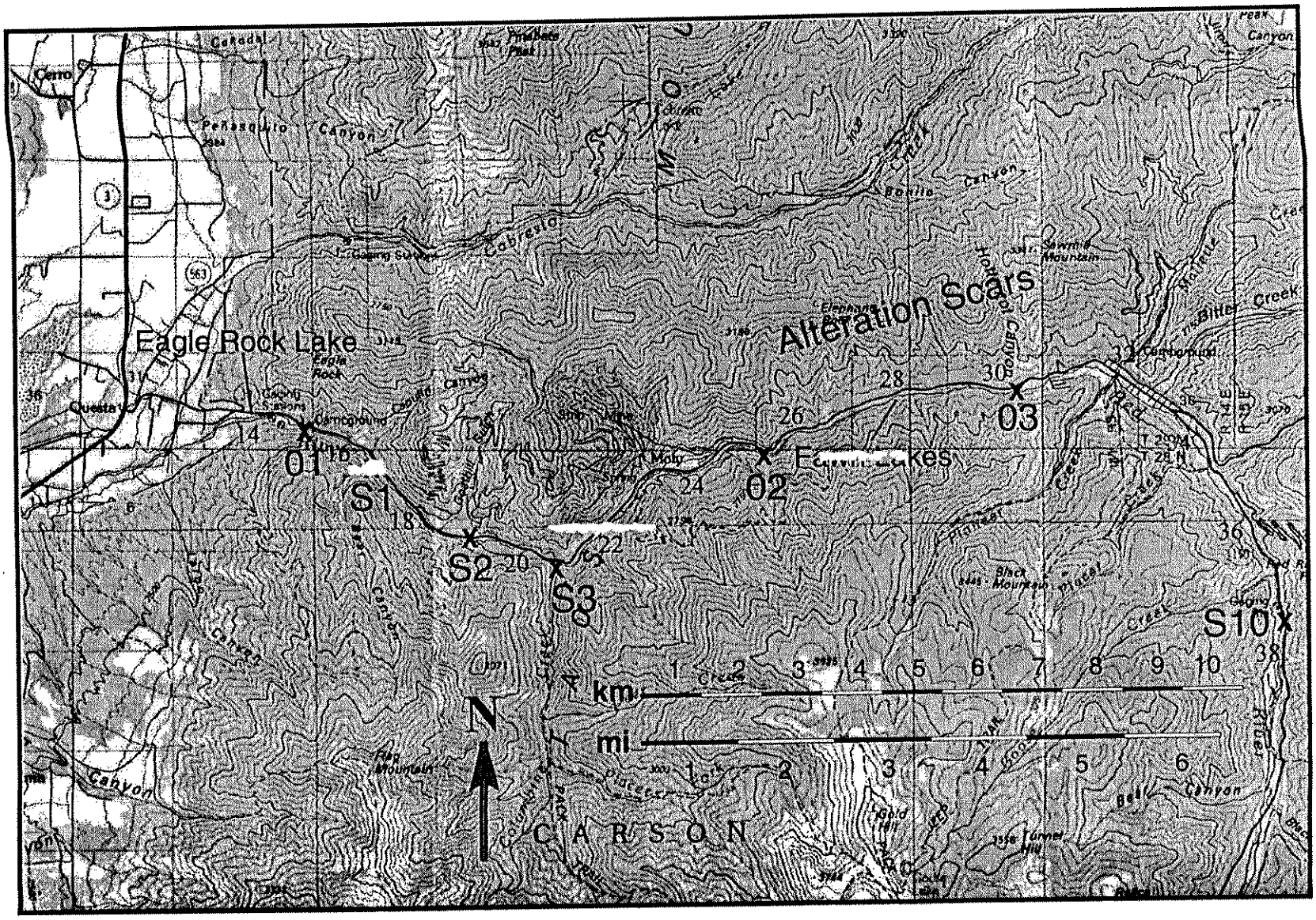

Figure 3. Sampling localities for water, stream sediment, tree wood, and biologic samples. River distance in km as indicated.

Table 1. Red River sampling localities for water-quality, sediment, tree wood, and biologic samples. Localities shown in Figure 3.

ID	Location	Water Sampling Frequency	Justification Criteria
01	Eagle Rock campground, downstream from mine; river distance 15.3 km.	Monthly, n=13 Primary location	Impacted by both mine and upstream alteration scars; mine impact chemistry.
S1	Upstream from mouth of Capulin Canyon, downstream from mine; river distance 16.8 km.	No water-quality samples from the Red River collected.	Impacted by both mine and upstream alteration scars; mine impact chemistry.
S2	Downstream from mill and Columbine Creek, upstream from mouth of Goat Hill Gulch; river distance 18.9 km.	Quarterly, n=5 Supplemental location	Impacted by both mine and upstream alteration scars; mine impact chemistry.
S3	Columbine Creek 100 meters upstream from confluence with Red River; river distance 20.9 km.	Quarterly, n=5 Supplemental location	Columbine Creek waters, not influenced by mine or alteration scars; dilutes Red River waters; background chemistry.
02	Upstream from mine property; river distance 25.5 km.	Monthly, n=13 Primary location	Impacted by alteration scars upstream from mine; mine baseline chemistry.
03	Downstream from town of Red River at mouth of Hottentot Canyon; river distance 30.2 km.	Monthly, n=13 Primary location	Impacted by Hottentot alteration scar drainage, town of Red River, and upstream scar areas (e.g. Bitter Creek); mine baseline chemistry.
S10	Upstream from town of Red River at abandoned USGS stream gage (Zwergle Dam); river distance 37.6 km.	Quarterly, n=5 Supplemental location	Not influenced by mine or alteration scars; background chemistry.

0.45 µm Gelman capsule; unfiltered samples were collected directly from the tubing. Acid-washed polyethylene bottles were used for collection of samples. Samples for metals analysis were preserved with HNO_3 to pH < 2. Samples for anions were transported to the lab on ice and kept under refrigeration until analyzed. Equipment blanks and field replicates were collected to check for contamination and reproducibility. Sample containers for all types of environmental samples were sealed in the field and chain-of-custody procedures were employed.

Sediment Samples

Stream and Pond Sediment

Stream sediments were collected from the channel of the Red River under different conditions of flow and analyzed for Al, Fe, Mn, Cu, Co, Mo, Ni, and Zn. Grab samples were collected from the stream channel in February, July, and October of 1998. Sediment traps were deployed in the stream to obtain samples directly from the water column. Sediment samples were collected from reaches of the stream affected by natural alteration scars and from localities within and below the mine area, in order to compare metal concentrations in sediments affected by both sources of acid rock drainage (ARD).

Sediment traps were deployed in the stream channel at localities 03, 02, and 01 (Fig. 3) and samples were collected monthly in conjunction with water sampling visits. Three traps were deployed at each locality to ensure that sufficient material for analyses was collected, and to provide replicate samples. Sediment-trap samples for the months of August, October, and December, 1997, and January, February, and April, 1998 were analyzed. In addition, sediment traps were deployed in Columbine Creek (locality S3) and in the Red River at locality S2 near the end of October, 1997. Collection tubes were retrieved from these traps near the end of February, so that these samples represent a 4-month period of collection.

In order to obtain information about possible temporal changes in the geochemistry of the Red River, samples were collected from two types of geologic archive. These archives contain stream sediments that were deposited prior to excavation of the open-pit mine. The first type of archive consists of sediment accumulations associated with a comparatively young fluvial terrace that extends along the Red River in the vicinity of the mine. The terrace tread lies 1 to 3 meters above the modern stream channel (Fig. 4) and growth rings in trees rooted on the abandoned surface indicate that the underlying fill is at least 60 years old. Sediments underlying the terrace were collected near localities 02, S2, S1, and 01 (Fig. 3).

Stream sediments are also accumulating in artificial impoundments along the Red River, two of which were sampled during this study. Eagle Rock Lake (ERL), constructed in the mid 1950s, is located downstream from the mine-impacted area, to the east of Questa. The Fawn Lakes (FL) impoundment, constructed in the early 1960s, is located upstream from the open-pit mine and within the area of alteration scars between the town of Red River and the mine (Fig. 1). Sediments from the two ponds provide information about the chemistry of the stream in areas affected by natural outcrops of mineralized rocks (FL) and by open-pit mining activities (ERL).

Both impoundments were created before excavation of the open-pit mine and bottom deposits in the ponds comprise a continuous record of changes in the

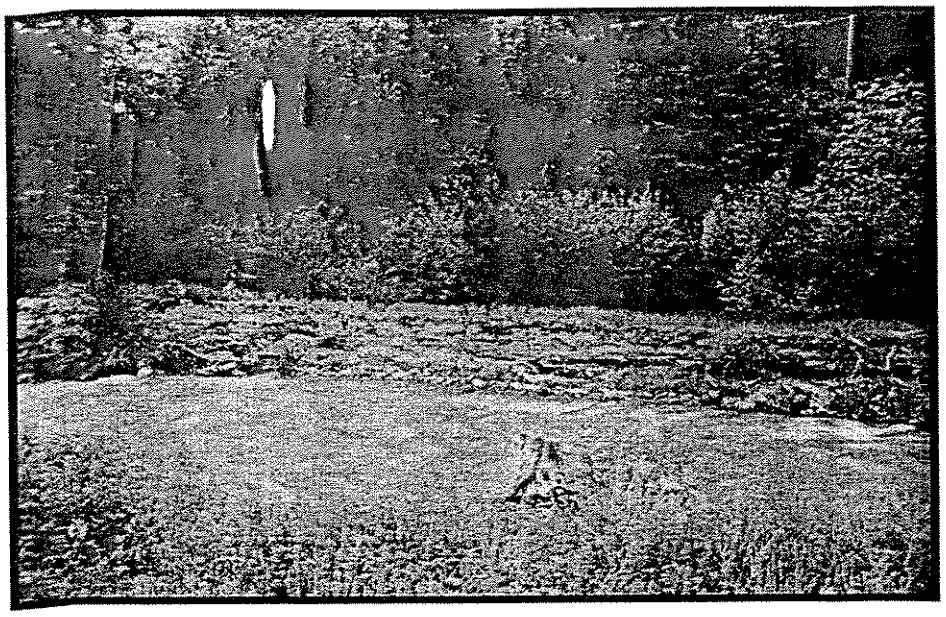

Figure 4. Red River showing prominent fluvial terrace that occurs along stream in vicinity of the molybdenum mine. Fill units beneath terrace (exposed in stream cut) pre-date open-pit mining activity.

geochemistry of sediments transported by the Red River. Preliminary cores were taken from the ponds in March, 1997 (ERL) and June, 1997 (FL) to assess the thickness of the accumulations and the consistency of the sediments. The thickest accumulation of sediments occur in the areas of the ponds nearest their inlet from the Red River. Core samples for geochemical analysis were collected in January, 1998. Two overlapping cores were required to recover the entire ~ 1.5 meters of pond sediment present near the inlets of both ponds. A core taken from the outlet end of ERL was also subsampled and analyzed for metal concentrations, and a second core taken nearby was subsampled to provide replicate samples. Coring localities are shown in Fig. 5.

Sediment accumulations toward the inlet of both ponds exhibit distinct layering related to seasonal changes in the composition of sediment transported by the Red River. In particular, surface runoff associated with rainfall events over scar areas is recorded in bottom sediments as yellow-tan layers of silty clay. These yellow, "runoff-season" layers are interlaminated with typical black pond sediments. In ERL upper portions of the pond sequence also contain milky colored, gelatinous layers enriched in aluminum, which are not present in FL.

Sediment traps were deployed in ERL and FL to collect sediments carried into the ponds. Traps were deployed in the ponds in June, 1997 with the trap opening ~0.5

meters below the water surface. Two traps were deployed on the same mooring in ERL to provide replicate samples. Collection tubes were retrieved in September, 1997 and June, 1998 (2 collection tubes from each sediment trap for the 1-year deployment). The contents of collection tubes from Fawn Lake were subsampled to provide 4 samples (2 samples from each tube). Collection tubes from one of the ERL traps were subsampled to provide 6 samples. Collection tubes from the other ERL trap were not subsampled, yielding 2 samples for the 1-year deployment.

Grab samples from the stream channel were collected using latex gloves, placed in sealable polyethylene bags, and stored on ice until returning to the laboratory. Sediment-trap samples were collected by removing the polycarbonate collection tube from the trap housing (Appendix III) and sealing the top of the tube with polyethylene film and tape. Collection tubes were transported to the laboratory on ice. Core samples from Eagle Rock and Fawn Lakes were collected using a square-rod piston corer (Wright et al., 1984) and 5-cm diameter, stainless-steel core barrels. Core barrels were cleaned in the laboratory and wrapped in polyethylene film to minimize contamination during transport to the field. Cores were collected through holes bored in the ice and were extruded into split sections of previously cleaned butyrate tubing lined with polyethylene film, and taped closed. Wet samples were kept under refrigeration until dried.

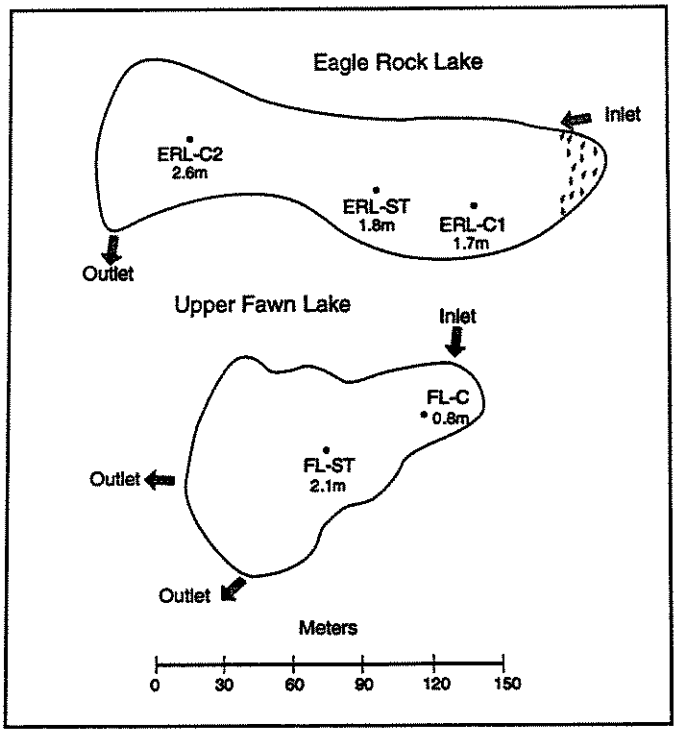

Figure 5. Eagle Rock and upper Fawn Lakes, showing sediment-trap (ST) and core (C) localities. Water depth at each locality as indicated.

Other Sediment Samples

Additional sediment samples analyzed during the investigation include five samples of alluvium associated with natural scar areas. Three samples were collected in the Hansen Creek drainage and one sample each from debris fans near locality 03 and near the mouth of Goathill Gulch (Fig 6). Samples of alluvium were analyzed in order to provide additional geochemical information about scar-area sediments.

Grab samples of comparatively dry sediments were exposed using a pick or shovel, then collected using latex gloves after brushing away materials that may have been contaminated during excavation. Dry samples were placed in polyethylene bags and transported to the laboratory without refrigeration.

Fe-Mn-Al Coatings and Cements

Early in the investigation it was thought that thick deposits of metal oxides might be found that have been accumulating over a period of time, potentially providing continuous records of changes in the chemistry of acidic seep waters. Such deposits were not identified during the investigation, but several samples enriched in metal oxyhydroxides, occurring either as thin coatings or as cement, were collected and analyzed to provide further information about the distribution of metals in the study area.

Samples enriched in iron were collected from low-pH seeps near the mouth of Capulin Canyon, and from the headwaters of the Hansen Creek scar area. The Capulin Canyon crusts are relatively porous accumulations enriched in iron that are chemically precipitated on the stream bank in association with abundant growths of yellow- and green-colored filamentous algae. The sample collected in the Hansen Creek drainage is a breccia consisting of rhyolite clasts held together by an iron oxide cement. Low-pH waters from Hansen Creek presently flow over the breccia and have deposited a ~2-mm thick, laminated Fe coating on its surface. The laminated coating and the underlying breccia were both sampled. The breccia was disaggregated in the lab and sieved to remove larger clasts of rhyolite.

Fluvial sand and gravel deposits were identified downstream from Columbine Creek along the modern channel of the Red River and at higher elevations along the north side of the stream that are cemented or coated with compounds enriched in iron and/or manganese. Three such samples were collected along the modern stream (2 samples near locality 01 and one near locality S1), and one sample from well above the modern stream channel near Goathill Gulch (Fig. 6). Cemented samples were disaggregated in the lab and sieved to remove larger clasts, retaining the finer (<100-mesh) fraction for analysis.

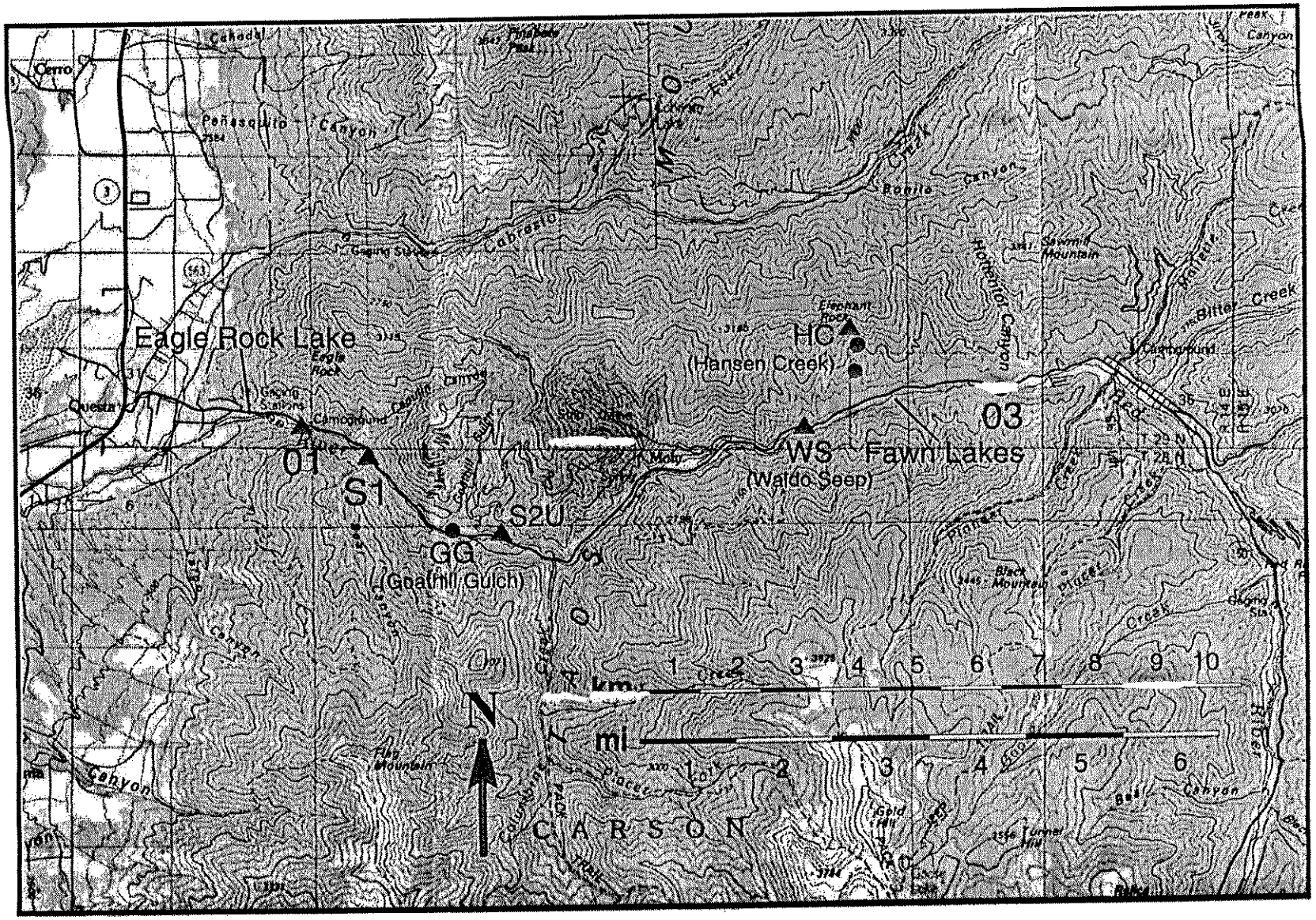

Figure 6. Sampling localities for alluvium associated with scars (circles) and Fe-Mn-Al crusts and cements (triangles).

Samples enriched in aluminum were collected from the Red River at locality S1 (upstream from mouth of Capulin Canyon), and from a small pool ("Waldo seep", Slifer, pers. commun.) located adjacent to the Red River upstream from locality 02 (Fig. 6). The Capulin Canyon sample consists of the white precipitate that blankets the streambed downstream from the mine in areas of ARD discharge. Coated cobbles from the streambed were collected and the white crust was mechanically removed in the lab using a polypropylene spatula. The Waldo seep sample was collected in the outflow channel of a small, low-pH pool that lies adjacent to the Red River in an abandoned channel of the stream. Flow velocities in the outlet channel are low, and the aluminum precipitate accumulates as a white floc, several cm in thickness, on the bottom of the channel. The sample was obtained using a peristaltic pump by holding the inlet tube over the floc and pumping the material into a bottle. After settling, most of the water in the bottle was decanted and the remaining sample was retained for analysis.

Tree Wood

Wood was collected from trees rooted near the Red River in order to assess the utility of trees as potential recorders of geochemical changes in the stream as it flows through mineralized portions of the study area. Concentrations of metals in plant tissues may reflect the abundance of metals in the plant's immediate soil, air, and water environment, and in some studies tree wood has been shown to yield geochemical concentration data that are consistent with inferred geochemical trends in the environment (e.g. Baes and McLaughlin, 1984; Latimer et al., 1996).

Samples of Douglas fir and ponderosa pine were collected near water and sediment sampling localities (Fig. 3). An attempt was made to locate trees close to the stream whose root systems extend to the depth of the water table (i.e. stream elevation) and were at least 40-years old, so that wood which grew before open-pit mining operations could be sampled. These conditions were met at the two upstream localities, S10 and 03. At downstream localities older trees were limited to the lowest prominent terrace adjacent to the Red River.

At localities S10 and 03 older trees growing near the stream were limited to firs, and wood samples from one tree rooted near the stream were collected at each of these localities. At locality 03 pine trees occur on the large debris fan associated with the Hottentot scar area, several meters above the elevation of the modern stream channel. Wood from one of these pine trees was sampled and analyzed. Wood samples from one fir and two pine trees near locality 02 were analyzed, but, as for all of the downstream wood samples, much of the root system of these trees may be above stream elevation. A pine tree was sampled near locality S1 growing about 2 meters above the elevation of the water table near an abandoned channel of the Red River, and near locality 01 one pine and one fir tree were sampled and analyzed.

Samples were collected using a 0.2-inch diameter increment borer. Three to five cores were taken from each tree in order to provide sufficient material for analysis. The increment borer was rinsed with acetone between samples to minimize contamination. Wood cores were wrapped in polyethylene film, placed in PVC tubes, and the tube ends taped shut for transportation to the lab.

Biota

Lysimeters for collecting macroinvertebrates from the streambed were installed in February, 1998, and capped for later sampling. Lysimeters were constructed by driving sections of 1/2-inch PVC pipe into the substrate to a depth of 30 to 40 cm using a steel drive rod (Appendix III). Samples were collected using a hand-operated diaphragm pump connected to the lysimeter. The outlet from the pump was held over a 50-mesh sieve to collect the sample. Approximately 10 liters of water was pumped from each lysimeter to ensure that similar volumes of the substrate were sampled. Sediment collected on the sieve was transferred to polyethylene bottles containing 95% ethanol. The sieve and pump were rinsed and purged between samples. Three lysimeters were installed at each of the seven localities shown in Figure 3.

Samples were collected on 19 March and 29-30 April, 1998. Spring runoff had begun before the second sampling round, and at each sampling locality, except for locality S3 (Columbine Creek), at least one of the lysimeters had been lost, presumably dislodged by debris in the stream. Remaining lysimeters were sampled.

In the laboratory, organisms were separated from the sediment matrix using a picking tray, forceps, and a 7-30X binocular microscope. Arthropods were identified to order and insects were identified further to family. Amphipods were identified to genus.

ANALYTICAL METHODS

Water

Field Measurements

Alkalinity, dissolved oxygen (DO), pH, oxidation reduction potential (ORP), electrical conductivity, and temperature (T) were measured in the field. Alkalinity was measured using a Hach field titrator, battery stir plate, and pH probe. DO was measured directly in the stream with a YSI 55B DO meter, calibrated at each location. pH and ORP were measured in the flow-through cell using an Orion 290A pH/millivolt meter with Orion ATC pH electrodes (pH) and bright platinum electrodes (ORP). pH drift during sampling events was within +/- 0.05 pH units except when temperatures were

below instrument operational limits, at which time pH drifted up to +/- 0.1 unit. ORP electrodes were checked with Zobell solution at the beginning of each sampling event. ORP values in Zobell solution were 230 +/- 10 mV. ORP values were converted to the standard hydrogen electrode and are reported as Eh. Electrical conductivity measurements were measured using a YSI 1500 conductivity probe and meter.

Laboratory Measurements

Major cations (Ca, Mg, Na, K) and Mn, Fe, and Al were determined by flame using a Perkin-Elmer model 303 atomic-absorption spectrophotometer. Anions (SO_4, Cl, F and NO_3) were analyzed using a Dionex-500X ion chromatograph. Trace element concentrations (Cd, Cu, Co, Ni and Zn) were determined by inductively coupled plasma-mass spectrometry using a VG Elemental Plasma Quad ICP-MS. Unfiltered water samples for metals analysis were digested at ~90°C using HNO_3 and HCl.

The mean concentration of equipment blanks collected in the field (n=13) were 0.06 mg/L for anions, 0.1 mg/L for cations, and below detection for trace metals. The mean relative percent difference (RPD) between lab duplicates and field replicates was within 10% for anions, major cations, and all trace metals except for iron, which yielded mean RPDs of 15%.

Sediment

Sediment samples were placed in polypropylene dishes, dried for 12 to 16 hours at 60 to 80°C, and stored in polypropylene bags. Sediment cores and sediment-trap collection tubes were photographed prior to subsampling. Subsamples from pond cores were taken at discrete depth intervals, yielding samples ~ 1 to 2 cm in thickness. This allowed the separation of yellow layers associated with scar-area runoff events from the remainder of the sediment core. Similarly, scar-area runoff layers in stream sediment traps were separated from the remaining sediments in order to obtain samples of consistent lithology. Sediment-trap samples were collected by extruding the sample from the collection tube.

Sediment cores were subsampled using a stainless steel knife and polyethylene spatulas. The outer ~3 mm was removed from core samples to eliminate material that may have been contaminated during retrieval and processing of the core. The upper ~20 cm of the pond sequence near the outlet end of ERL (core ERL-C2, Fig. 5) was extremely loose and unconsolidated, containing thick layers of aluminum-enriched floc, and disturbance of sediment layers during coring prevented the separation of typical pond sediments from this portion of the core. Thus, plots of elemental concentrations against depth (presented in a later section) show a relatively large gap in data near the top of core

ERL-C2. Two aluminum-enriched layers were collected from the upper part of ERL-C2, however.

Dried samples were disaggregated, homogenized by passing through clean polypropylene and nylon sieves, and stored in glass, snap-cap containers. Some samples had to be disaggregated using a ceramic mortar, which was washed, soaked in 20% HNO_3, and rinsed with deionized water between samples. Crushing of samples was avoided, except for crust samples, which were pulverized if necessary to allow the entire sample to pass through a 100-mesh sieve.

Pond sediments were disaggregated to the extent that the entire sample, with the exception of large organic fragments, would pass through a 60-mesh sieve. Stream-channel samples were passed through a 100-mesh sieve, without crushing, and the finer fraction was retained for analysis in order to obtain samples with similar grain-size distributions.

Prior to weighing, samples were dried for 12 to 16 hours at 105°C. For pond sediments, 0.5 gram of sample was analyzed, and for stream sediments 1.0 gram was analyzed. Weight loss on ignition (LOI) for 1 hr at 500°C was determined in order to provide a qualitative assessment of the percentage of organic carbon plus other volatile components present in the samples.

Weighed samples were digested at ~90°C to dryness in teflon beakers using a 1:1:1.5 mixture of HNO_3, $HClO_4$, and HF. The residue was dissolved in HCl + Cs, and diluted to 100 ml, producing a solution containing 1000 mg/l Cs in 10% HCl. Blanks were prepared for each group of samples using the same procedure and reagents used for the preparation of samples and standards. Samples were analyzed for Al, Fe, Mn, Co, Cu, Mo, Ni, and Zn by flame using Perkin-Elmer model 303 and Thermo Jarrell Ash model S12 atomic-absorption spectrophotometers. Sample concentrations were determined using standard calibration curves based on a basalt working standard (UNM-B1). Reported concentration values reflect rounding to significant digits, which was done after calculating precision and other quality-control parameters.

The mean recovery of analyte in spiked samples (n=9) was within +/- 10% of the expected value for all elements. The mean, relative percent differences between lab duplicates (n=19) and field replicates (n=14) were less than 10% and 20%, respectively, for all elements. Mean concentrations determined from 4 samples of an independent standard (NBS-1645, river sediment) were within 10% of reported values (Govindaraju, 1994) for all elements except Ni. The mean concentration obtained for Ni was within 20% of the reported value.

Tree Wood

Wood cores were rinsed in 10% HNO_3 and deionized water, and air dried shortly after returning from the field. Digital images were taken of one core from each tree prior to subsampling. Samples consisting of the outer 10 years of growth, excluding the bark, were taken from cores obtained at each of the sample localities. The outer 10-year increments from locality S1 and 01 wood cores were subsampled into 5-year increments, and the entire length of cores obtained from localities 02, S1, and 01 were subsampled into 5- or 10-year increments. Growth layers in the pine tree growing on the debris fan at locality 03 were very tightly spaced, and subsamples representing the outer 60 years of growth were obtained from this tree.

Samples were oven-dried at 70°C for 16 hours. 0.5 to 1 gram of dried sample was ashed at 500°C in ceramic crucibles and digested using the same procedure as for sediment samples. Residue from the digestion was dissolved in HCl + Cs and diluted to 25 ml, producing a solution containing 1000 mg/l Cs in 10% HCl. Samples were analyzed by flame for the same analytes, and using the same instruments and procedures, as for sediment samples. Of the measured analytes, only Mn, Cu, and Zn were present in sufficient amounts to be detected with the solution strengths and methods utilized.

Analytical precision for wood samples was not determined because of difficulties in producing a homogeneous powder from the fibrous wood samples. Replicate samples for two trees were prepared using separate cores from the same tree. The relative percent difference between replicate samples ranged from 2 % for manganese to 31% for copper, which was present in replicate samples at concentrations near the detection limit. The percent recovery of analyte in spiked samples was within 10% of expected values.

RESULTS

Water

Water-quality data and time-variant plots of selected analytes are shown in Appendix I. As expected, concentrations of chemical constituents in the Red River fluctuate during the annual cycle. The impact of ARD on the Red River is more pronounced during winter months when baseflow conditions exist, and is less pronounced during spring snowmelt and runoff, when maximum dilution of groundwater seepage occurs. In general, concentrations of dissolved constituents increase in a downstream direction.

Chloride concentrations through an annual cycle are shown in Figure A1. Chloride concentrations from alteration scar and mine impact locations are of the same magnitude, and increase somewhat in a downstream direction. Application of salt in the

town of Red River as a de-icing agent during winter, followed by flushing into the stream during snowmelt, may account for the early-spring peak in chloride concentrations (Fig. A1).

Sulfate concentrations in the Red River are higher during winter baseflow and lower during spring runoff (Fig. A2), and increase downstream. Background concentrations (locality S10) are relatively constant throughout an annual cycle, ranging from 10 to 14 mg/L. Sulfate concentrations in reaches of the stream impacted by seepage from extensive natural scars range from 15 to 70 mg/L (locality 03) and 20 to 100 mg/L (locality 02), representing an increase from background levels. Downstream from the mine (locality 01) sulfate ranges from 35 to 180 mg/L, representing an additional increase from upstream scar areas.

The temporal and spatial distribution of major cations (Ca, Mg, Na and K; Figs. A3 through A6) generally exhibit similar trends during an annual cycle. Calcium and magnesium concentrations increase systematically downstream. The temporal and spatial distribution of sodium is similar to chloride. Potassium shows little tendency for downstream enrichment in stream water.

Alkalinity is a measure of the acid-buffering capacity of waters, with low values suggesting impact from ARD. Alkalinity decreases downstream from approximately 85 mg/L in background waters (locality S10), to 30-60 mg/L at locality 01 (Fig. A7). The distribution of hydrogen ions (pH) varies from 8.5 in background waters to approximately 7.5 downstream from the mine. The downstream decreases in alkalinity and pH are consistent with ARD impacts from scar and mine-disturbed areas.

Comparatively high concentrations of manganese in stream waters were measured at locality 01 during baseflow, with peaks in September, December and February (Fig. A8). At locality 01, manganese increased from 140 ug/L during June, 1997, to 950 ug/L during December, 1997. Manganese concentration in reaches impacted by alteration-scar seepage above the mine ranged seasonally from <100 ug/L during spring runoff to about 200 ug/L during baseflow. Manganese concentrations of <100 ug/L were measured at locality S10 for all sampling events.

Trends in the distribution of zinc are similar to that of manganese (Fig. A9). At locality 01 zinc concentrations range from 30 ug/L during June to 400 ug/L during December, 1997. Mean daily discharge at the nearby USGS gage (Fig. 1) was ~280 cfs during the June sampling round, and ~9 cfs during the December round. Zinc concentrations at upstream localities impacted by scar seepage ranged from 18 to 56 ug/L (locality 02) and 2 to 40 ug/L (locality 03) during the June and December sampling rounds. Background zinc concentrations (locality S10) were < 1 ug/L for all sampling events.

Nickel and cobalt show similar temporal and spatial trends to that of manganese and zinc (Figures A10 and A11). Concentrations of nickel varied from <2 to 60 ug/L (locality 01), <2 to 18 ug/L (locality 2), and <2 to 8 ug/L (locality 03). Cobalt varied from 1 to 11 ug/L (locality 01), <1 to 4 ug/L (locality 02), and <1 to 2 ug/L (locality 03). Concentrations of Ni and Co were consistently less than 2 and 1 ug/L, respectively, at locality S10 during the annual cycle.

In general, the concentration of dissolved aluminum in stream water is somewhat higher downstream from the mine than in localities affected only by natural scar drainage (Fig. A12). Dissolved aluminum was at or slightly above detection limit (150 ug/L) above the mine, with somewhat higher concentrations downstream from the mine at locality 01. Total-aluminum values reflect dissolved aluminum species, colloidal aluminum compounds, and suspended clays. Comparatively high concentrations of total aluminum were obtained in samples collected at localities 01 and 02 (Table A1). Although the total-aluminum concentration data do not distinguish between colloidal aluminum compounds and aluminum associated with clays, visible clouding of the stream by colloidal aluminum compounds was observed at locality 01 during baseflow, but was not apparent at localities 02 and 03.

Sediment

Modern Stream Sediment

Analytical results for stream-sediment san ples and plots of concentration data against river distance are presented in Appendix I. In constructing the plots, no attempt was made to distinguish between data from each locality having the same numerical value. That is, two or more samples from the same locality, each yielding the same concentration for a particular element, appear on the plots as a single symbol. Plots of concentration vs. river distance for stream sediment-trap and grab samples are plotted using the same vertical axes as for older stream sediments associated with fluvial terraces, in order to facilitate visual comparison of data.

Metal concentrations in stream-channel grab samples (Fig. A13) reveal two general trends. First, concentrations of most metals (Al, Mn, Co, Cu, Ni, and Zn) are relatively similar at localities upstream from the mine-disturbed area, whereas concentrations at localities within and downstream from the mine area are more variable. Second, and related to this downstream increase in variability, are significant increases in metal concentrations in some downstream samples. Samples with high concentrations of iron, in contrast, are not associated with a particular reach of the stream, and molybdenum concentrations are comparatively uniform at all sample localities and increase downstream.

Concentration data for sediment-trap samples (Fig. A14) are summarized in Table 2, and show that Al, Mn, Co, Mo, Ni, and Zn are consistently more abundant in stream sediments collected at locality 01 (below the mine-disturbed area) relative to localities above the mine. Copper concentrations are generally higher at locality 01 relative to locality 02, but are also relatively high at locality 03. The pattern for iron is similar to that of copper.

Table 2. Summary data for stream sediment-trap samples.

	Al %	Fe %	Mn ppm	Co ppm	Cu ppm	Mo ppm	Ni ppm	Zn ppm
Loc. 01 (n=8)	8.9	3.7	2,694	49	378	46	94	1,194
Loc. 02 (n=8)	6.8	3.3	854	22	108	15	37	383
Loc. 03 (n=7)	6.9	4.0	944	25	289	15	41	494

Metal concentrations in stream-channel sediments are qualitatively similar to downstream trends observed in water-quality data, in that comparatively strong increases in the concentrations of certain metals occur below the mine-disturbed area. In contrast, increases in the concentration of metals between locality S10 (background) and downstream localities 03 and 02 are comparatively minor (Fig. A13), even though locality 03 and 02 samples reflect impact from extensive scar areas.

Concentration data for yellow, storm-runoff layers collected in sediment-traps at localities 02 and 01 during July-August are listed in Table A8. Surface runoff from scar areas is capable of increasing the suspended load of the stream enormously (Smolka and Tague, 1989; Slifer, 1996) and produced, during the summer and fall of 1997, discrete layers of yellow-tan silty clay in sediment traps (Fig. A19). Concentration data for these runoff samples indicate that sediments derived from the scar areas are not enriched in trace metals relative to typical stream sediments. This finding is consistent with analyses of similar layers in the pond cores, and with analyses of alluvium directly associated with three of the scar areas, as shown in Table A8.

Older Stream Sediment

Analytical results for stream sediments underlying fluvial terraces are listed in Table A4. As discussed earlier, these stream sediments were deposited prior to excavation of the open-pit mine. Concentration data for these "terrace samples" are plotted in Figure A15.

Concentrations of measured elements in terrace samples are generally similar to concentrations in modern stream sediments collected upstream from the mine. Samples were collected from localities S2 and S1, however, that contained more molybdenum than in any of the modern stream-channel sediments collected during the investigation (Table A4). The high concentration of molybdenum in these samples suggest erosion from a nearby source, consistent with molybdenite mineralization in the area now occupied by the mine.

A terrace sample was collected from locality 01 (sample 01-FT-1, 10/23/97) that is not included in the plots of Figure A15 because it is lithologically distinct from the other stream-sediment samples analyzed. The sample was collected from a several-cm thick peat layer, which may have accumulated in a low area adjacent to the stream before the stream incised to its present elevation. Similar accumulations of peaty material were recognized in exposures of the fill beneath the terrace at other localities along the Red River. The sample contains a substantial amount of organic matter, as indicated by a LOI value of 27%, and yielded a relatively high value for nickel concentration (110 ppm, Table A4).

Analytical results for terrace samples suggest that elevated concentrations of certain metals in stream sediments collected downstream from mine seepage, as presently observed, is a relatively recent trend. Fill units beneath stream terraces, however, are in places coated or cemented with oxyhydroxides of iron and/or manganese. Analyses of samples derived from such units are presented in the section on crusts and cements.

Pond Sediment

As mentioned earlier, both pond sequences exhibit distinct color-banding related to runoff from scar areas (Fig. 7). Analyses of yellow runoff layers from both ponds are included in Table A8, along with analyses of other sediments related to scar areas. Sedimentation rates towards the inlet ends of the ponds are on the order of a few centimeters per year, and successive runoff-season layers are thick enough to be resolved over the entire length of the pond sequence. Counts of yellow layers in cores collected towards the inlets of both ponds are in general agreement with the number of years that have elapsed since the ponds were constructed, and can be used to provide an approximate chronology for these cores (Fig. A20), with an estimated possible error in

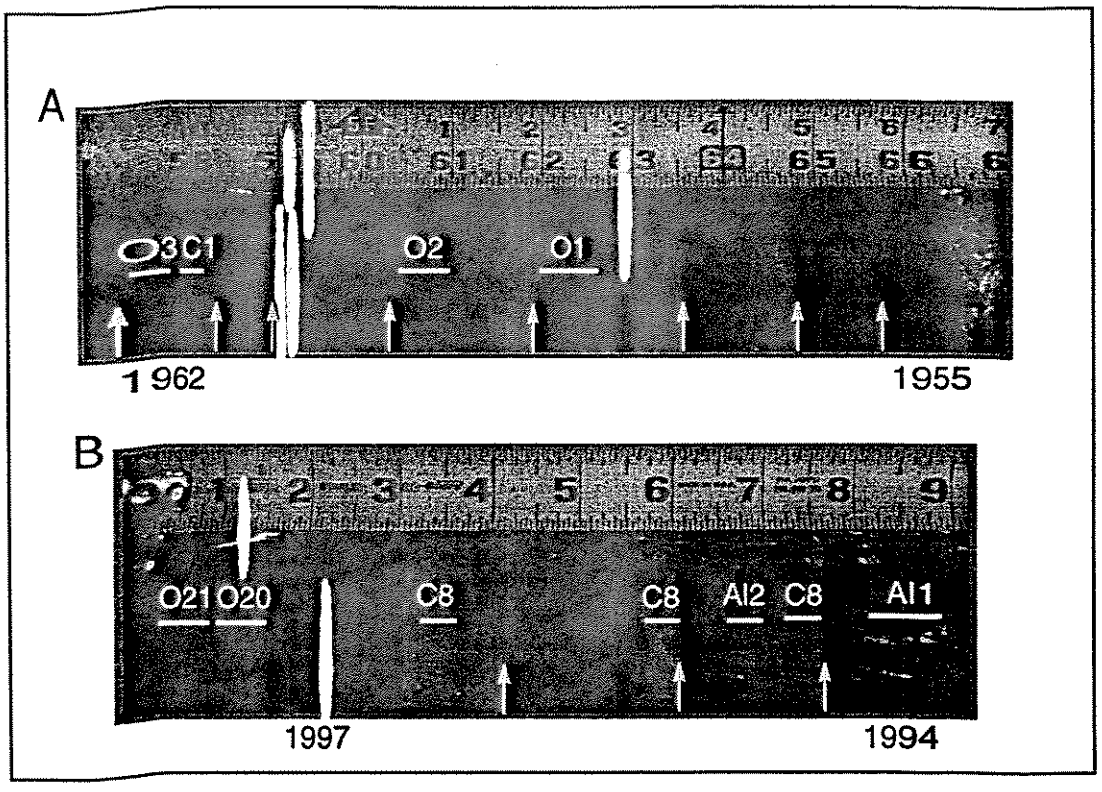

Figure 7. Sediment core from Eagle Rock Lake (ERL-C1) showing bottom (A) and top (B) portions of core, and associated sample intervals (labeled bars). Light-colored layers (base of layers indicated by arrows) are yellow and result from seasonal storm runoff derived from scar areas. Runoff layers alternate with dark-colored pond sediment. Sediments near inlet end of Fawn Lake have similar yellow and dark-colored layers, but do not contain gelatinous layers enriched in aluminum (e.g. layers Al1 and Al2 in (B) above) that occur in upper part of Eagle Rock Lake sequence. Geochemical profiles (Table A6; Figs. A16-A18) were obtained from dark-colored layers. Analytical results for yellow runoff layers and gelatinous, aluminum-enriched layers are tabulated in Tables A8 and A7, respectively.

the middle part of the cored interval of 5 years. The resolution of the seasonal layering decreases a short distance from the pond inlets because yellow runoff layers become thinner and overall sedimentation rate decreases with increasing distance from the inlet to the ponds.

Analytical results for sediment-trap samples collected in Fawn and Eagle Rock Lakes during 1997-1998 are listed in Table A5. All of the metals determined, with the exception of iron and molybdenum, are more concentrated in ERL sediments than in FL sediments. Enrichment of metals in recently deposited ERL sediments, relative to FL sediments, was previously documented in pond-bottom grab samples collected by the NM Environment Department in 1991 (Smolka, 1992).

Analytical results for dark-colored layers in sediment cores from Eagle Rock and Fawn Lakes are listed in Table A6. Plots of concentration vs. depth are shown in Figs. A16, A17, and A18. The FL profiles (Fig. A18) suggest that concentrations of metals in sediments carried into the pond have not varied much since the pond was created. In contrast, profiles for the ERL cores reveal considerable variability with depth. Concentrations of Al, Co, Ni, and Zn increase noticeably towards the top of both ERL cores, and peaks in molybdenum are present in older parts of the sequence. In addition, milky-colored, gelatinous layers are present in the upper part of the ERL sequence that are not present in lower portions of the ERL sequence, or in the FL sequence. The gelatinous layers contain up to 20% aluminum and are apparently associated with the white chemical precipitate that occurs in the channel of the Red River in reaches below the mine property, particularly during baseflow conditions. The layer count for ERL-C1, collected near the inlet to the pond, suggests that increases in concentration of aluminum and trace metals in that core (Fig. A16) occur in sediments deposited after the mid 1980s. Analytical results for aluminum-enriched gelatinous layers in ERL sediments are listed in Table A7, along with other chemical precipitates (crusts and cements).

Mean concentrations of metals in sediment-trap samples and core samples from ERL and FL are summarized in Table 3. Mean concentrations were calculated for the lower part of ERL-C1 (below increases in metal concentrations), the upper part of ERL-C1 (increased metal concentrations), the FL core, and the ERL and FL sediment traps. Mean trace-metal concentrations in the lower (older) part of ERL-C1 are less than 2-times greater than corresponding concentrations in the FL core, except for molybdenum, which is almost 15-times more abundant in the older ERL samples and will be discussed later. In contrast, trace-metal concentrations in recently deposited sediments from the two ponds are quite different. For example, Ni and Zn are greater than 5 times more abundant in the ERL sediment-trap samples than in the FL samples. Similar comparisons between groups of samples lead to the conclusion that concentrations of aluminum and some trace-metals in ERL, particularly Ni and Zn, have increased significantly since the pond was constructed.

Because aluminum is a major constituent of mineral sediments, differences in aluminum content between samples, even if large in an absolute sense, will not be reflected in a large fractional difference between samples that have undergone whole-rock analysis. For example, mean aluminum concentration in ERL sediment-trap samples relative to FL samples (11.3% vs. 8.8%, Table 3) is a seemingly small 1.28-times fractional increase, but represents a substantial 25 grams of aluminum per kilogram of sediment.

Molybdenum in ERL sediments is relatively abundant in lower portions of the sequence, and decreases to comparatively low levels towards the top (Figs. A16 and A17). The distribution of molybdenum in the pond sequence is consistent with the history of mining activity at the molybdenum mine. Prior to open-pit mining operations,

Table 3. Summary data for core and sediment-trap samples, ERL and FL.

	Al %	Fe %	Mn ppm	Co ppm	Cu ppm	Mo ppm	Ni ppm	Zn ppm
ERL-C1 (upper part, n=6)	11.8	5.0	5245	85	523	72	216	2733
ERL-C1 (lower part, n=14)	9.1	5.5	757	34	241	474	56	537
FL (n=11)	8.0	5.1	595	31	150	32	37	285
ERL Sed. Traps (n=8)	11.3	4.4	12,025	111	548	31	296	3375
FL Sed. Traps (n=4)	8.8	4.9	1,633	33	233	28	59	625

mill tailings were disposed of at the mill site, near the Red River and upstream from ERL. Comparatively high concentrations of molybdenum in lower parts of the pond sequence probably reflect erosion and transport of these mill tailings into the Red River. Molybdenum may also have been introduced into ERL when breakages occurred in the pipeline used to convey tailing away from the mill site. Low levels of molybdenum in the upper part of the ERL sequence suggest that problems associated with erosion and pipeline breakages have been minimized in recent years.

Crusts and Cements

Analytical results for Al-Fe-Mn coatings and cements are listed in Table A7. The iron crusts from the Capulin Canyon seep area and from the Hansen Creek alteration scar yielded high concentration values for iron (48% and 41% iron respectively) and comparatively low concentrations for the other metals determined, with the exception of copper in the Capulin Canyon sample, which measured 110 ppm. The iron-enriched cement in the rhyolite breccia collected in Hansen Creek contained about 17% iron and low concentrations of manganese and trace metals.

The manganese-enriched cements from locality 01 and S2U (Fig. 6) contain from 6.4% to 8.5% Mn and are relatively enriched in Co, Cu, Mo, Ni, and Zn. The sample

collected well above the modern stream channel (sample S2U-FT-1, 7/16/98) yielded higher trace-metal concentrations than the two samples collected at stream level near locality 01. The Fe-Mn crust collected from sediments beneath the terrace at locality S1 (sample S1-FT-1, 7/16/98) yielded 1.8% Mn, 7.7 % Fe, and a comparatively high molybdenum concentration (450 ppm). The presence of trace-metal enriched, Fe-Mn cements and crusts at various elevations above the modern stream channel suggests that generation of ARD and discharge of metal-laden waters has been occurring for a long period of time in the reach of the Red River between Goathill Gulch and locality 01. Hence, it seems likely that the buffering capacity of sediments and rocks along these ancient flow paths for ARD have been largely depleted.

The aluminum-enriched chemical precipitate collected from the stream channel in the vicinity of the Capulin Canyon ARD seeps contains about 19 % Al and comparatively high concentrations of Cu (1330 ppm) and Zn (970 ppm) and relatively low concentrations of other trace metals. The sample collected from Waldo seep contains 24% aluminum and relatively low concentration of other metals. Analytical results obtained from four samples of gelatinous, aluminum-enriched layers in the ERL cores are also included in Table A7. The pond samples range from ~14% to 21% aluminum, and contain comparatively high concentrations of copper and zinc, similar to the Capulin Canyon seep sample.

Tree Wood

Analytical results for Mn, Cu, and Zn in tree-wood samples are listed in Table A9. Analyses of the outer 10 years (1989-98) of wood reveal comparatively high concentrations of copper and zinc at the two upstream localities, S10 and 03. Concentrations of copper and zinc at downstream localities 02, S1, and 01 are similar, and comparatively low. In contrast, manganese concentrations are low at upstream localities S10 and 03, and comparatively high in samples collected at downstream localities. Furthermore, manganese concentrations appear to be more variable than copper or zinc at localities where more than one tree was sampled. Concentrations of metals in the pine tree growing on the debris fan at locality 03 are similar to those in wood samples collected at downstream localities, with comparatively low copper and zinc values, and relatively high concentrations of manganese.

Sample increments of wood grown prior to 1989-1998 were analyzed from four trees growing at downstream localities. Results for these older wood samples show that, for 3 of the 4 trees, concentrations of manganese and zinc are highest in the older wood, and decrease in successively younger samples. Copper concentrations in wood from these samples are generally similar.

Invertebrate Biota

Census results for hyporheic samples are listed in Tables A10 and A11, and are plotted in Figure 8. In lysimeter samples taken in March, the number of invertebrate taxa collected at localities S10, 03, and 02, which are located upstream from the potential influence of mining activities, ranged from 6 to 10. On the same date, only one dipteran taxon was collected at locality 01, located downstream from the mining operations. In the April samples, the number of invertebrate taxa ranged from 12 to 14 at localities S10, 02, and S3 (Columbine Creek), which are located outside the area influenced by mining. On the same date, the number of taxa collected downstream from the mine, at localities S2, S1, and 01, ranged from 0 to 7. The number of invertebrate individuals at localities upstream and downstream from mining activities also contrasted sharply during both the March and April collections (Fig. 8).

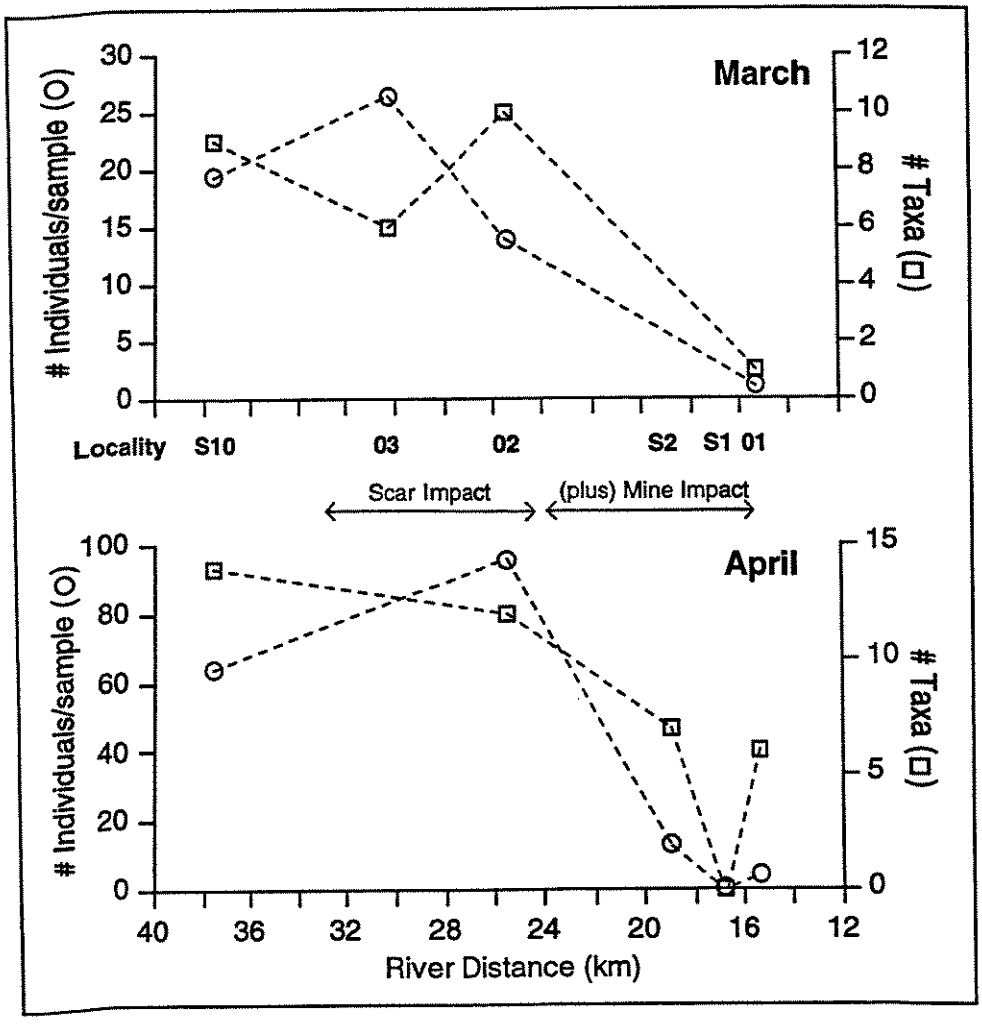

Figure 8. Hyporheic invertebrates collected in the Red River, March and April, 1998, showing number of taxa and individuals collected at stream localities shown in Table 1. Census data are listed in Tables A10 and A11.

The composition of the fauna indicates the presence of a true groundwater invertebrate community above the mining activity. Particularly notable is the presence of the blind phreatic amphipod *Stygobromus sp.* at locality S10 which is upstream from any mining activities and from the town of Red River. Several of the Plecoptera taxa collected had little or no pigmentation and reduced numbers of eye facets, indicating that they were also apparently associated with groundwater. Rich communities of Ephemeroptera, Plecoptera, and Trichoptera were collected at all sites upstream from mining activities but were absent or uncommon at locations below mining activities.

EVALUATION OF RESULTS

Spatial Differences in Metal Loading: Alteration Scars vs. Waste-Rock Dumps

Numerous water-quality surveys have been conducted on the Red River in recent decades that show that the middle reach of the Red River, between the towns of Red River and Questa, is being loaded with metals. The greatest increases in some dissolved species have been shown to occur below the mine property, near the U.S. Forest Service office (Smolka and Tague, 1989). Existing water-quality data also suggest that the high concentrations of some metals presently observed downstream from the mine is a relatively recent trend, and post-dates excavation of the open-pit mine (Kent, 1995; Slifer, 1996). Little water-quality data for the 1960s and 1970s exist, however, making it difficult to quantify the increase in metal loading due to mining activity.

Recently, efforts have been made to obtain water-quality data for surface and groundwaters associated with suspected, ARD-generating source areas (SRK, 1995; SPRI, 1995). In general, water-quality results from these studies show that low pH and elevated levels of sulfate and dissolved metals characterize waters associated with both natural, and mine-disturbed areas. Because relationships between mining activity and perceived declines in water quality are complicated by natural inputs from scar areas, an understanding of the Red River hydrologic/geochemical system that includes the river, scar areas, and mine-disturbed areas is needed. Continued monitoring of the Red River will provide information for calibration and validation of numerical models, and may be critical for evaluating possible future changes in stream chemistry (e.g. due to remediation efforts). Thus, one aspect of this investigation involved the collection and analysis of water samples from the Red River at key localities in the vicinity of the mine.

Differences in Stream Water

Weathering of natural exposures of sulfide-mineralized rocks contribute ARD to the Red River upstream, within, and downstream from mine-disturbed areas. Weathering reactions and generation of ARD in natural exposures probably occurs to a large extent

within several meters of the land surface, although oxygenated surface waters may penetrate along fractures and other permeable zones to form ARD.

The stable forms of most metals in low-pH, moderately oxidizing solutions are ionic species capable of being transported long distances from source areas along groundwater flowpaths. The essential chemical reaction involved in the release of metals from sulfide-mineralized rocks is the oxidation of the mineral pyrite (FeS_2) and the formation of low-pH solutions capable of releasing metals as mobile species in solution. The formation of such acidic solutions, which are often referred to as acid mine drainage or acid rock drainage (ARD), occurs when pyrite (FeS_2) is exposed to atmospheric oxygen and may be symbolically depicted by the reaction:

$$4FeS_2 + 15O_2 + 8H_20 = 2Fe_2O_3 + 8SO_4^{-2} + 16H^+$$

The weathering of pyrite in the field is much more complex, involving intermediate reactions and the catalyzing action of bacteria. The basic result, however, entails the conversion of reduced sulfur to sulfate ion, and increased acidity (lower pH) of associated solutions. Hence, measurements of pH and concentration of sulfate, in conjunction with analyses of metal concentrations, have routinely been utilized in studies of the Red River as indicators of ARD (e.g. Vail, 1993; Kent, 1995).

If mineralized rocks in the vicinity of the mine contain comparatively high concentrations of sulfides and trace metals, sharp increases in metal concentrations in stream waters below mining operations might be part of a natural response to this increased mineralization. Conversely, if rocks in the vicinity of the mine are anomalously enriched in sulfides, the geochemical impact on the stream system associated with their excavation and emplacement above the water table could be especially significant.

The waste dumps resulting from excavation of the open-pit mine represent a new source of ARD within the Red River watershed (SRK, 1995). Waste rock comprising these dumps have been significantly modified by mining activity. The surface area exposed to oxidation of these materials has been increased by several orders of magnitude due to mechanical disaggregation associated with blasting and excavation of the pit. Furthermore, the mining waste has been placed above the water table, and is susceptible to enhanced weathering due to exposure to atmospheric oxygen. These modifications may be expected to lead to the generation of ARD at accelerated rates compared to the original, intact rock body.

Key constituents that appear to be entering the stream system at increased rates due to mining disturbances include Al, Mn, Co, Ni, and Zn. This inference is based on marked increases in these elements in downstream water-quality transects and their distribution in modern and historical accumulations of sediment.

If alteration scars were the primary source of metal loading to the Red River, a somewhat linear, downstream increase in trace-metal concentrations might be expected, due to the similar surface distribution of scars in upstream and downstream reaches (Fig. 2). Results from this investigation and previous studies, however, suggest that concentrations of certain constituents increase somewhat in the area of scars, and then increase more sharply below the mine-disturbed area. Mean concentrations of Ni and Zn in stream waters, calculated over the one-year sampling period, illustrate this sharp increase (Fig. 9A).

Another way to examine downstream trends in metal loading is to compare the annual variability in concentrations of constituents as the stream flows through mineralized reaches of the canyon. The annual cycle of stream discharge is generally characterized by seasonal fluctuations in concentrations of dissolved constituents (Figs. A1 through A11), with high concentrations during winter baseflow (minimum dilution of

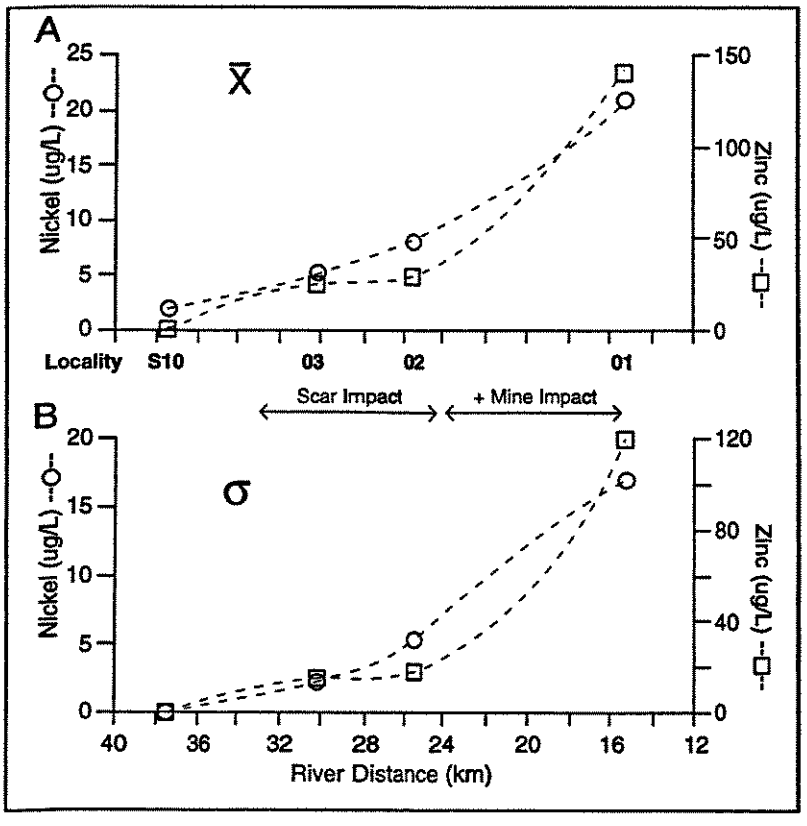

Figure 9. (A) Mean concentrations vs. river distance for Ni and Zn in Red River water samples, showing nonlinear increase below mining operations. N = 13, except for locality S10 (n=5). (B) Downstream variability (σ) of Ni and Zn concentrations, showing increase in seasonal variability below mining operations. Variability is assumed to be minimal at background locality S10.

groundwater seepage) and low concentrations during spring runoff (maximum dilution). Annual variability in concentrations of nickel and zinc, expressed as the standard deviation of concentrations in samples collected over an annual cycle, are depicted in Figure 9B. Annual variability is less pronounced in upstream reaches of the stream, and greater in reaches downstream from the mine, suggesting that loading of these elements in seepage increases below the mine.

The spatial distributions of total aluminum and dissolved nickel and zinc, from the Woodward-Clyde data of November, 1995 (Woodward-Clyde, 1996) are shown in Figure 10. These data, representing stream waters collected at closely spaced sampling localities, show significant increases in concentration about midway through the mine property, and another sharp increase below Capulin Canyon.

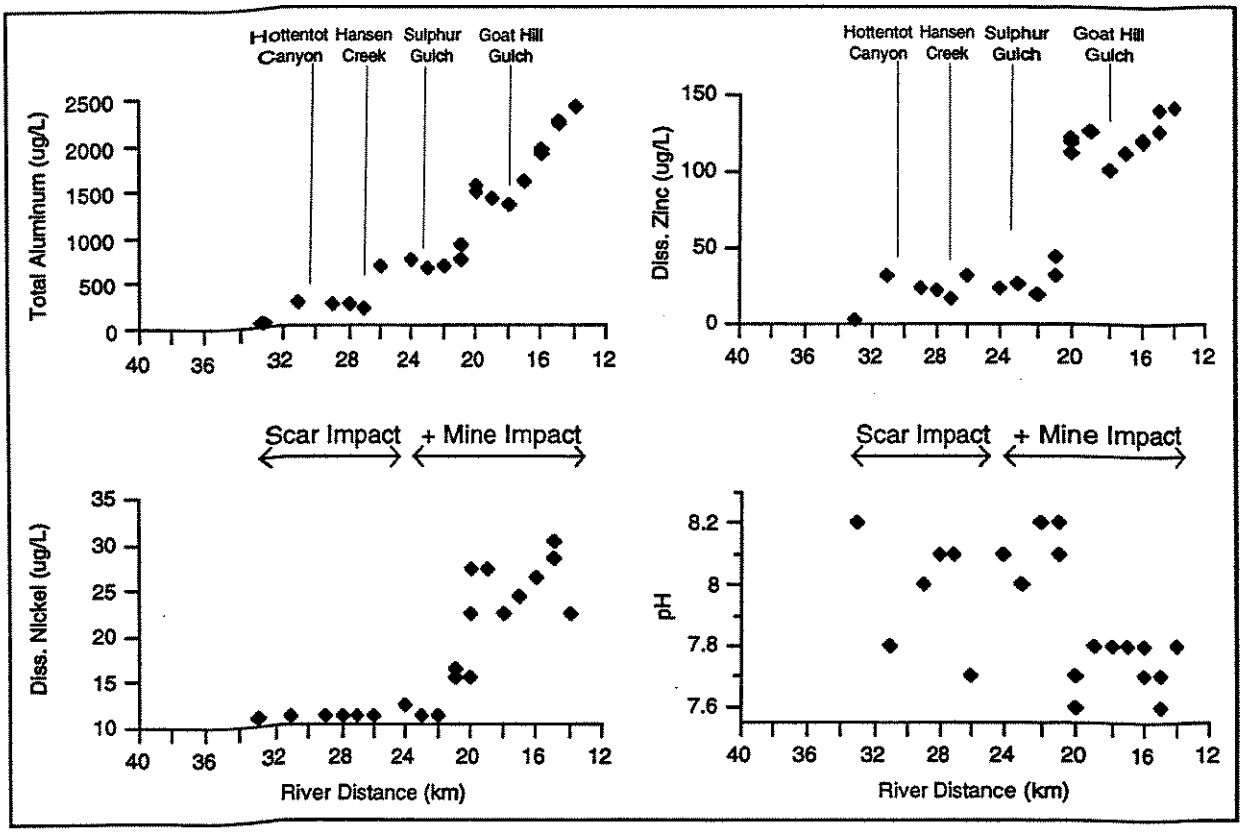

Figure 10. Concentration and pH data collected from Red River at closely spaced sample localities, showing sharp increases in concentration of certain metals below waste-rock dumps. Data collected November, 1995 (Woodward-Clyde, 1996). Sulphur Gulch (now buried) and Goathill Gulch drained the two extensive natural scar areas on the mine property. Increases in concentration occur downslope from areas of waste-rock dumps. Total-aluminum concentrations include aluminum-hydroxide compounds that are visible in stream below the mine during baseflow.

Differences in Stream Sediment

During this investigation sediments associated with the modern stream channel were collected in conjunction with water-quality samples to provide additional information about downstream changes in the chemistry of the Red River in the vicinity of the open-pit mine. The rationale for studying sediments relies on a tendency for the chemical composition of sediments to reflect, to some degree, the composition of waters with which they have been in contact. Practitioners of geochemical prospecting utilize this tendency to locate mineralized rock bodies that are poorly exposed at the earth's surface, the underlying assumption being that concentrations of metals in sediment samples will increase with proximity to a suspected ore body.

Significant changes in acidity (pH) and oxidation potential (Eh) that occur when ARD mixes with oxygen-saturated, near-neutral-pH surface waters generally result in the chemical precipitation of insoluble metal oxides. Low-pH seeps near the mouth of Capulin Canyon (Fig. 3, locality S1), for example, are characterized by accumulations of iron and aluminum. Discharge of ARD to the surface and mixing with dilute stream waters, resulting in the deposition of iron and aluminum, is a simple example of how metal ions in ARD may become associated with sediments. Other geochemical processes result in the removal of ions from solution and their incorporation in suspended and bedload sediments of the stream. Certain compounds, such as oxyhydroxides of iron and manganese, organic matter, and clay minerals, may accumulate dissolved metal ions. A substantial literature exists regarding the sorbtion of metals by various solid phases.

Anomalous concentrations of metals in sediment samples may also occur by erosion of mineralized sediments into surface waters. Prior to excavation of the open-pit mine tailings from milling operations were subject to erosion and downslope transport into the stream. The construction of berms and settling areas below waste dumps, and the removal of mill tailings by pipeline to another area, have apparently minimized the potential for direct release of mining-related sediments to surface waters in the vicinity of the mine (SRK, 1995).

Few systematic studies of sediments have been conducted in the Red River watershed. The work performed by SRK (1995) was primarily aimed at characterizing the geochemistry of rocks within the mine property, although some rock samples and unconsolidated sediments from adjacent areas were studied. An effort was made to distinguish between rocks associated with natural scar areas and those associated with excavation of the open-pit mine. SRK's (1995) data indicate that, in general, both "types" of rock have the potential to generate ARD. This conclusion is supported by water-quality data (SRK, 1995, Table 1.2) showing that low pH and elevated levels of sulfate and dissolved metals characterize seep waters associated with both natural and mine-disturbed areas.

Geochemical analyses of stream sediments collected in the Red River (Figs. A13 and A14) are consistent with water-quality data which suggest that increased loading of Al, Mn, Co, Ni, and Zn occurs downstream from the mine area. Concentrations of these metals in stream sediments increase downstream from the mine, similar to corresponding changes in dissolved species in water samples. Similarly, sediment samples collected in traps in ERL contain elevated levels of these metals compared to samples collected in FL, upstream from the mine.

Differences During the Annual Cycle

Dissolved aluminum concentrations appear to be somewhat consistent throughout an annual cycle (Fig. A12), suggesting an approach to equilibrium between solid aluminum phases and dissolved aluminum species. Preliminary geochemical modeling of stream waters using MINTEQA2 (Allison et al., 1991) suggests that the predominant inorganic aluminum species present in the stream are $Al(OH)^-_4$, $Al(OH)^+_2$, and $Al(OH)^0_{3\ (aq)}$. These species, especially $Al(OH)^0_{3\ (aq)}$, form hydrous bridges with one another (oligomers) and flocculate in the water column at high concentrations. Model calculations indicate that the solid phases alunite, gibbsite, and $Al(OH)_{3\ (amorphous)}$ are over-saturated with respect to stream water at downstream localities during baseflow. The visible accumulations and clouding of stream waters observed downstream from the mine in winter suggests that elevated total aluminum concentrations in downstream reaches during baseflow conditions (e.g. Fig. 10) are primarily due to the presence of aluminum hydroxide-compounds, and not suspended clays.

Debris flow and other processes of mass wasting from natural scar areas result in the downslope transport of large quantities of sediment from these areas, and significant loading of particulate matter to the Red River has been observed as a result of rainfall events over scar areas (Smolka and Tague, 1989; Slifer, 1996). Sediments derived from scar areas are yellow-tan in color and can be traced considerable distances downstream as layers of sediment in impoundments along the Red River. Metal concentrations in these seasonally transported sediments appear to be comparatively low (Table A8).

Temporal Differences in Metal Loading: Historical Records in Pond Sediments

Sediment cores collected from impoundments along the Red River at Fawn Lakes, upstream from the mine, and at Eagle Rock lake, downstream from the mine, provide information about historical changes in metal loading associated with open-pit mining operations. The two impoundments receive water from the stream through gates and channels, and discharge through outlets to the stream. Suspended stream sediment constitutes the bulk of the material deposited in the ponds.

Aluminum and other metals are more abundant in the upper part of sediment cores collected from ERL than in lower portions of the cores (Figs. 11, A16, A17). This increase in aluminum and certain trace metals in ERL occurs in sediments deposited after the mid 1980s, based on counts of seasonal layers in the pond sequence. The increase in metal concentrations apparently occurred more than 20 years after the initial development of the open pit and the disposal of associated waste-rock in dumps around the periphery of the mine. The lag between the start of open-pit operations and the geochemical response, assuming a direct connection, suggests a finite reaction time for weathering and mobilization of metals in the waste rock, followed by groundwater transport to the Red River.

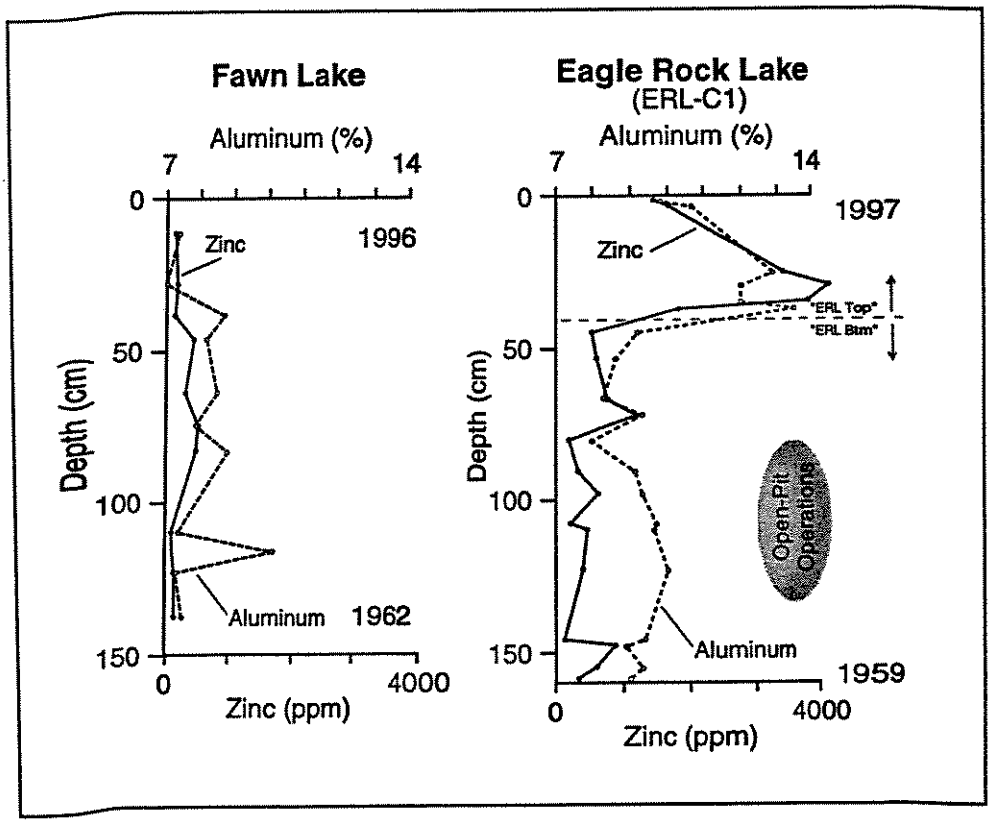

Figure 11. Profiles of aluminum and zinc concentration in Fawn Lake (FL) and Eagle Rock Lake (ERL) sediment cores. Note that Al and Zn concentrations increase markedly towards top of ERL sequence. Age of lower and upper sediment samples in each core, estimated from counts of seasonal layers, are indicated. Increased metal concentrations in ERL occur in sediments deposited after excavation of open-pit mine and emplacement of waste rock dumps. Mean metal concentrations for the ERL core, depicted in Fig. 12, represent samples collected from below (ERL Btm) and above (ERL Top) the dashed horizontal line shown on the ERL profile.

In comparison to ERL, concentration data for sediments from FL, located in an area impacted by drainage from natural alteration sc s, show no apparent vertical trends or increase over the time interval when metal loading apparently increased in ERL (Fig. 11, A18). Mean concentrations of metals in upper and lower parts of the cores, in conjunction with concentration data measured in the ponds with sediment-trap samples (Fig. 12), suggest that some of the increased loading in downstream reaches has occurred subsequent to disturbances associated with open-pit mining.

Alternative explanations for the concentration profiles from ERL include geochemical processes that might mobilize metals and concentrate them in the upper portion of the pond sequence, or upward increases in components such as organic carbon that are known to concentrate metals. For example, LOI values increase concomitantly

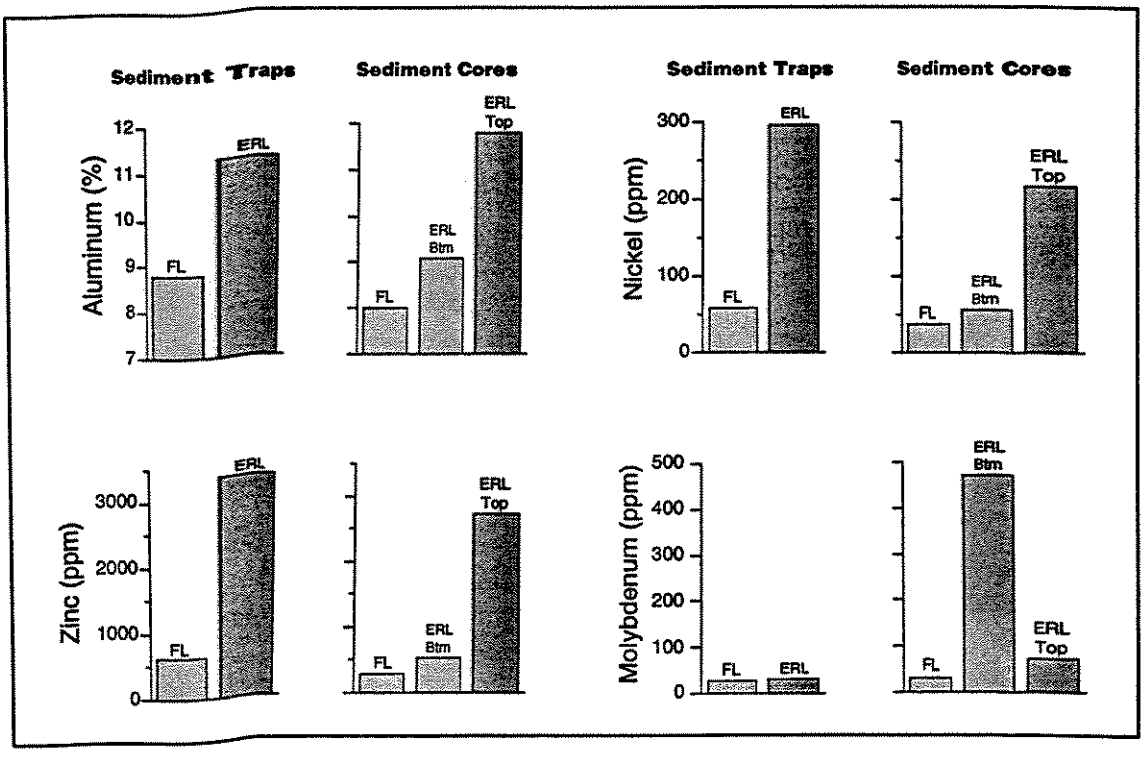

Figure 12. Mean concentrations of metals in sediment-trap samples and core samples from upper Fawn Lake (FL) and Eagle Rock Lake (ERL). ERL core samples are from core ERL-C1 (Fig. 5). Mean concentrations for ERL-C1 samples are from lower (older) portion of the sequence (ERL Btm, n = 14) and upper (younger) portion of the sediment sequence (ERL Top, n = 6). Sediment-trap samples were collected in 1997-98. See Table 3 for tabulation of mean concentration data. Concentrations of Al, Ni, and Zn have apparently increased several-fold in ERL sediments since excavation of the open-pit mine. Molybdenum concentration has decreased in ERL sediments, probably due to measures taken to prevent erosion of tailings and molybdenite-bearing sediments into the Red River.

with increases in trace-metal concentrations in ERL, suggesting that a greater abundance of organic compounds may be partly responsible for the increases. However, the higher LOI values also coincide with increases in aluminum concentration and the appearance of milky-colored, gelatinous layers in the pond sequence. Thus, some of the increase in LOI values towards the top of the ERL profiles is attributable to volatilization of water associated with aluminum-hydroxide compounds. A similar relationship between LOI values and aluminum concentration is exhibited by stream sediment samples (Fig. A14) and sediment-trap samples from ERL and FL (Table A5). If it is assumed that LOI values are due entirely to organic carbon, and that trace metals are strictly associated with organic carbon, then increases in some trace metals in ERL might be explained by relative increases in the abundance of organic compounds.

Mobilization of certain solid-phase metals, particularly manganese, might occur in the reducing environment within the sequence of pond sediments. Upward movement of mobilized metal species might occur by diffusion, and re-precipitation of mobile species might occur within the upper, oxygenated portion of the sediment sequence. Although this explanation for the concentration profiles in ERL might apply to some metals, it would not account for upward increases in aluminum, which is virtually unaffected by changes in oxidation potential. The fact that aluminum and other metals increase together, even though their geochemical behaviors are quite different, suggest that the core profiles from ERL reflect changes in the chemistry of sediments carried into the pond. Furthermore, form tion of authigenic sulfides within the pond sediments, if occurring, would tend to fix (ertain trace metals and minin ize mobilization and re-precipitation at some oxic-an xic boundary. Possible evid nce for redistribution in the ERL sequence is the spike in manganese concentration in core ERL-C1, at a depth of ~30 cm (Fig. A16).

Analytical results from older stream sediments collected beneath a fluvial terrace along the Red River (Fig. A15) suggest that observed increases in aluminum and certain trace metals in modern stream sediments downstream from the mine is a relatively recent trend. Geochemical data from terrace samples, however, represent a relatively limited number of samples (n = 9), and additional work will be needed to document downstream distributions of metals in such samples. Investigations of terrace samples are complicated by the occurrence of iron-stained and manganese-cemented sediments that occur at various levels above the modern channel of the Red River. Occurrences of metal oxyhydroxides in older alluvium represents discharge of low-pH solutions and chemical precipitation of compounds enriched in iron and manganese over undetermined periods of geologic time.

Metals in Tree Wood

Although analytical results of tree-wood samples appear to show some weak trends (Table A9), it is difficult to draw conclusions about possible changes in the chemistry of the Red River due to mining activity from these data. It may be that the relative enrichment of copper and zinc in wood collected at upstream localities is related to the proximity of the trees to the stream and water table, since the upstream samples (localities S10 and 03) were collected from trees rooted very close to stream level, and downstream samples were collected from trees rooted on a terrace above the stream. The relative enrichment of manganese and zinc in older wood collected at downstream localities is an interesting aspect of the trace-metal distributions in wood samples that may warrant further investigation.

Biologic Impacts of Mining Activity

Research conducted in recent years has demonstrated that much of stream ecosystem function takes place not in the water column or benthic zone but below the benthic zone in the hyporheic, a zone of active mixing of surface water and groundwater (Boulton et al., 1998). Several studies have indicated that hyporheic invertebrate communities are sensitive indicators of stream health and stream ecosystem integrity (e.g. Brunke and Gonser, 1997; Richter et al., 1998). Because flows within the hyporheic zone are necessarily interstitial, water velocities are relatively low compared to surface waters and oxygen levels are easily reduced by oxygen-demanding chemical reactions, especially biological activity. In addition, interstitial flows are sensitive to sedimentation by fine particles. These characteristics combine to make the hyporheic zone of streams simultaneously very important to overall stream ecosystem function and very vulnerable to many forms of pollution.

The patterns of hyporheic invertebrate diversity, abundance, and composition all indicate substantial negative impact of mining activities on the hyporheic portion of the Red River ecosystem. Hyporheic invertebrates were abundant and diverse at all localities upstream from mining activities and uncommon and species poor at all localities downstream from mining activities. The reduction of hyporheic invertebrate abundance and diversity are likely the result of reduced water circulation through the hyporheic due to sedimentation (Boulton et al., 1998), and may also reflect the presence of heavy metals, which have been shown to be toxic to stream invertebrates, particularly at low pH (e.g. Plenet et al., 1996; Gilbert et al., 1995).

The greatest diversity and population density occurs upstream from the reach adjacent to extensive natural mineralization and scars, and in Columbine Creek (Table A10, Fig. 8). Diversity and number of individuals remain high at upstream localities adjacent to natural scars and are significantly reduced below the area of mine seeps. The

specific conditions that have reduced and excluded sub-bottom invertebrates is unknown, but there is a strong suspicion that the aluminum-hydroxide precipitate is a major factor. This white aluminum-hydroxide compound coats the stream bottom in reaches downstream from the mine seeps, and during periods of low flow clouds the stream. None of this material was observed in the upstream sediment layers deposited in FL, but it appears consistently in sediments within the upper part of the ERL sequence.

CONCLUSIONS

Geochemical differences measured at localities along the Red River, selected to compare metal loadings in areas of natural exposures of mineralized rock (scars), and in areas of mining and waste-rock dumps, confirm the results of previous investigations, which indicate a significant increase in reaches of the stream adjacent to and below the mine area. Increases below the mine exceed the systematic trend of increasing concentration that begins upstream near the town of Red River and includes scar areas.

Metal concentrations in river water and stream sediments downstream from the mine are in some cases more than 5 times the values in the natural scar areas. Water-quality data from the Red River obtained by Woodward-Clyde (1996), collected at closely spaced localities, suggest that the increases in certain metals, including total aluminum and dissolved nickel and zinc, occurs about midway through the mine-disturbed area, downstream from areas receiving drainage from waste-rock dumps.

Increases in metal loading downstream from the mine area are recognizable in geochemical profiles obtained from pond sediments in Eagle Rock Lake. Significant increases in the concentrations of aluminum and certain trace metals apparently begin after the mid-1980s. Geochemical profiles from a similar pond in the scar area above the mine do not show a corresponding increase in metal concentrations. The apparent time lag between the initiation of open-pit operations and the appearance of increased metal loading suggests a finite reaction time by weathering and hydrologic processes after construction of waste-rock dumps.

Measurements of metal concentrations in terrace deposits collected downstream from the mine area show metal concentrations similar to those measured in the present stream channel upstream from mining operations in the vicinity of natural scar areas. Evidence for low-pH, metal-laden seeps are also present in older alluvial deposits as iron and manganese oxyhydroxide coating and cements. Measurements of metal concentrations in tree wood at localities near the stream do not appear to show a relationship to mineralization or mine activity.

A census of invertebrate organisms living beneath the stream bed reveals a spatial pattern of abundance and diversity that corresponds with metal concentration in

the river and metal loading of sediment, with reduced numbers and diversity of organisms found in the reach of high metal loading below the mine.

The appearance of aluminum-hydroxide layers late in the history of ERL, and more than a decade after exposure of mine-related waste-rock to weathering, indicates that the Red River has only recently begun to be affected by the mobilization of metals and other environmental changes related to open-pit mining activity. If this interpretation is correct, then high concentrations of aluminum and associated metals may continue indefinitely, into the future.

RECOMMENDATIONS

Excavation and dumping of sulfide-mineralized rocks adjacent to the Red River may be expected to change the chemistry of the stream, but the time required to induce change is unknown. Processes of chemical weathering leading to generation of ARD, and establishment of groundwater flowpaths with depleted capacities to buffer or attenuate low-pH solutions, could take years or decades to develop. This study has not attempted to identify a specific geometry, groundwater flow paths, concentrations, and rates, or the climatic factors which will ultimately determine the duration and magnitude of the effects of mining on the river system. We suggest that a program of detailed hydrologic investigation and modeling be initiated and that available information, including data obtained in this investigation, be used to design a long-term program of monitoring of the stream environment, with a final goal of remediation.

REFERENCES

Allison, J.D., Brown, D.S., Novo-Gradac, 1991, MINTEQA2/PRODEFA2, a geochemical assessment model for environmental systems: Version 3.0 user's manual: EPA/600/3-91/021.

Baes, C.F., III, and McLaughlin, S.B., 1984, Trace elements in tree rings: evidence of recent and historical air pollution: Science, v. 224, p. 494-497.

Boulton, A. J., Findlay, S., Marmonier, P., Stanley, E.H., and Valett, H.M., 1998, The functional significance of the hyporheic zone in streams and rivers: Annual Review of Ecology and Systematics, v. 29, p. 59-81.

Brunke, M., and Gonser, T., 1997, The ecological significance of exchange processes between rivers and groundwater: Freshwater Biology, v. 37, p. 1-33.

Gilbert, J., Marmonier, P., Vanek, V., and Plenet, S., 1995, Hydrological exchange and sediment characteristics in a riverbank: relationship between heavy-meatals and invertebrate community structure: Canadian Journal of Fisheries and Aquatic Sciences, v. 52, p. 2084-2097.

Govindaraju, K. (ed.), 1994, Geostandards Newsletter, Special Issue, v. 18, July, 158 p.

Jacobi, G.Z., and Smolka, L.R., 1984, Intensive survey of the Red River in the vicinity of the Red River and Questa wastewater treatment facilities and the Molycorp complex, Taos County, New Mexico, January 25-27, 1984: Santa Fe, New Mexico Environmental Improvement Division, Surface Water Quality Bureau, EID/SWQ-84/1, 29 p.

Jacobi, G.Z., and Smolka, L.R., 1986, Water quality survey of the Red River, Taos County, New Mexico, April 15-17, 1985: Santa Fe, New Mexico Environmental Improvement Division, Surface Water Quality Bureau, EID/SWQ-86/11, 63 p.

Kent, S., 1995, Expanded site inspection report on Molycorp, Inc., Questa Division, Taos County, New Mexico (investigation conducted under CERCLA authority): Santa Fe, New Mexico Environment Department, Groundwater Protection and Remediation Bureau- Superfund Program, 36 p. plus tables, figures, and attachments.

Latimer, S.D., Devall, M.S., Thomas, C., Ellgaard, E.G., Kumar, S.D., and Thien, L.B., 1996, Dendrochronology and heavy metal deposition in tree rings of baldcypress: Journal of Environmental Quality, v. 25, p. 1411-1419.

Lipman, P.W., and Reed, J.C., Jr., 1989, Geologic map of the Latir volcanic field and adjacent areas, northern New Mexico: U.S. Geological Survey, Miscellaneous Investigations Map I-1907, 1:48,000.

Plenet, S., Hugueny, H., and Gibert, J, 1996, Invertebrate community responses to physical and chemical factors at the river aquifer interaction zone. 2. Downstream from the city of Lyon: Archiv fur Hydrobiologie, v. 136, p. 65-88.

Richter, B. D., Baumgartner, J.V., Braun, D.P., and Powell, J., 1998, A spatial assessment of hydrologic alteration within a river network: Regulated Rivers-Research & Management, v. 14, p. 329-340.

Roberts, T.T., Parkison, G.A., and McLemore, V.T., 1990, Geology of the Red River District, Taos County, New Mexico: New Mexico Geological Society, Guidebook 41, p. 375-380.

Schilling, J.H., 1956, Geology of the Questa Molybdenum (Moly) mine area, Taos County, New Mexico: New Mexico Bureau of Mines and Mineral Resources, Bulletin 51, 87 p.

Slifer, D., 1996, Red River groundwater investigation (report prepared for USEPA, Region VI): Santa Fe, New Mexico Environment Department, Surface Water Quality Bureau, 79 p. plus figures, tables, appendices, and illustrations.

Smolka, L.R., 1992, Water quality survey of Fawn and Eagle Rock Lakes in Taos County, New Mexico, April 9 and 23-25, 1991, *in* Intensive water quality stream surveys and lake water quality assessment surveys, 1991: Santa Fe, New Mexico Environment Department, Surface Water Quality Bureau, NMED/SWQ-92/2, p. 165-178.

Smolka, L.R., 1993, Special water quality survey of the Red River, Taos County, New Mexico, February - December, 1992, *in* Intensive water quality stream surveys, 1991: Santa Fe, New Mexico Environment Department, Surface Water Quality Bureau, NMED/SWQ-93/1, p. 107-138.

Smolka, L.R., and Tague, D.F., 1987, Intensive survey of the Red River, Taos County, New Mexico, August 18-21, 1986: Santa Fe, New Mexico Environmental Improvement Division, Surface Water Quality Bureau, EID/SWQ-86/22, 55 p.

Smolka, L.R., and Tague, D.F., 1989, Intensive water quality survey of the middle Red River, Taos County, New Mexico, September 12 - October 25, 1988: Santa Fe, New Mexico Environmental Improvement Division, Surface Water Quality Bureau, EID/SWQ-88/8, 89 p.

SPRI, 1995, Progress report on the geology, hydrogeology, and water quality of the mine area, Molycorp facility, Taos County, New Mexico (report prepared for Molycorp, Inc.): Scottsdale, AZ, South Pass Resources, Inc., 19 p. plus appendices, figures, and tables.

SRK, 1995, Questa molybdenum mine geochemical assessment (report prepared for Molycorp Inc.): Lakewood, CO, Steffen Robertson and Kirsten (U.S.) Inc., 44 p. plus tables, figures and appendices.

USDHEW, 1966, A water quality survey, Red River of the Rio Grande, New Mexico: Ada, OK, U.S. Department of Health, Education, and Welfare, Federal Water Pollution Control Administration, variously paged.

USEPA, 1971, A water quality survey, Red River and Rio Grande, New Mexico: Ada, OK, U.S. Environmental Protection Agency, Region VI Surveillance and Analysis Division, 52 p.

USGS, 1988, Water Resources Data, New Mexico: U.S. Geological Survey, Water-Data Reports.

Vail, R.E., 1993, Interim study of the acidic drainage to the middle Red River, Taos County, New Mexico (report prepared for Molycorp, Inc.): Santa Fe, NM, Vail Engineering Inc., 53 p. plus appendices and figures.

Woodward-Clyde, 1996, Preliminary surface water analytical results for the Red River (data prepared for Molycorp, Inc.): Denver, Woodward-Clyde, data tables.

Wright, H.E., Jr., Mann, D.H., and Glaser, P.H., 1984, Piston corers for peat and lake sediments: Ecology, v. 65, p. 657-659.

APPENDIX I

Tabulated Analytical Results and Data Plots

Table A1. Analytical results, water-quality samples.

Location 01	Sample Date												
Constituent	06/10/97	07/17/97	08/14/97	09/18/97	10/23/97	11/20/97	12/19/97	01/14/98	02/20/98	03/19/98	04/30/98	06/04/98	07/16/98
Alk (as $CaCO_3$)	47.5	45.5	62.0	48.5	49.5	42.8	26.0	39.5	32.8	42.0	51.5	56.5	39.0
HCO_3 (mg/L)	57.9	55.5	75.6	59.1	60.4	52.1	31.7	48.2	39.9	51.2	62.8	68.9	47.5
pH (su)	7.44	7.62	7.76	7.55	7.62	7.60	7.18	7.47	7.15	7.57	7.78	7.71	7.71
T (deg C)	10.7	10.8	10.5	14.3	9.7	2.6	1	1	4.6	8.8	9.8	13.1	15.6
EC (umhos/cm)	40	132	50	95	99	234	477	400	60	268	80	178	45
DO (mg/L)	8.1	12.9	8.0	7.6	8.9	10.1	10.2	10.9	9.8	9.1	9.0	8.7	6.4
NFR (mg/L)	**	8	11	21	10	27	15	10	18	20	22	19	11
Eh (mV)	402	**	346	471	362	535	379	**	335	275	423	380	393
Discharge (cfs)*	283	53	43	22	19	9	9	17	12	16	54	137	57
F (mg/L)	0.3	0.7	0.7	0.8	0.8	0.7	3.1	1.6	1.0	0.7	0.5	0.3	0.7
Cl (mg/L)	1.1	2.0	2.3	3.2	2.9	4.4	4.2	4.5	4.7	5.5	5.2	1.2	2.6
NO_3 (mg/L)	0.8	0.4	0.9	1.4	0.8	1.2	2.5	2.3	2.6	1.3	1.7	**	0.3
SO_4 (mg/L)	34.9	70.8	83.6	126.1	109.2	112.6	177.1	140.9	166.3	135.6	68.9	36.8	67.4
Ca (mg/L)	23.1	35.3	39.7	49.8	47.1	47.5	65.3	51.5	56.2	55.8	30.4	23.9	32.4
K (mg/L)	0.9	1.3	1.2	1.3	1.2	1.2	1.4	1.3	1.2	1.2	0.9	0.6	0.9
Na (mg/L)	2.8	3.9	3.9	5.1	4.6	4.7	5.8	5.7	6.7	6.4	4.0	2.4	3.4
Mg (mg/L)	4.0	7.5	8.2	10.9	9.9	10.4	14.6	11.9	13.9	12.4	6.3	4.2	6.2
Fe (ug/L)	< 200	< 200	< 200	< 200	217	< 200	295	< 200	217	< 200	< 200	< 200	< 200
Fe tot (ug/L)		< 200			758			< 200			383		290
Mn (ug/L)	143	504	525	676	570	603	953	481	581	453	162	137	195
Mn tot (ug/L)		315			440			493			187		211
Ni (ug/L)	<2	7	16	27	17	16	37	39	59	32	10	6	4
Ni tot (ug/L)		11			15			17			11		9
Co (ug/L)	1	3	5	8	5	5	11	6	6	5	2	1	2
Co tot (ug/L)		3			4			5			2		1
Cu (ug/L)	1	1	<1	<1	<1	<1	<1	<1	<1	<1	14	2	2
Cu tot (ug/L)	<1	5			11			9			15		<1
Zn (ug/L)	30	78	197	180	64	72	413	233	288	181	25	38	37
Zn tot (ug/L)		75			97			114			74		54
Cd (ug/L)	<2	<2	<2	<2	<2	<2	<2	<2	<2	<2	<2	<2	<2
Cd tot (ug/L)	<2	<2			<2			<2			<2		<2
Al (ug/L)	340	230	250	230	190	200	<150	<150	<150	200	<150	260	270
AL tot (ug/L)		1000			2400			2100			1500		1100

* Mean daily discharge at USGS gage near Questa.
** Not measured.

Table A1, continued.

Location S2	Sample Date				
Constituent	08/14/97	11/20/97	02/20/98	04/30/98	07/16/98
Alk (mg/L $CaCO_3$)	55.7	58.0	50.3	54.0	51.1
HCO_3 (mg/L)	67.9	70.7	61.3	65.8	62.3
pH (su)	7.46	7.50	7.41	7.76	7.81
T (deg C)	16.1	1.8	5.9	5.0	17.0
EC (umhos/cm)	148	200	40	51	46
DO (mg/L)	6.2	9.5	9.7	9.3	7.7
NFR (mg/L)	**	26	7	18	6
Eh (mV)	416	553	391	377	371
Discharge (cfs)*	43	9	12	54	57
F (mg/L)	0.6	0.6	0.6	0.4	0.5
Cl (mg/L)	2.1	2.3	3.4	3.1	1.6
NO_3 (mg/L)	0.7	1.1	2.4	0.7	0.3
SO_4 (mg/L)	64.5	93.5	91.2	60.9	61.6
Ca (mg/L)	36.0	41.8	45.0	29.5	31.9
K (mg/L)	1.2	1.1	0.9	1.7	0.8
Na (mg/L)	4.2	4.4	5.6	4.7	3.2
Mg (mg/L)	7.4	8.8	10.8	6.0	6.0
Fe (mg/L)	<200	<200	<200	<200	<200
Fe tot (mg/L)				605	317
Mn (mg/L)	373	267	<100	<100	<100
Mn tot (mg/L)				<100	123
Nl (ug/L)	11	12	74	6	<2
Nl tot (ug/L)				10	<2
Co (ug/L)	3	2	5	1	1
Co tot (ug/L)				1	<1
Cu (ug/L)	<1	<1	<1	2	1
Cu tot (ug/L)				7	<1
Zn (ug/L)	37	34	139	26	34
Zn tot (ug/L)				37	45
Cd (ug/L)	<2	<2	29	<2	<2
Cd tot (ug/L)				<2	<2
Al (ug/L)	200	<150	<150	<150	500
AL tot (ug/L)				1000	100

Table A1, continued.

Location S3	Sample Date				
Constituent	08/14/97	11/20/97	02/20/98	04/30/98	07/16/98
Alk (mg/L $CaCO_3$)	66.5	59.8	68.8	53.0	61.0
HCO_3 (mg/L)	81.1	72.9	83.9	64.6	74.4
pH (su)	8.22	8.23	8.30	8.21	8.32
T (deg C)	11.6	3.0	2.0	1.9	11.8
EC (umhos/cm)	75	153	60	32	25
DO (mg/L)	7.5	10.0	10.7	12.9	7.6
NFR (mg/L)	**	3	2	4	<2
Eh (mV)	416	495	**	424	383
Discharge (cfs)*	43	9	12	54	57
F (mg/L)	0.2	0.3	0.4	0.3	0.2
Cl (mg/L)	0.8	0.4	1.3	0.5	0.1
NO_3 (mg/L)	0.4	0.6	1.7	0.5	0.4
SO_4 (mg/L)	6.5	7.8	10.6	6.8	6.7
Ca (mg/L)	24.7	26.1	23.6	19.3	23.2
K (mg/L)	0.9	0.9	0.6	0.7	0.6
Na (mg/L)	2.1	2.1	2.1	1.9	1.7
Mg (mg/L)	2.1	2.4	2.9	2.0	2.2
Fe (mg/L)	<200	<200	<200	<200	<200
Fe tot (mg/L)				<200	<200
Mn (mg/L)	<100	<100	<100	<100	<100
Mn tot (mg/L)				<100	<100
Ni (ug/L)	<2	<2	<2	<2	<2
Ni tot (ug/L)				<2	<2
Co (ug/L)	<1	<1	<1	<1	<1
Co tot (ug/L)				<1	<1
Cu (ug/L)	<1	<1	<1	<1	<1
Cu tot (ug/L)				<1	<1
Zn (ug/L)	<1	<1	<1	<1	<1
Zn tot (ug/L)				3	<1
Cd (ug/L)	<2	<2	<2	<2	<2
Cd tot (ug/L)				<2	<2
Al (ug/L)	<150	<150	<150	<150	<150
AL tot (ug/L)				200	200

Table A1, continued.

Location 02	Sample Date												
Constituent	06/10/97	07/17/97	08/14/97	09/18/97	10/23/97	11/20/97	12/19/97	01/14/98	02/20/98	03/19/98	04/30/98	06/04/98	07/16/98
Alk (mg/L $CaCO_3$)	60.5	55.5	60.0	58.5	54.7	62.5	45.0	55.8	42.0	57.0	50.0	58.5	54.3
HCO_3 (mg/L)	73.8	73.8	67.7	73.2	71.3	66.7	76.2	54.9	68.0	51.2	69.5	61.0	71.3
pH (su)	7.96	8.37	8.20	7.93	7.79	7.99	7.85	7.95	8.03	7.70	7.94	7.69	7.88
T (deg C)	12.7	12.8	13.4	15.9	6.7	3.0	1.4	1.5	3.0	1.9	10.1	11.9	15.4
EC (umhos/cm)	33	**	50	251	32	286	78	321	60	52	54	45	**
DO (mg/L)	9.3	8.3	7.7	7.5	9.0	9.9	10.3	10.6	10.0	10.2	8.2	9.5	6.3
NFR (mg/L)	**	4	8	17	10	36	8	8	6	15	28	17	11
Eh (mV)	371	**	400	485	390	499	421	**	356	354	394	390	423
Discharge (cfs)*	283	53	43	22	19	9	9	17	12	16	54	137	57
F (mg/L)	0.1	0.2	0.2	**	0.5	0.3	**	1.3	0.7	0.5	1.1	0.1	0.5
Cl (mg/L)	1.3	1.7	2.0	2.7	2.3	2.5	3.4	4.1	3.7	6.4	5.6	1.0	2.5
NO_3 (mg/L)	0.8	0.1	0.7	1.5	0.7	0.9	2.5	1.7	2.0	2.0	1.4	**	0.5
SO_4 (mg/L)	22.6	53.3	51.7	75.6	76.8	76.6	84.0	96.9	103.1	92.8	53.1	26.1	43.1
Ca (mg/L)	19.5	30.5	31.3	37.8	39.1	38.6	42.5	37.8	43.4	43.4	25.7	22.3	27.7
K (mg/L)	0.6	1.1	1.1	1.3	1.3	1.1	1.2	0.8	1.1	1.4	1.0	0.6	0.8
Na (mg/L)	2.3	3.6	3.8	4.8	4.4	4.5	5.2	4.4	6.3	7.2	4.4	2.3	3.4
Mg (mg/L)	3.3	5.7	5.9	7.7	10.8	8.2	10.1	9.4	12.2	10.6	5.9	4.0	5.3
Fe (ug/L)	<200	<200	<200	<200	<200	<200	<200	<200	<200	<200	<200	<200	<200
Fe tot (ug/L)					<200			2355			1046		802
Mn (ug/L)	<100	109	135	135	170	170	210	153	216	203	<100	<100	<100
Mn tot (ug/L)		<100			131			245			<100		<100
Ni (ug/L)	<2	3	5	7	9	18	10	10	16	13	7	2	<2
Ni tot (ug/L)		5			8			12			10		4
Co (ug/L)	<1	1	2	2	3	4	3	3	3	3	1	<1	1
Co tot (ug/L)		1			3			5			1		<1
Cu (ug/L)	<1	1	<1	<1	<1	<1	<1	<1	<1	<1	<1	<1	2
Cu tot (ug/L)		1			2			6			17		1
Zn (ug/L)	18	12	18	23	19	48	56	50	46	48	23	9	6
Zn tot (ug/L)		13			31			69			43		25
Cd (ug/L)	<2	<2	<2	<2	<2	<2	<2	<2	<2	<2	<2	<2	<2
Cd tot (ug/L)		<2			<2			<2			<2		<2
Al (ug/L)	<150	190	230	150	170	<150	<150	170	<150	<150	<150	<150	<150
AL tot (ug/L)		300			780			1600			1500		630

Table A1, continued.

Location 03	Sample Date												
Constituent	06/10/97	07/17/97	08/14/97	09/18/97	10/23/97	11/20/97	12/19/97	01/14/98	02/20/98	03/19/98	04/30/98	06/04/98	07/16/98
Alk (mg/L $CaCO_3$)	48.0	57.0	66.0	77.0	61.0	67.5	66.0	64.0	75.0	67.5	48.5	50.5	49.5
HCO_3 (mg/L)	58.5	69.5	80.5	93.9	74.4	82.3	80.5	78.0	91.4	82.3	59.1	61.6	60.4
pH (su)	7.57	7.74	7.88	7.74	7.74	7.78	7.48	7.51	7.76	7.81	7.84	7.90	7.62
T (deg C)	10.6	13.6	14.1	13.5	2.6	0.4	1.9	0.9	3.2	3.4	10.7	11.8	16.3
EC (umhos/cm)	20	19	43	171	49	266	49	285	30	39	40	28	38
DO (mg/L)	8.8	8.4	7.4	7.6	9.8	10.6	9.9	10.0	9.6	9.4	8.1	8.9	6.2
NFR (mg/L)	**	6	3	12	5	12	<2	7.00	3	27	16	15	10
Eh (mV)	383	**	358	474	319	395	379	**	325	248	371	495	404
Discharge (cfs)*	283	53	43	22	19	9	9	17	12	16	54	137	57
F (mg/L)	0.1	0.2	0.2	0.2	0.4	0.3	0.3	1.3	0.6	0.3	0.3	0.1	0.4
Cl (mg/L)	0.9	1.4	1.7	2.4	1.9	2.1	3.6	3.8	3.5	8.0	3.8	0.8	1.2
NO_3 (mg/L)	0.6	0.2	0.2	0.2	0.4	0.6	**	**	1.4	0.3	0.3	**	**
SO_4 (mg/L)	15.3	34.2	37.1	57.0	49.7	60.3	50.9	69.5	46.5	62.1	42.7	18.9	29.2
Ca (mg/L)	18.5	25.6	29.1	36.0	33.8	37.4	38.0	42.2	36.2	40.3	25.2	20.4	24.6
K (mg/L)	0.7	1.0	0.9	1.3	1.0	1.1	1.2	0.8	0.7	0.9	1.0	0.5	1.0
Na (mg/L)	2.0	2.8	3.1	4.0	3.9	4.3	3.9	4.4	5.1	7.5	4.1	1.8	2.3
Mg (mg/L)	3.1	4.5	7.0	6.5	6.7	7.6	7.9	8.6	8.5	9.8	5.1	3.0	4.4
Fe (ug/L)	<200	<200	<200	<200	<200	<200	<200	<200	<200	<200	<200	<200	<200
Fe tot (ug/L)		604			250			383			919		301
Mn (ug/L)	<100	150	<100	124	180	210	170	116	123	145	<100	<100	<100
Mn tot (ug/L)		<100			180			120			<100		<100
Ni (ug/L)	<2	<2	4	8	6	7	7	8	6	5	5	<2	<2
Ni tot (ug/L)		5			5			7			8		2
Co (ug/L)	<1	1	1	2	1	2	2	2	2	2	1	<1	<1
Co tot (ug/L)		2			1			1			1		<1
Cu (ug/L)	<1	5	<1	<1	<1	<1	<1	<1	<1	<1	<1	<1	1
Cu tot (ug/L)		5			3			10			15		<1
Zn (ug/L)	2	31	16	42	18	19	39	38	37	39	24	2	4
Zn tot (ug/L)		49			23			55			30		11
Cd (ug/L)	<2	<2	<2	<2	<2	<2	<2	2	<2	<2	<2	<2	<2
Cd tot (ug/L)		<2			<2			<2			<2		<2
Al (ug/L)	150	<150	<150	<150	170	<150	<150	<150	<150	<150	<150	<150	150
AL tot (ug/L)		450			250			350			1200		350

Table A1, continued.

Location S10	Sample Date				
Constituent	09/18/97	11/20/97	02/20/98	04/30/98	07/16/98
Alk (mg/L $CaCO_3$)	84.5	84.0	91.5	77.5	56.5
HCO_3 (mg/L)	103.0	102.4	111.6	94.5	68.9
pH (su)	8.36	8.33	8.15	8.67	8.56
T (deg C)	14.2	0.1	0.3	7.6	10.8
EC (umhos/cm)	85	205	30	48	32
DO (mg/L)	7.6	10.4	10.3	9.3	8.7
NFR (mg/L)	4	5	<2	8	4
Eh (mV)	531	432	400	404	411
Discharge (cfs)*	22	9	12	54	57
F (mg/L)	**	0.2	0.1	0.1	0.0
Cl (mg/L)	1.2	1.2	1.1	2.1	0.5
NO_3 (mg/L)	0.1	0.6	0.7	0.3	0.1
SO_4 (mg/L)	14.1	13.8	12.1	10.5	13.0
Ca (mg/L)	32.3	33.6	29.9	22.9	22.0
K (mg/L)	0.9	0.7	0.7	0.6	0.5
Na (mg/L)	2.5	2.9	3.3	2.7	1.6
Mg (mg/L)	3.9	4.4	5.5	3.9	3.2
Fe (mg/L)	<200	<200	<200	<200	<200
Fe tot (mg/L)				<200	<200
Mn (mg/L)	<100	<100	<100	<100	<100
Mn tot (mg/L)				<100	<100
Ni (ug/L)	<2	<2	<2	<2	<2
Ni tot (ug/L)				2	2
Co (ug/L)	<1	<1	<1	<1	<1
Co tot (ug/L)				<1	<1
Cu (ug/L)	<1	<1	<1	<1	<1
Cu tot (ug/L)				<1	<1
Zn (ug/L)	<1	<1	<1	<1	<1
Zn tot (ug/L)				2	<1
Cd (ug/L)	<2	<2	<2	<2	<2
Cd tot (ug/L)				<2	<2
Al (ug/L)	<150	<150	<150	<150	<150
AL tot (ug/L)				400	150

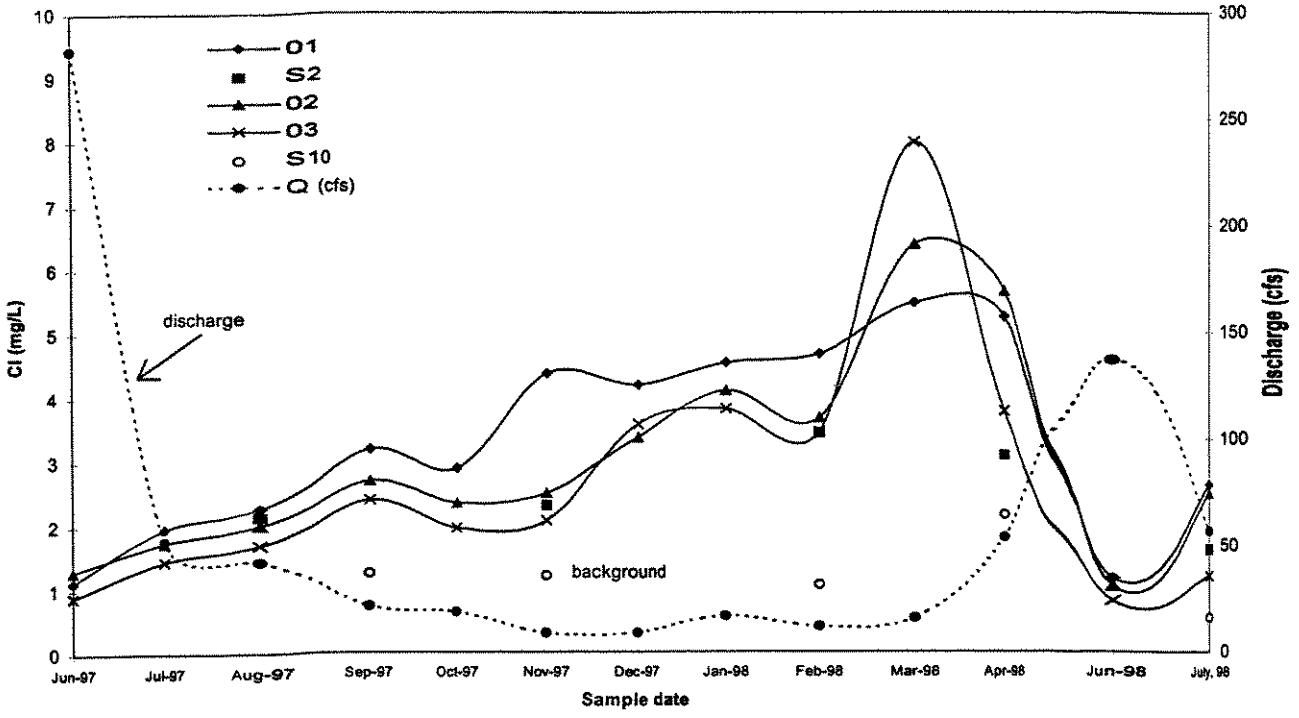

Figure A1. Cl and stream discharge (at the USGS gage near Questa) in the Red River during an annual cycle.

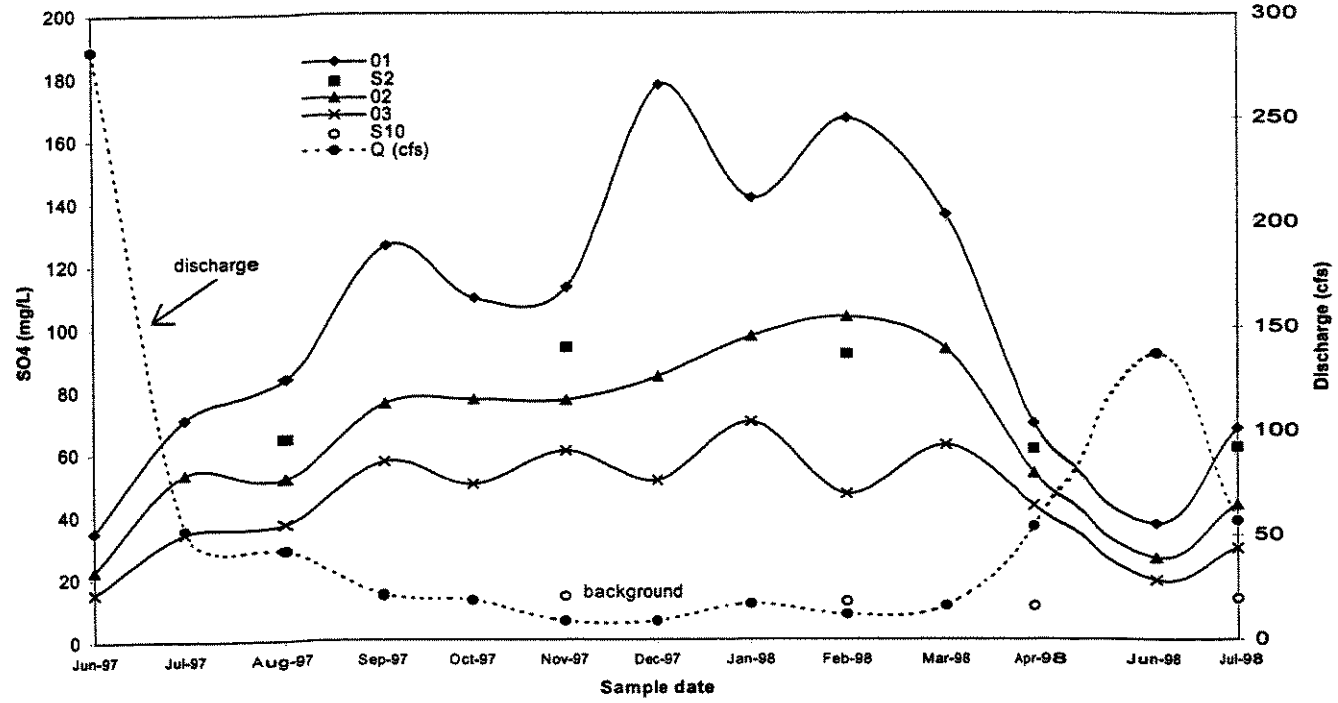

Figure A2. SO4 and stream discharge (at the USGS gage near Questa) in the Red River during an annual cycle.

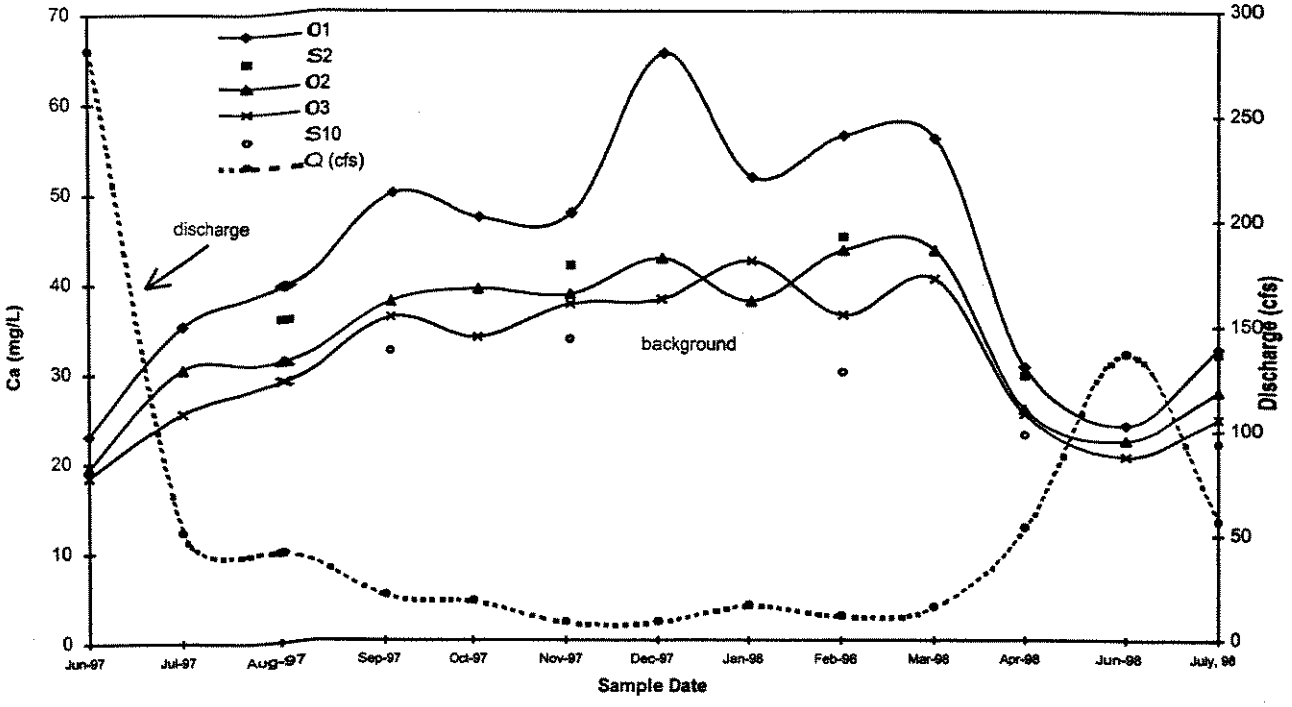

Figure A3. Ca and stream discharge (at the USGS gage near Questa) in the Red River during an annual cycle.

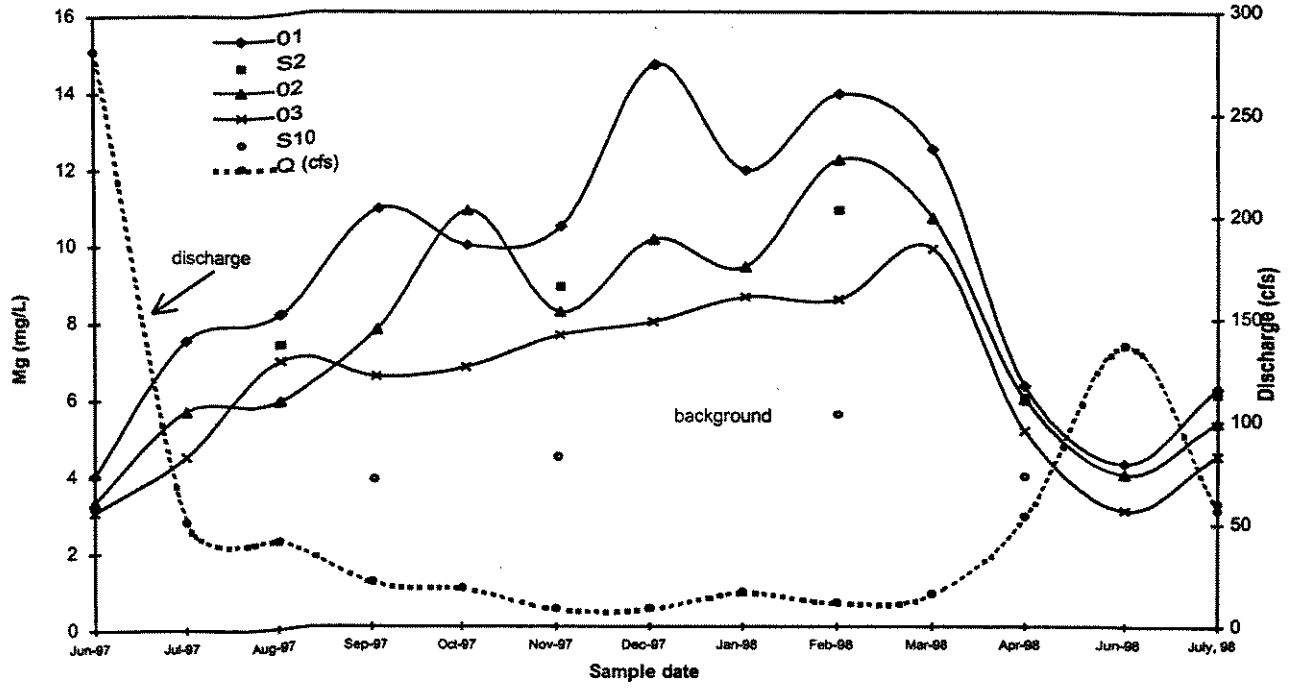

Figure A4. Mg and stream discharge (at the USGS gage near Questa) in the Red River during an annual cycle.

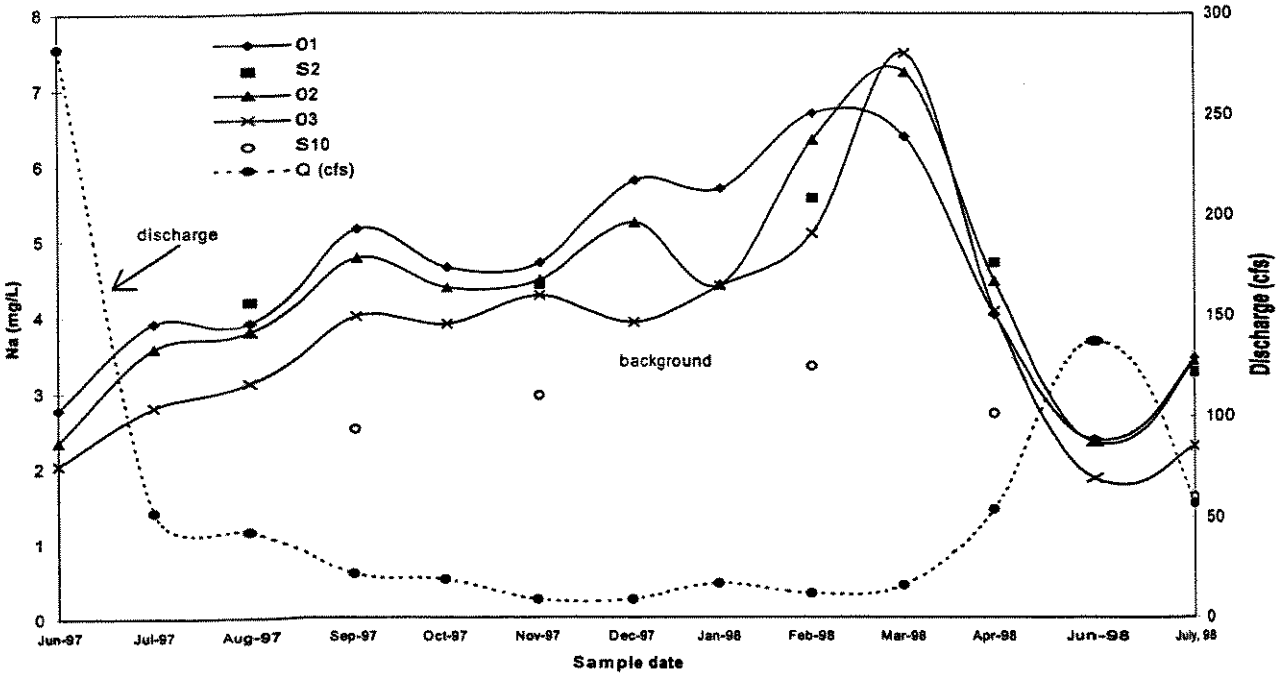

Figure A5. Na and stream discharge (at the USGS gage near Questa) in the Red River during an annual cycle.

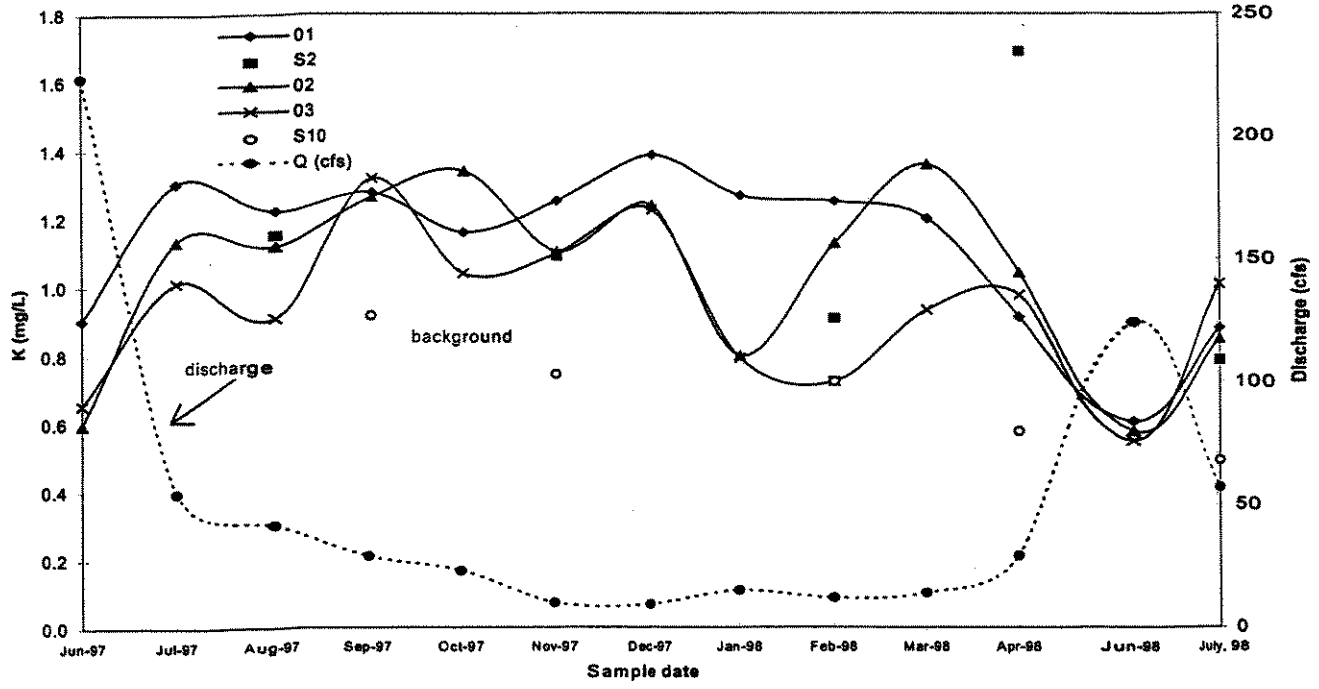

Figure A6. K and stream discharge (at the USGS gage near Questa) in the Red River during an annual cycle.

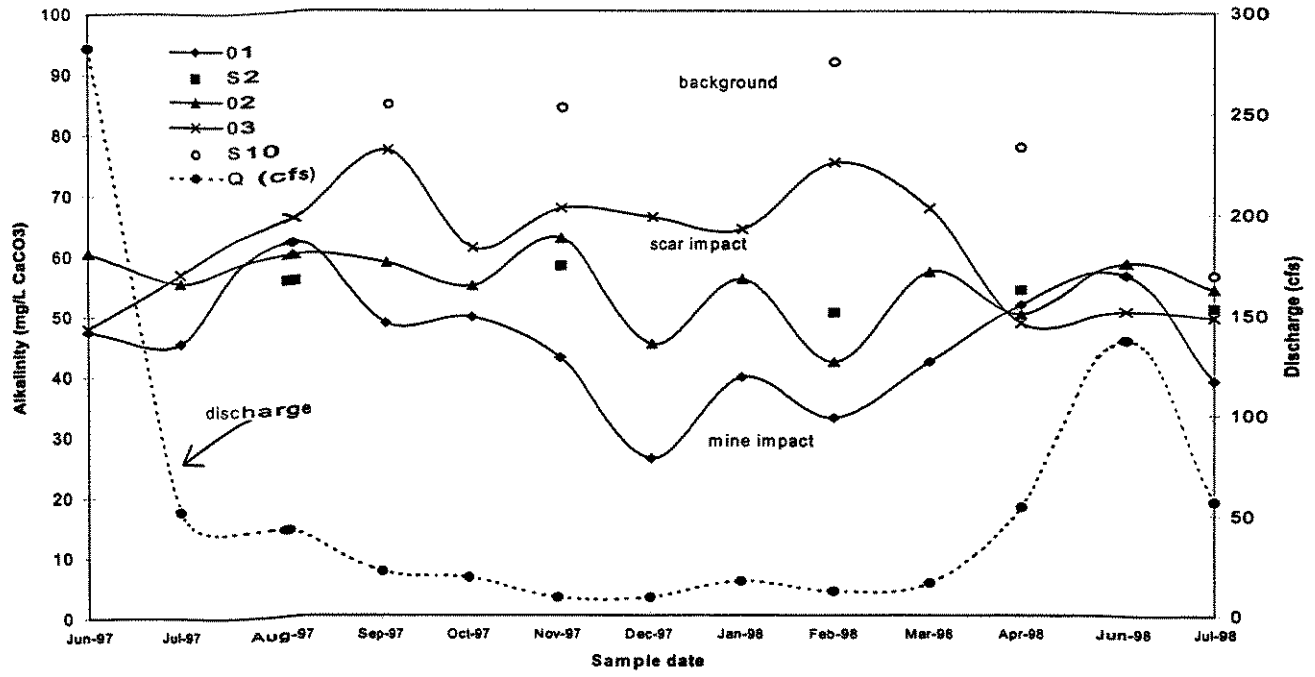

Figure A7. Alkalinity and stream discharge (at the USGS gage near Questa) in the Red River during an annual cycle.

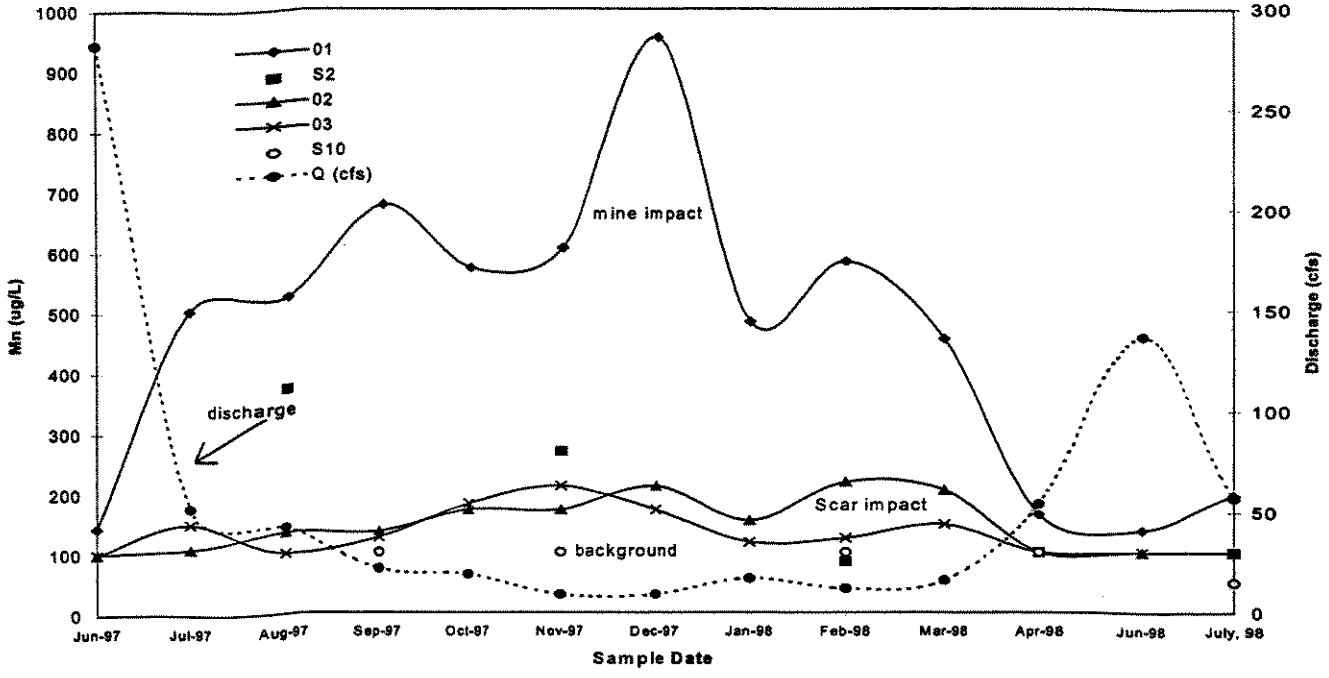

Figure A8. Mn and stream discharge (at the USGS gage near Questa) in the Red River during an annual cycle.

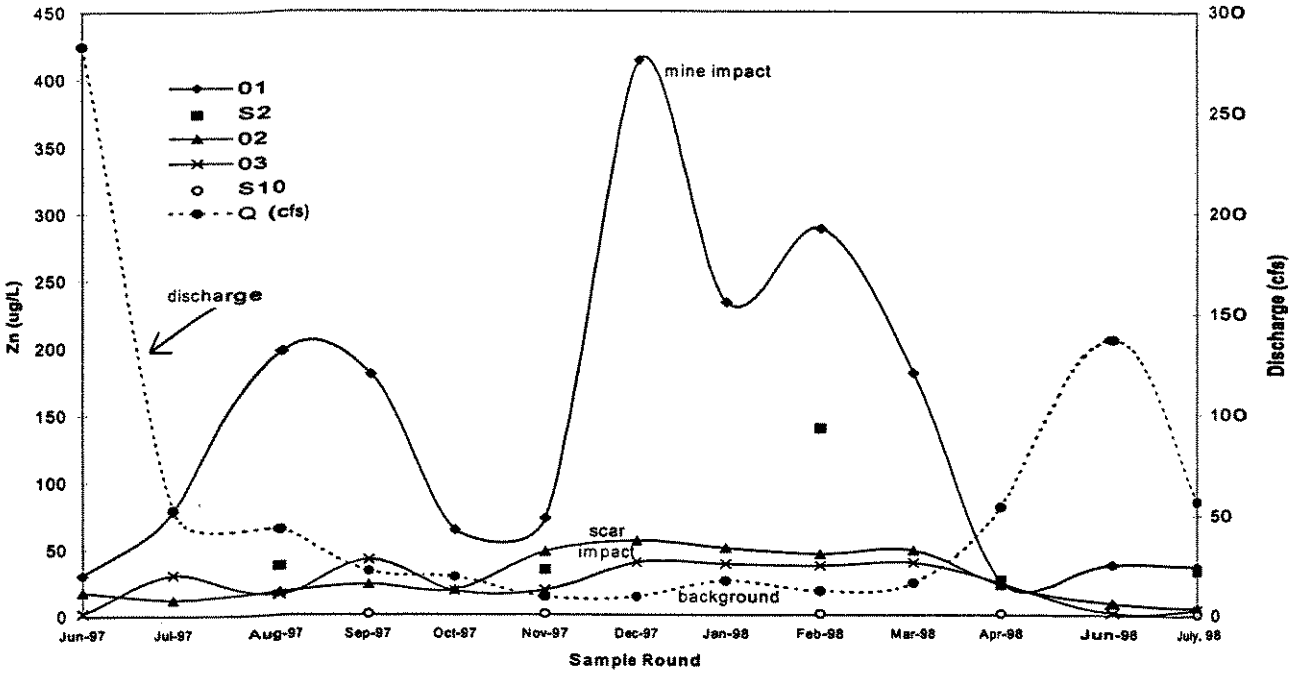

Figure A9. Zn and stream discharge (at the USGS gage near Questa) in the Red River during an annual cycle.

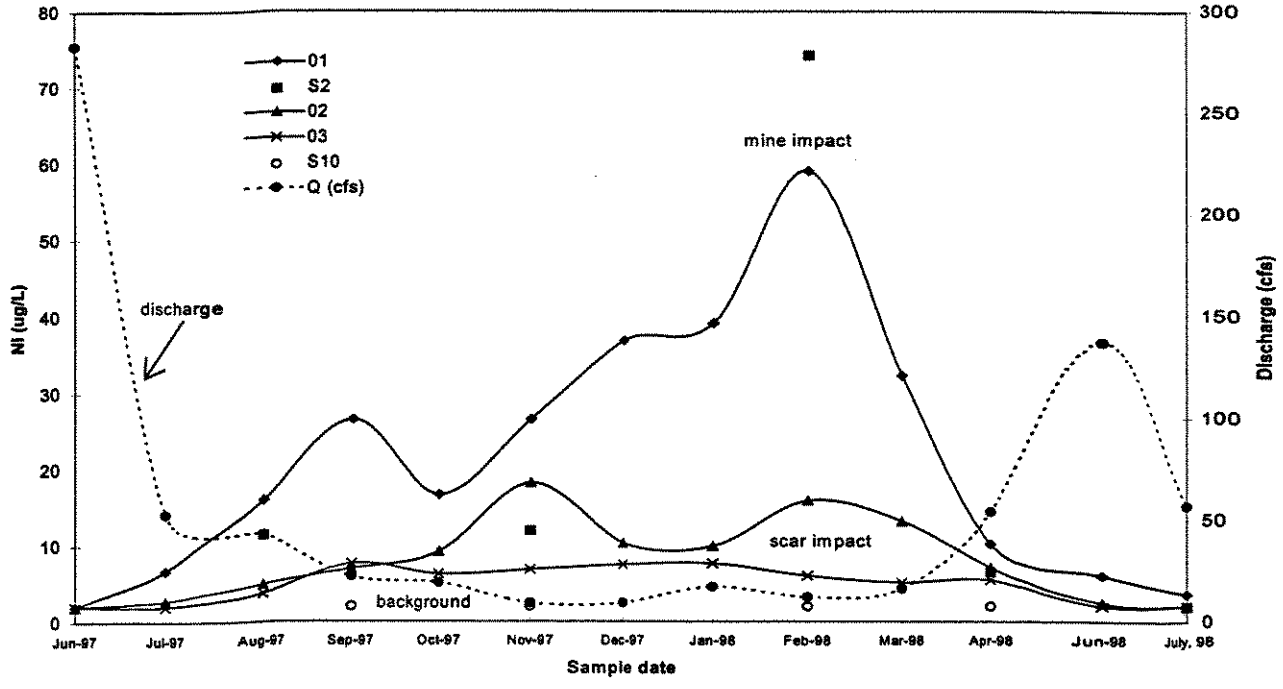

Figure A10. Ni and stream discharge (at the USGS gage near Questa) in the Red River during an annual cycle.

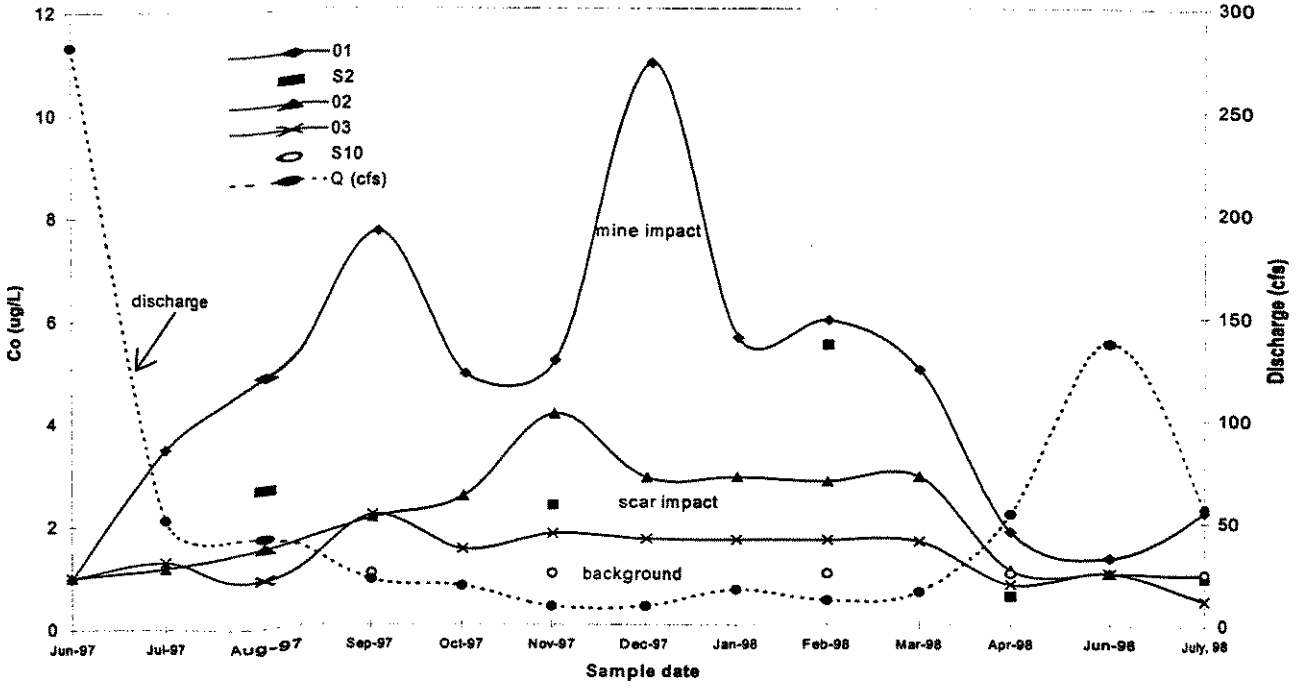

Figure A11. Co and stream discharge (at the USGS gage near Questa) in the Red River during an annual cycle.

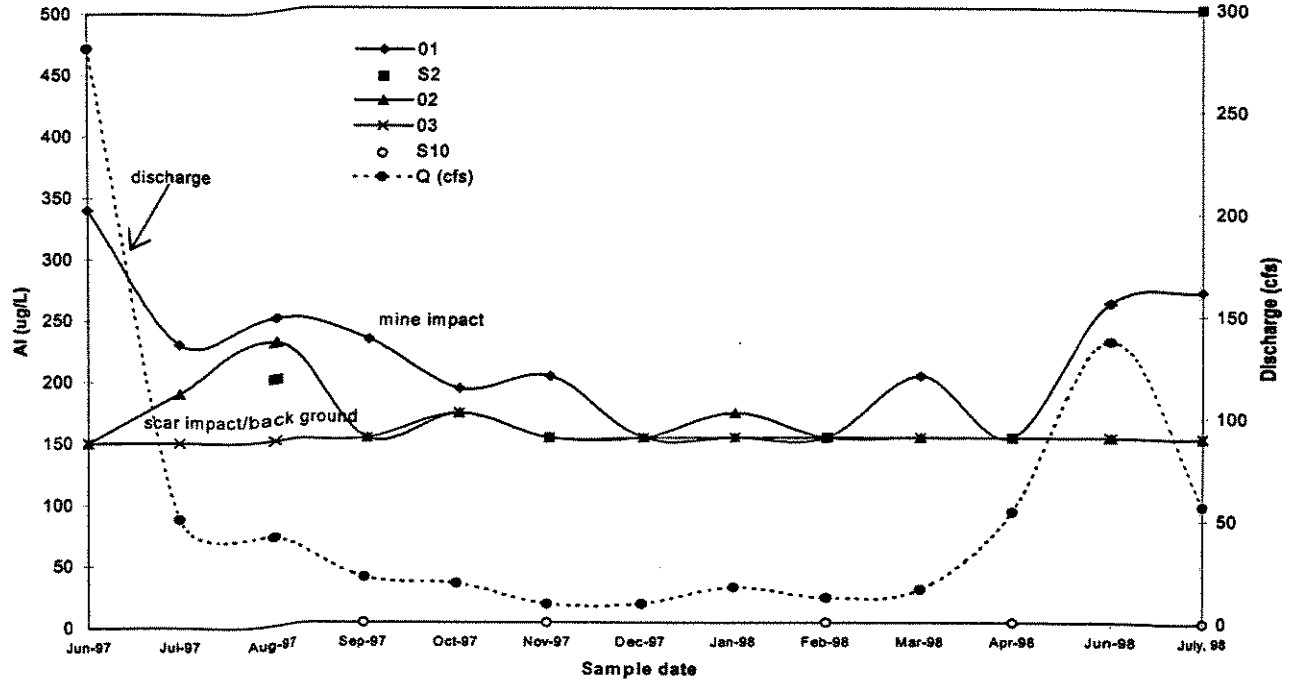

Figure A12. Al and stream discharge (at the USGS gage near Questa) in the Red River during an annual cycle.

Table A2. Analytical results, Red River grab samples.

		Concentration in dry sediment sample*								
Sample ID	Date	Al %	Fe %	Mn ppm	Co ppm	Cu ppm	Mo ppm	Ni ppm	Zn ppm	LOI 500 C %
S10-SCG-1	2/21/98	6.7	5.6	920	15	30	10	20	130	4.1
S10-SCG-1	7/16/98	7.1	4.2	1050	20	40	10	20	100	5.2
S10-SCG-1	10/22/98	6.4	4.3	970	20	35	10	25	110	3.6
03-SCG-1	2/21/98	7.0	3.3	720	20	145	20	25	260	3.1
03-SCG-1	7/16/98	6.8	5.1	830	15	125	25	25	220	3.7
03-SCG-1	10/22/98	7.2	3.7	780	15	160	20	30	310	3.7
02-SCG-1	2/21/98	6.8	3.4	700	20	80	15	35	310	2.4
02-SCG-2	2/21/98	6.7	3.7	570	15	60	10	20	220	2.3
02-SCG-1	7/[illegible]	6.9	4.4	490	15	140	30	15	150	2.2
02-SCG-2	7/16/98	6.9	4.4	560	15	140	35	20	170	2.1
02-SCG-1	10/22/98	6.9	3.6	600	15	75	20	25	210	1.8
S2-SCG-1	2/21/98	6.8	4.0	1550	25	115	30	50	520	2.5
S2-SCG-1	7/16/98	7.1	3.8	1150	25	135	30	45	450	4.7
S1-SCG-1	2/21/98	8.2	4.9	450	15	160	35	25	210	5.4
S1-SCG-2	2/21/98	10.3	5.4	880	20	250	35	35	330	8.6
S1-SCG-1	7/16/98	6.9	5.0	380	10	130	45	25	180	3.5
S1-SCG-1	10/22/98	6.8	4.7	400	10	95	30	20	140	2.7
01-SCG-1	2/21/98	8.3	3.8	4150	60	280	45	110	1250	4.9
01-SCG-1	7/16/98	7.1	3.6	1600	25	130	30	60	570	2.6
01-SCG-2	7/16/98	8.1	4.5	820	20	185	45	40	430	6.3
01-SCG-1	10/22/98	8.4	3.9	3750	60	285	35	130	1350	5.6
01-SCG-2	10/22/98	7.6	4.1	2400	40	210	35	100	990	4.4

* Bold values- Actual concentration is less than shown.

Table A3. Analytical results, Red River sediment-trap samples.

		Concentration in dry sediment sample*								
Sample ID	Date	Al %	Fe %	Mn ppm	Co ppm	Cu ppm	Mo ppm	Ni ppm	Zn ppm	LOI 500 C %
03-ST-3	8/14/97	6.3	3.8	730	25	175	10	35	410	8.2
03-ST-2	10/24/97	7.0	4.2	1000	25	260	10	50	530	6.4
03-ST-3	10/23/97	5.8	3.9	900	25	245	15	40	[illegible]	5.9
03-ST-1+3	12/19/97	7.2	4.1	1050	25	355	20	40	570	6.4
03-ST-1+3	1/14/98	7.4	3.8	1000	25	310	15	40	480	4.9
03-ST-1+3	2/20/98	7.1	4.1	1100	25	425	20	45	580	7.2
03-ST-1	4/29/98	7.3	4.0	830	25	255	15	35	430	5.3
02-ST-2 (13-23 cm)	8/15/97	6.7	2.6	560	20	75	**10**	30	270	3.8
02-ST-2 (7-14 cm)	10/23/97	6.4	3.5	330	**10**	40	**10**	20	120	1.9
02-ST-2	12/19/97	6.3	3.2	750	20	85	10	30	340	2.9
02-ST-3	12/19/97	6.9	3.4	870	20	110	15	35	420	3.1
02-ST-2	1/14/98	7.2	3.3	970	25	105	20	45	400	3.2
02-ST-3	1/14/98	6.5	3.3	1050	25	125	15	40	440	3.6
02-ST-1	2/20/98	7.3	3.4	1100	25	140	15	45	440	4.3
02-ST-1	4/29/98	7.3	3.4	1200	30	185	25	50	630	6.4
S2-ST-1	2/20/98	8.1	3.9	1950	35	240	40	70	810	6.8
01-ST-1 (8-15 cm)	8/15/97	7.6	3.3	1400	35	165	40	110	900	7.9
01-ST-2 (6-10 cm)	10/23/97	8.7	4.3	1500	35	270	40	75	1100	8.3
01-ST-1+2	12/19/97	8.9	3.5	2950	50	480	45	90	1300	9.3
01-ST-3	1/14/98	9.0	3.5	2700	45	375	45	75	1050	6.1
01-ST-2	2/20/98	10.2	3.7	3700	60	540	45	100	1450	11.2
01-ST-3	2/20/98	10.3	3.7	3700	65	535	45	110	1450	11.1
01-ST-2	4/29/98	8.4	3.6	2700	55	340	50	100	1200	10.2
01-ST-3	4/29/98	7.8	3.8	2900	50	320	55	90	1100	11.6
S3-ST-1+2+3	2/20/98	4.6	2.6	710	**10**	60	15	**15**	210	37.6

* Bold values- Actual concentration is less than shown.

Table A4. Analytical results, Red River terrace samples.

		Concentration in dry sediment sample*								
Sample ID	Date	Al %	Fe %	Mn ppm	Co ppm	Cu ppm	Mo ppm	Ni ppm	Zn ppm	LOI 500 C %
02-FT-1	9/19/97	7.0	3.7	490	15	105	**10**	35	480	5.9
02-FT-2	9/19/97	6.5	3.4	1650	20	110	**10**	35	280	6.7
02-FT-3	9/19/97	7.0	3.7	560	10	115	10	20	150	2.5
S2-FT-1	7/16/98	6.9	4.6	1000	20	105	440	35	130	4.4
S1-FT-2	7/16/98	6.8	3.1	450	15	70	65	30	220	7.6
S1-FT-3	7/16/98	6.0	2.9	380	10	55	60	**15**	120	7.9
S1-FT-1	10/22/98	6.8	3.2	380	**10**	100	420	**15**	85	2.0
01-FT-1	10/23/97	5.9	2.6	340	25	115	35	130	330	26.6
01-FT-1	7/16/98	6.5	3.3	420	10	70	35	**15**	100	2.0
01-FT-2	7/16/98	6.4	3.1	400	**10**	60	30	15	95	1.9

* Bold values- Actual concentration is less than shown.

Table A5. Analytical results, Eagle Rock and Fawn Lakes sediment-trap samples.

		Concentration in dry sediment sample*								
Sample ID	Date	Al %	Fe %	Mn ppm	Co ppm	Cu ppm	Mo ppm	Ni ppm	Zn ppm	LOI 500 C %
ERL-ST1 (3-4.5 cm)	9/18/97	10.8	4.3	11300	100	485	30	300	3150	14.3
ERL-ST1 (4.5-8 cm)	9/18/97	11.5	4.5	13700	110	470	30	310	3150	13.5
ERL-ST2	9/18/97	10.9	4.2	12000	110	505	30	280	3200	15.3
ERL-ST1 (1.5-6 cm)	6/4/98	11.9	5.3	8800	80	425	35	230	2600	12.3
ERL-ST1 (6-11 cm)	6/4/98	12.4	4.1	13900	125	685	30	330	4000	16.6
ERL-ST1 (11-14 cm)	6/4/98	11.1	4.1	12300	120	625	30	330	3750	17.8
ERL-ST1 (14-19 cm)	6/4/98	10.8	4.4	11500	115	585	30	290	3550	16.0
ERL-ST2	6/4/98	11.2	4.4	12700	125	605	30	300	3600	14.7
FL-ST (1.5-8 cm)	9/18/97	7.4	4.4	1400	30	205	25	60	570	13.5
FL-ST (8-17 cm)	9/18/97	9.0	4.5	1350	**30**	140	**20**	40	390	8.6
FL-ST (2-8 cm)	6/4/98	9.6	5.5	2100	40	315	35	70	860	9.8
FL-ST (8-12 cm)	6/4/98	9.1	5.1	1800	**30**	270	30	65	680	11.3

* Bold values- Actual concentration is less than shown.

Table A6. Analytical results, Eagle Rock and Fawn Lakes sediment cores.

Sample ID	Depth (cm)*	Concentration in dry sediment sample** Al	Fe	Mn	Co	Cu	Mo	Ni	Zn	LOI 500 C
		%	%	ppm	ppm	ppm	ppm	ppm	ppm	%
ERL-C1-O1	158.6	9.0	4.6	510	35	180	200	55	340	6.09
ERL-C1-O2	154.9	9.3	4.6	540	35	240	500	75	640	6.8
ERL-C1-O3	148.1	8.9	5.1	520	60	305	2900	110	900	7.9
ERL-C1-O4	145.7	9.4	7.0	670	**30**	210	390	40	130	5.0
ERL-C1-O5	123.0	10.0	5.5	900	**30**	200	210	50	410	6.35
ERL-C1-O6	109.9	9.6	6.6	1500	**30**	195	360	45	470	6.5
ERL-C1-O7	107.8	9.7	7.2	740	**30**	260	55	25	230	5.4
ERL-C1-O8	98.4	9.3	5.5	940	**30**	325	860	65	650	7.4
ERL-C1-O9	90.5	9.1	5.6	1100	**30**	220	630	35	360	5.4
ERL-C1-O10	80.5	8.0	4.2	640	**30**	130	70	35	220	5.29
ERL-C1-O11	71.8	9.3	5.4	1000	40	390	220	85	1200	8.6
ERL-C1-O12	66.5	8.3	6.0	830	35	270	100	75	800	8.7
ERL-C1-O13	53.3	8.6	4.8	760	**30**	240	60	45	620	6.5
ERL-C1-O14	44.9	9.2	4.8	850	**30**	215	80	45	550	5.9
ERL-C1-O15	37.5	13.5	4.9	1400	40	645	110	85	1850	12.92
ERL-C1-O16	34.6	12.0	5.4	3750	140	625	100	360	3850	13.9
ERL-C1-O17	29.2	12.0	5.0	20500	150	610	65	390	4150	16.30
ERL-C1-O18	25.4	12.9	5.4	870	95	570	85	220	3400	11.8
ERL-C1-O20	3.5	10.7	5.1	2600	40	320	35	130	1700	13.3
ERL-C1-O21	1.6	9.8	4.4	2100	45	370	35	110	1450	11.1

* Depth to center of sample interval.

** Bold values- Actual concentration is less than shown.

Table A6, continued.

Sample ID	Depth (cm)*	Concentration in dry sediment sample** Al	Fe	Mn	Co	Cu	Mo	Ni	Zn	LOI 500 C
		%	%	ppm	ppm	ppm	ppm	ppm	ppm	%
ERL-C2-O1	65.1	9.1	4.4	1100	30	235	40	75	670	7.2
ERL-C2-O2	61.0	9.4	4.6	1100	45	275	55	95	860	7.7
ERL-C2-O3	51.4	8.2	4.8	820	30	65	30	35	310	8.2
ERL-C2-O4	47.6	9.4	6.0	940	30	255	180	65	610	7.2
ERL-C2-O5	41.0	8.9	6.1	970	45	340	480	130	1020	10.3
ERL-C2-O6	40.6	9.2	6.0	740	65	345	150	160	1350	11.5
ERL-C2-O7	38.1	11.3	6.0	560	70	485	120	130	2200	13.5
ERL-C2-O8	34.1	11.2	4.3	590	65	440	45	150	1900	9.1
ERL-C2-O9	31.0	14.7	4.6	700	70	890	100	210	3250	16.0
ERL-C2-O10	29.4	13.8	5.3	720	105	855	80	250	3950	17.1
ERL-C2-O11	25.9	14.7	3.9	1050	125	815	75	340	4100	17.9
ERL-C2-O12	3.81	11.8	4.9	1650	60	495	35	160	2450	nd

Sample ID	Depth (cm)*	Concentration in dry sediment sample** Al	Fe	Mn	Co	Cu	Mo	Ni	Zn	LOI 500 C
		%	%	ppm	ppm	ppm	ppm	ppm	ppm	%
FL-C2-O1	137.8	7.5	4.4	480	30	125	20	30	170	8.4
FL-C2-O2	123.0	7.3	5.1	520	30	115	30	30	170	7.6
FL-C2-O3	116.2	10.1	5.3	490	30	95	25	25	150	4.9
FL-C2-O4	109.7	7.4	4.3	420	30	95	35	30	140	7.06
FL-C2-O5	83.2	8.8	6.0	950	30	185	45	65	530	7.5
FL-C2-O6	74.6	7.9	5.2	650	35	205	30	60	560	7.4
FL-C2-O7	64.1	8.5	5.4	590	30	190	60	40	350	7.4
FL-C2-O8	46.2	8.2	4.7	590	30	210	30	50	480	8.0
FL-C2-O9	38.6	8.7	7.4	670	30	215	35	25	180	5.9
FL-C2-O10	27.9	7.0	4.3	670	30	115	20	30	220	9.0
FL-C2-O11	11.6	7.4	3.5	510	30	100	20	25	190	3.85

Table A7. Analytical results, Fe-Mn-Al crusts, cements, etc.

		Concentration in dry sediment sample*								
		Al	Fe	Mn	Co	Cu	Mo	Ni	Zn	LOI 500 C
Sample ID	Date	%	%	ppm	ppm	ppm	ppm	ppm	ppm	%
IRON-ENRICHED CRUSTS AND CEMENTS										
CC-FC-1	6/4/98	0.5	48.1	30	**10**	110	**10**	**15**	30	16.6
HC-FC-1 (Crust)	6/4/98	2.2	40.7	40	**10**	25	15	**15**	35	14.4
HC-FC-1 (Cement)	6/4/98	5.6	17.5	40	**10**	45	**10**	20	75	5.4
MANGANESE/IRON-ENRICHED CRUSTS AND CEMENTS										
S1-FT-1	7/16/98	6.2	7.7	17900	55	120	450	110	280	3.8
01-FT-2	10/23/97	9.2	4.4	69500	1750	580	470	310	2400	7.0
01-FT-3	7/16/98	8.4	4.7	84800	2000	475	780	300	1750	4.3
S2U-FT-1	7/16/98	22.3	2.0	64500	3950	3280	550	2650	2650	18.8
ALUMINUM-ENRICHED CHEMICAL PRECIPITATES										
Red River										
WS-Al-1	8/15/97	24.1	0.2	95	15	200	35	**15**	120	28.4
S1-Al-1	10/23/98	18.7	2.7	90	**10**	1330	20	20	970	27.8
pond cores	Depth (cm)									
ERL-C1-Al1	21.3	20.9	2.5	300	**30**	1210	50	35	1100	14.4
ERL-C1-Al2	17.3	13.6	3.9	500	**30**	585	55	55	1300	10.8
ERL-C2-Al1	16.2	19.5	3.6	360	**30**	985	70	45	1050	18.5
ERL-C2-Al2	7.6	16.2	3.3	370	20	970	65	45	1000	15.0

*** Bold values- Actual concentration is less than shown.**

Table A8. Analytical results, sediments associated with scar areas.

Sample ID	Date	Concentration in dry sediment sample* Al %	Fe %	Mn ppm	Co ppm	Cu ppm	Mo ppm	Ni ppm	Zn ppm	LOI 500 C %
ALLUVIUM										
HC-C-1	6/4/98	7.0	10.3	310	**10**	25	15	**15**	50	5.5
HC-C-2	6/4/98	9.1	3.9	180	**10**	55	20	**15**	55	2.9
HC-C-3	6/4/98	7.8	4.0	220	**10**	30	10	**15**	60	2.8
03-C-1	7/16/98	8.5	4.1	120	**10**	25	25	**15**	35	4.0
GHG-C-1	7/16/98	6.9	5.1	240	**10**	60	45	**15**	35	3.2
RUNOFF LAYERS**										
stream sed. traps										
02-ST-2 (2-6 cm)	8/15/97	9.3	4.0	340	10	45	20	**15**	75	7.6
01-ST-1 (3-5 cm)	8/15/97	11.2	4.5	620	10	50	25	**15**	115	6.2
pond cores	Depth (cm)									
ERL-C1-C1	149.2	10.3	7.0	490	**30**	80	60	**25**	120	6.2
ERL-C1-C3	113.2	10.4	6.6	540	**30**	100	60	**25**	120	5.2
ERL-C1-C6	62.2	10.9	5.5	440	**30**	55	25	**25**	70	5.0
ERL-C1-C8	***	10.6	5.7	520	**30**	100	25	**25**	290	6.5
FL-C2-C1	140.3	9.1	6.3	490	**30**	185	45	30	250	4.4
FL-C2-C3	114.9	9.7	4.4	360	**30**	40	**20**	**25**	70	4.7
FL-C2-C6	24.3	8.7	9.1	640	**30**	220	45	**25**	200	5.9

* Bold values- Actual concentration is less than shown.

** Yellow-tan silty clay layers derived from scar areas.

*** Composite of upper 3 runoff layers.

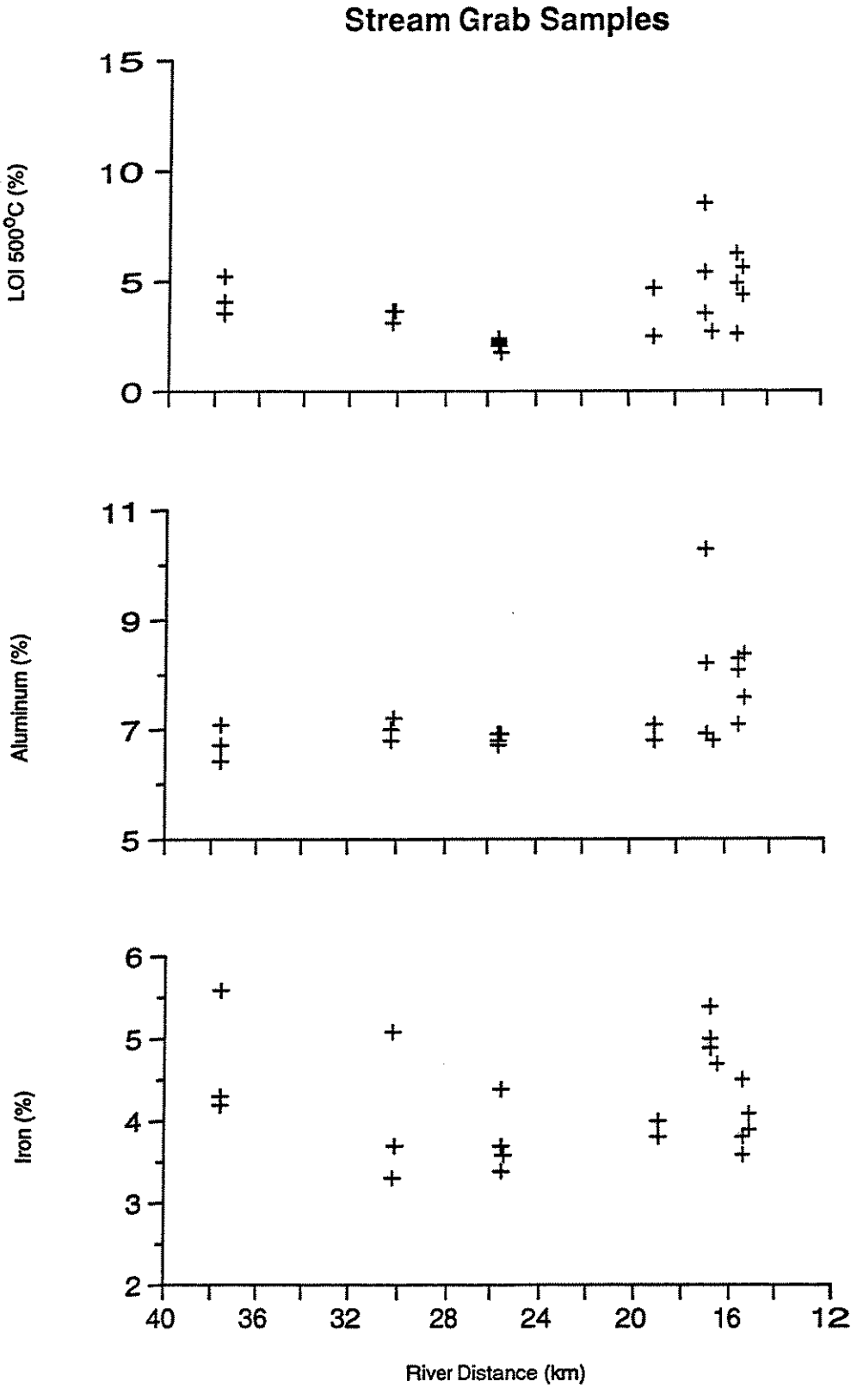

Figure A13. Concentration vs. river distance, Red River grab samples.

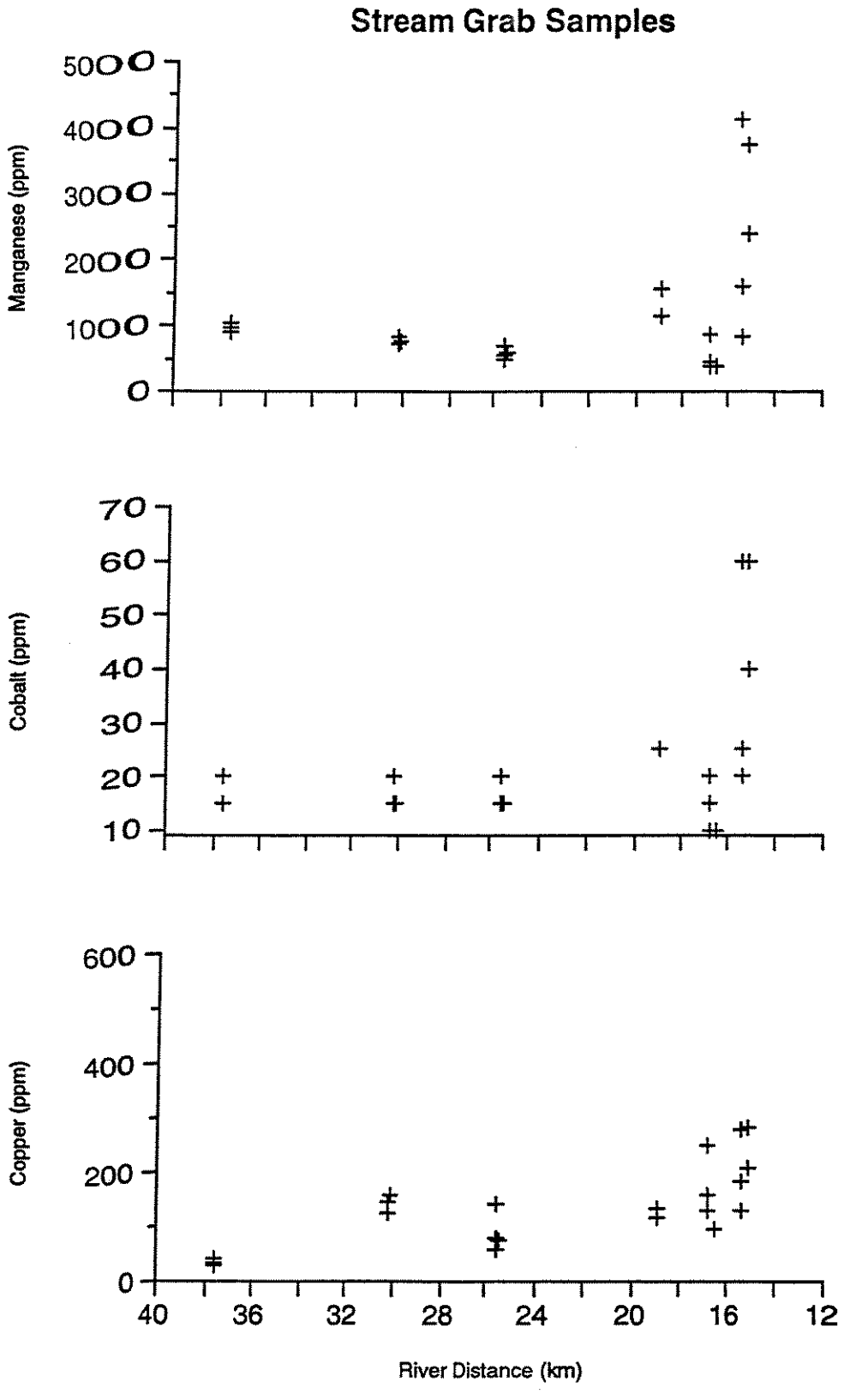

Figure A13, continued.

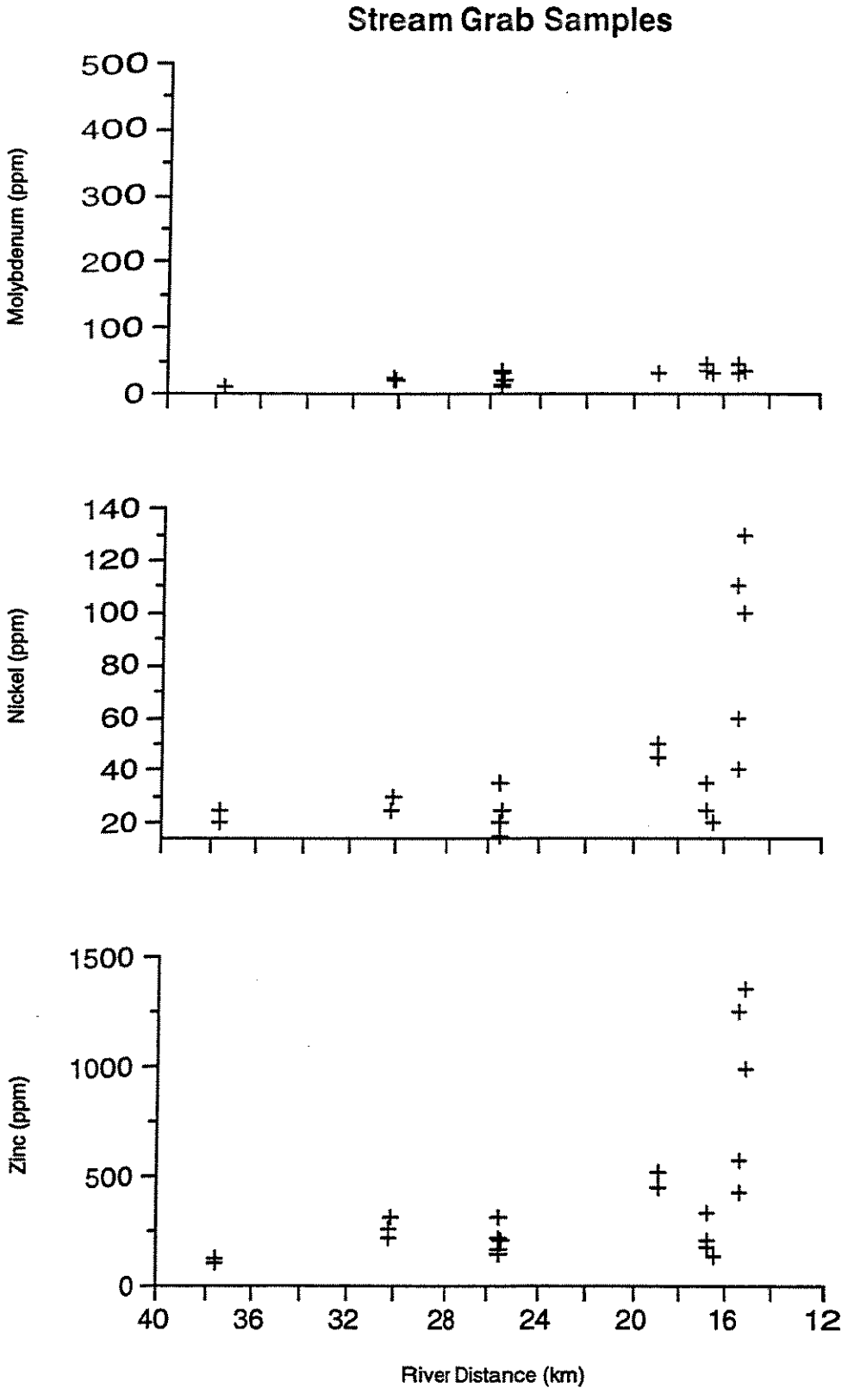

Figure A13, continued.

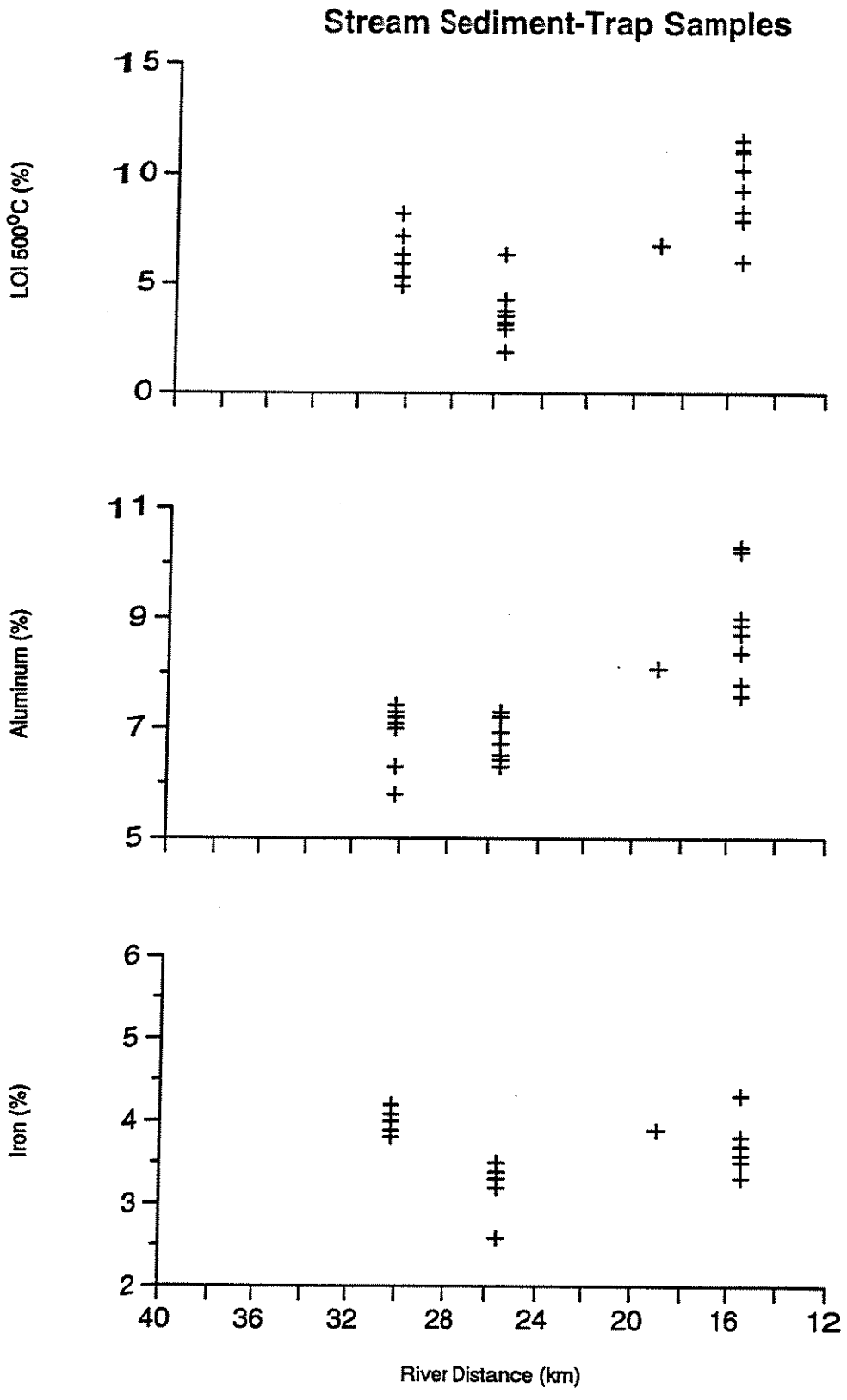

Figure A14. Concentration vs. river distance, Red River sediment-trap samples.

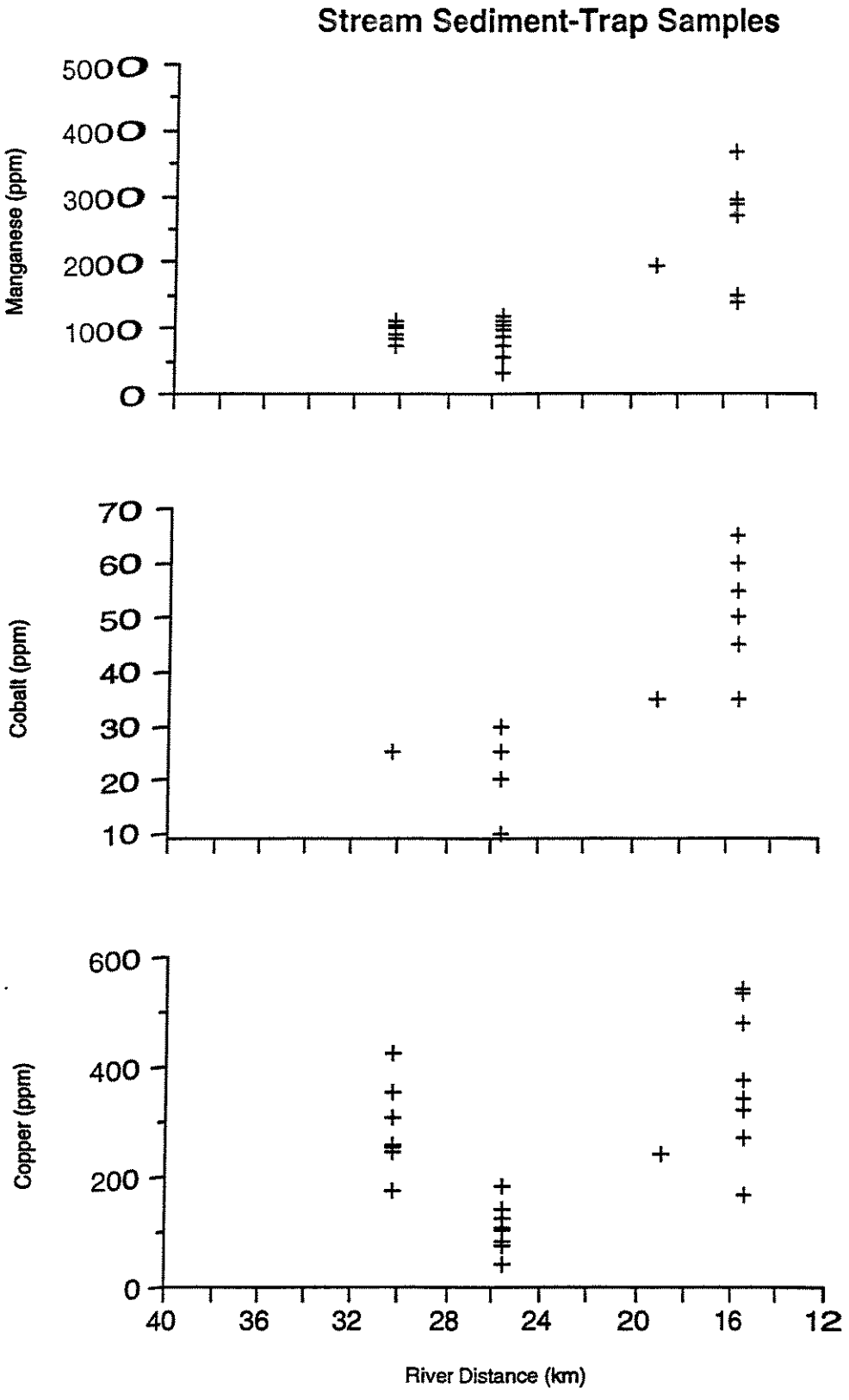

Figure A14, continued.

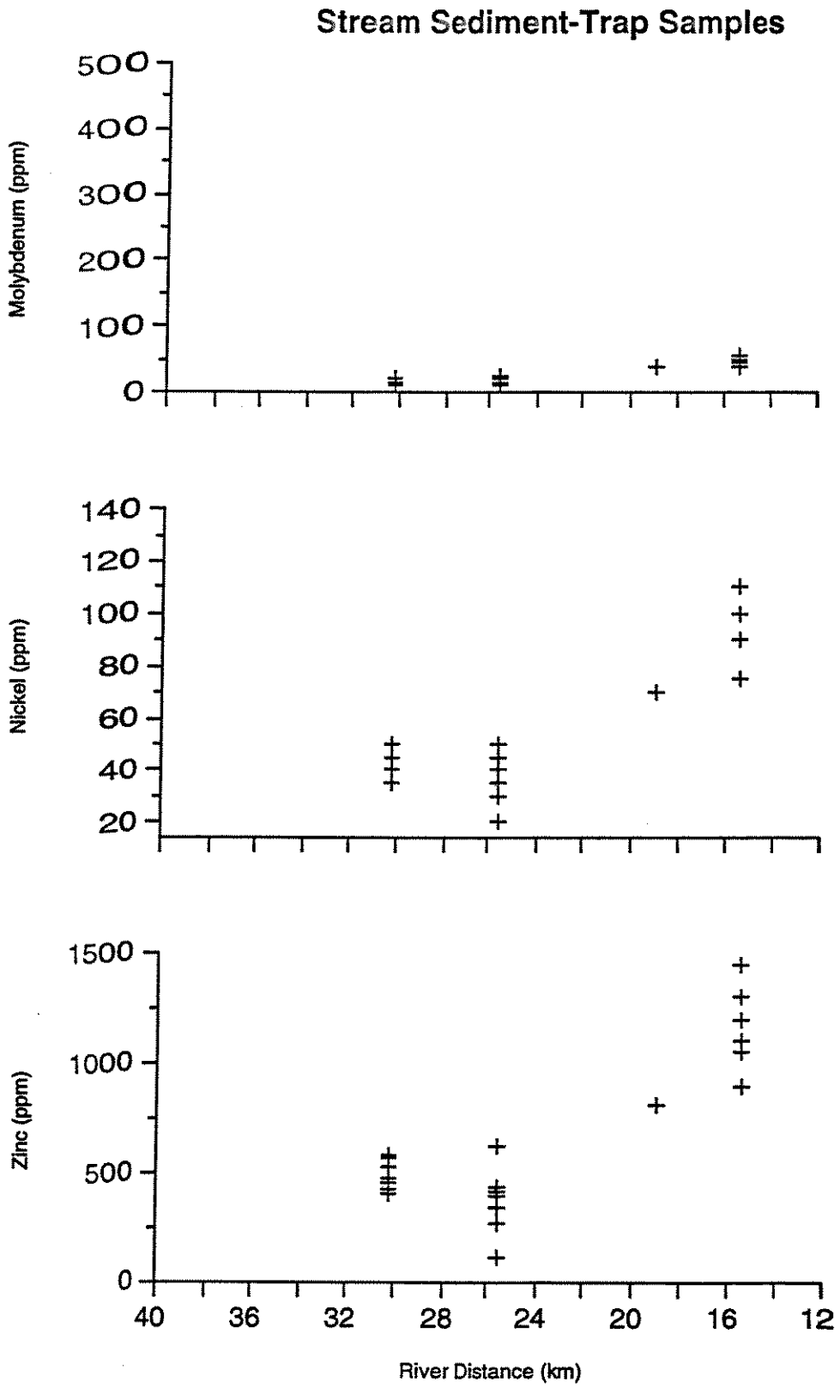

Figure A14, continued.

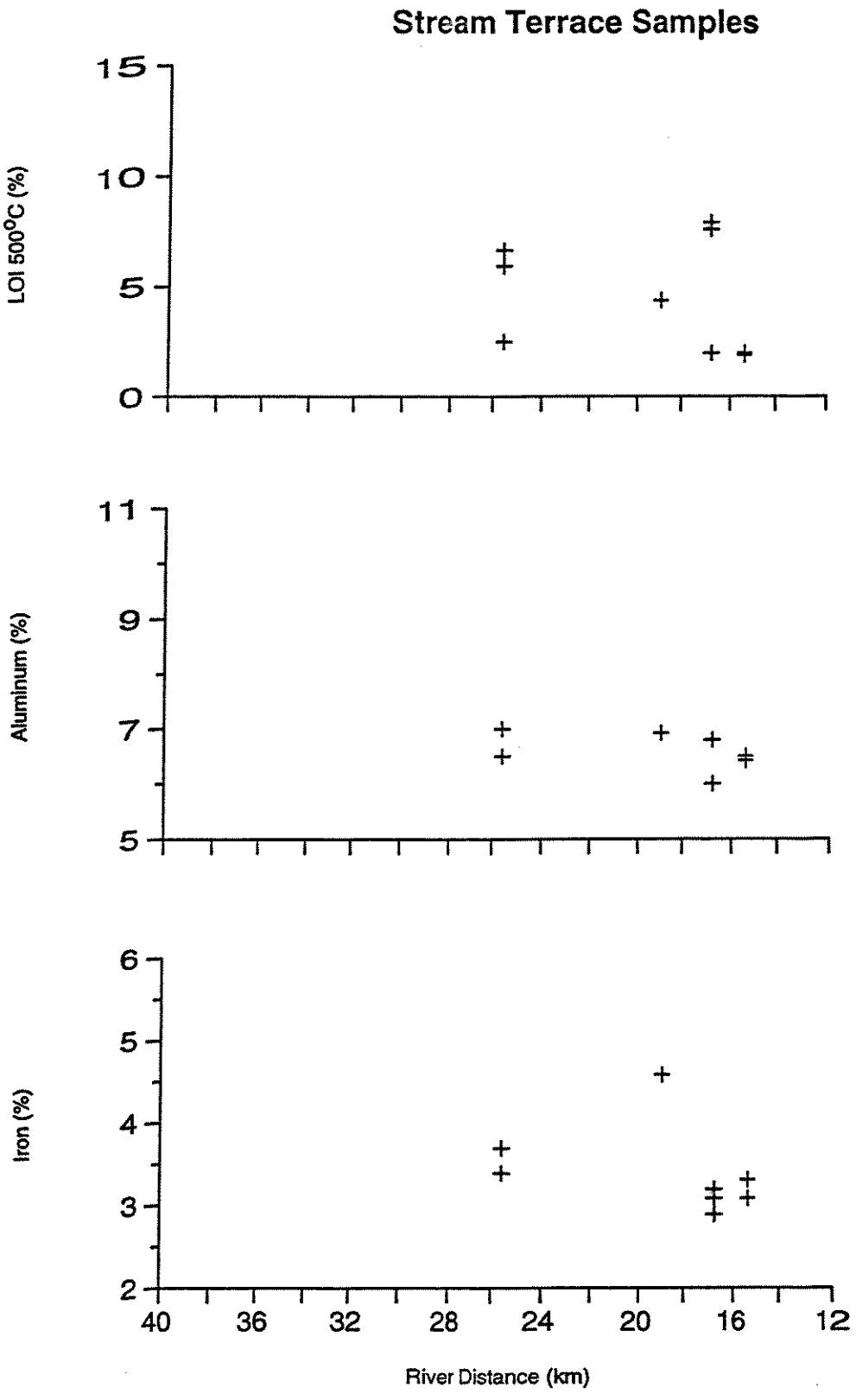

Figure A15. Concentration vs. river distance, Red River stream terrace samples.

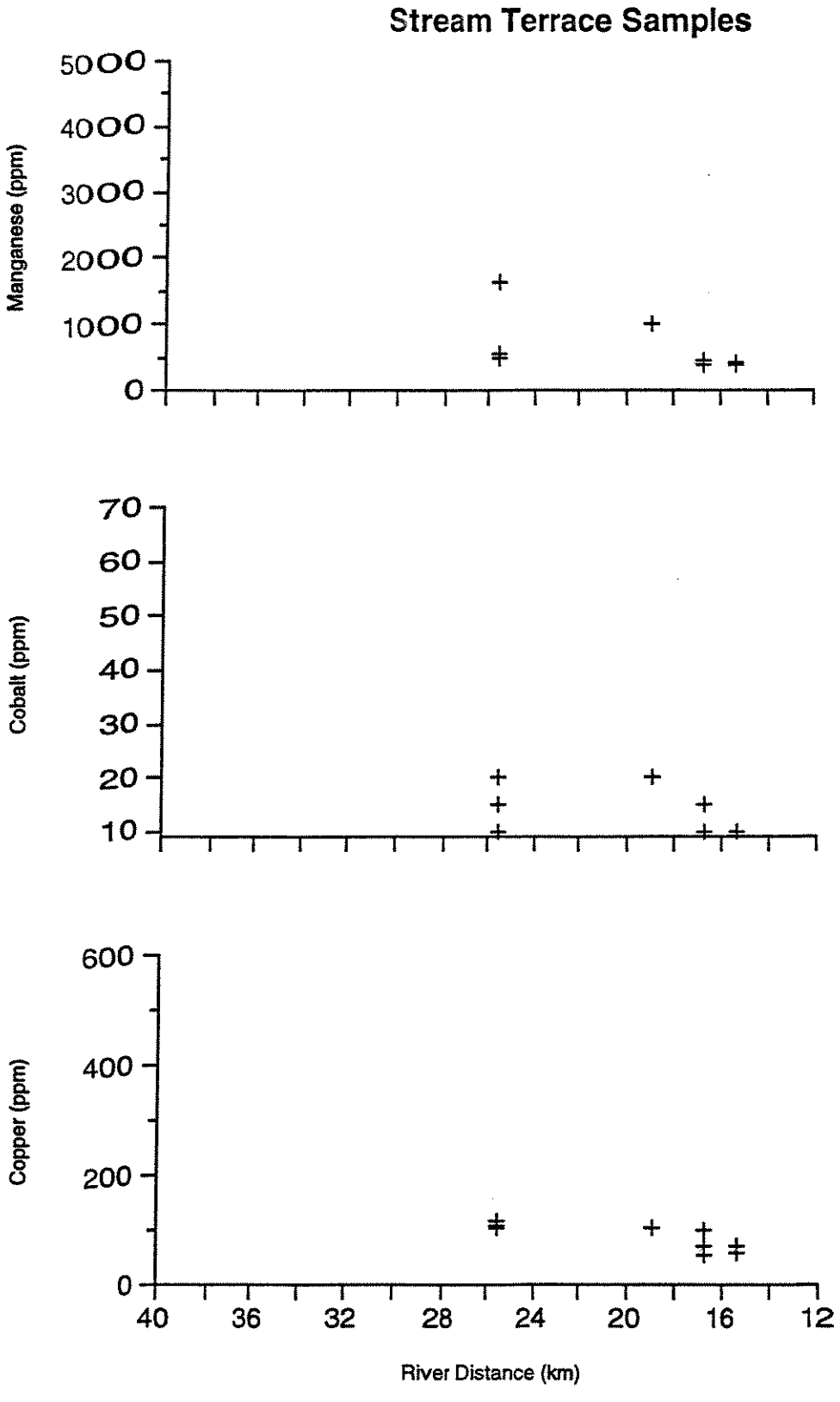

Figure A15, continued.

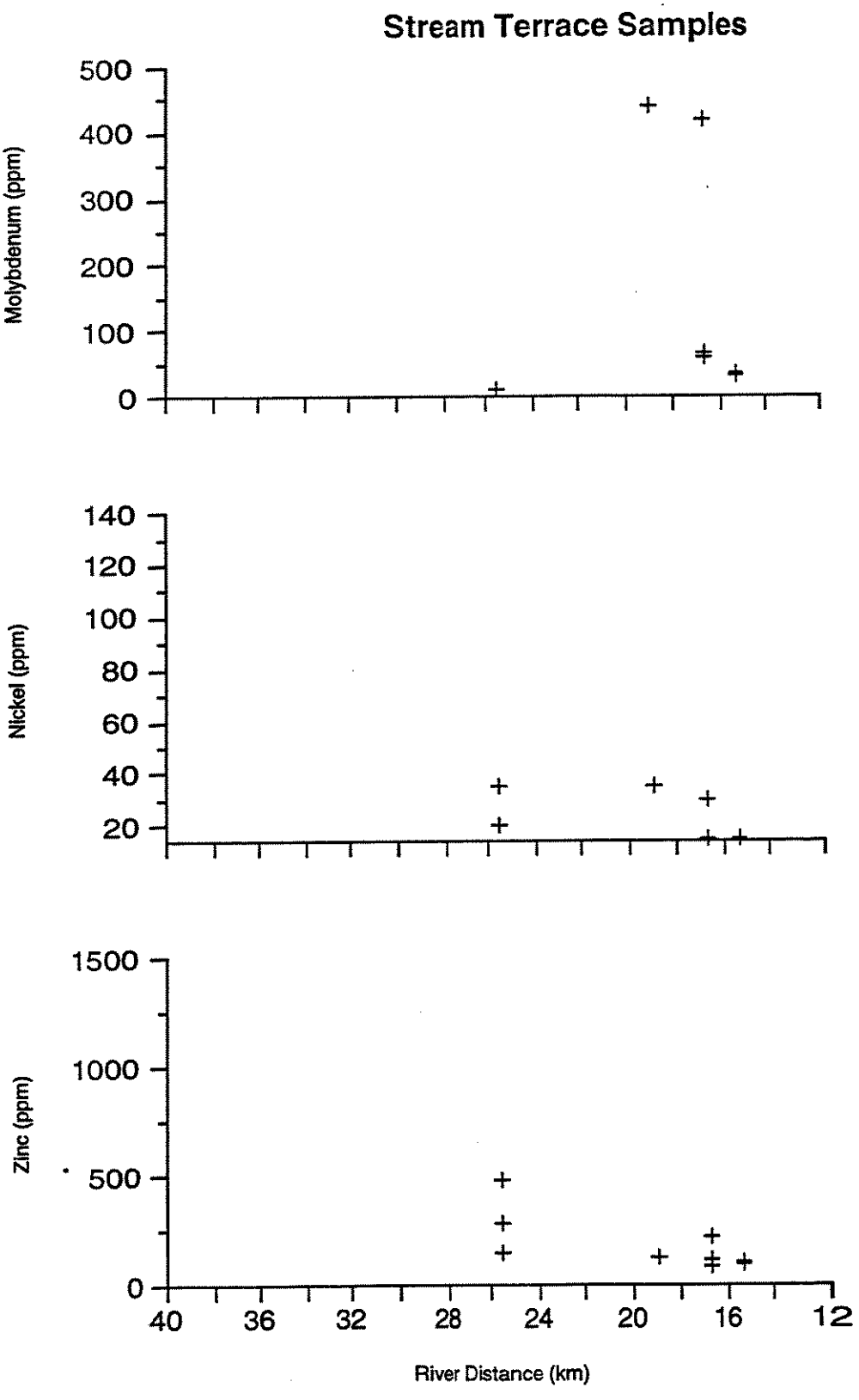

Figure A15, continued.

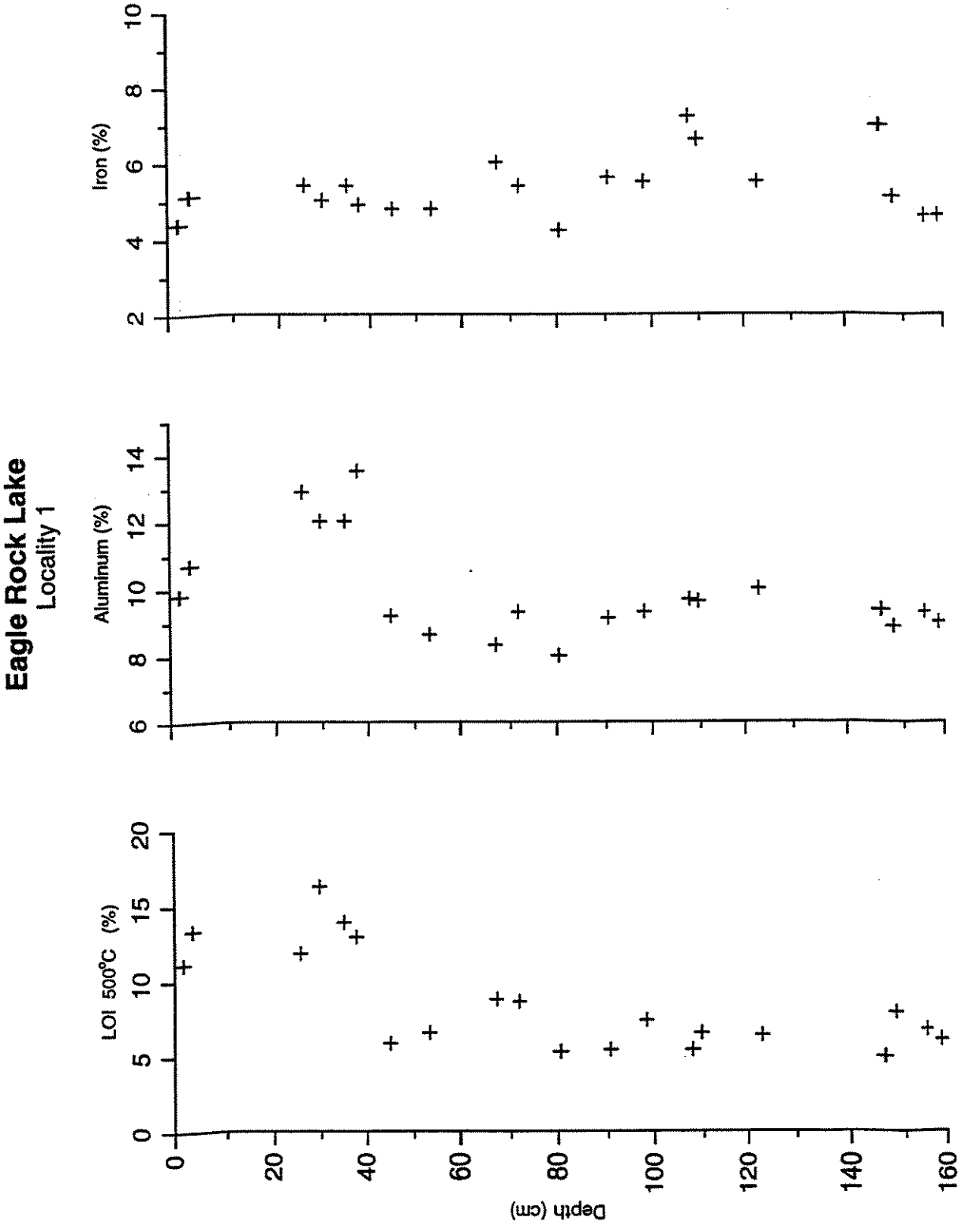

Figure A16. Concentration vs. depth, core ERL-C1.

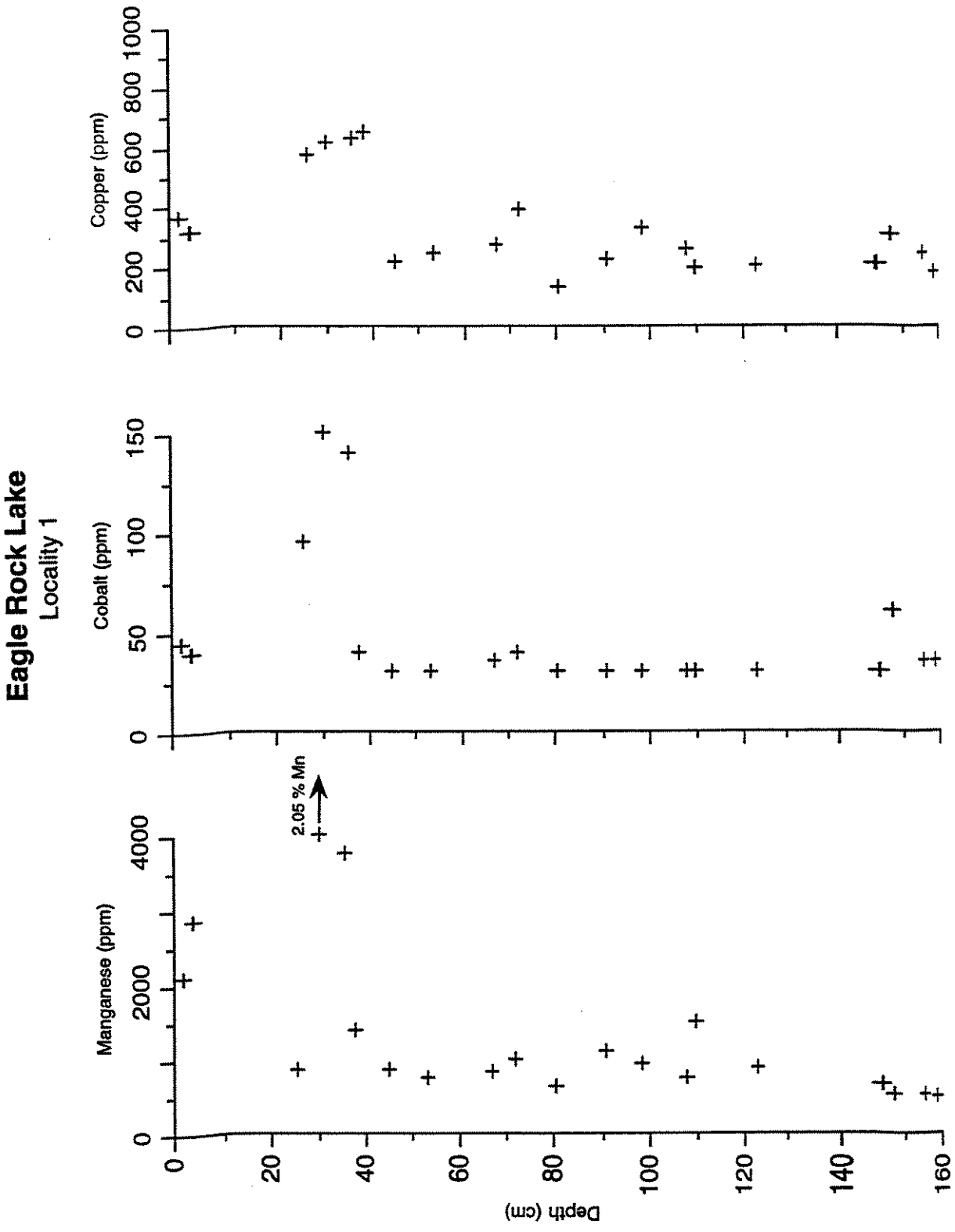

Figure A16, continued.

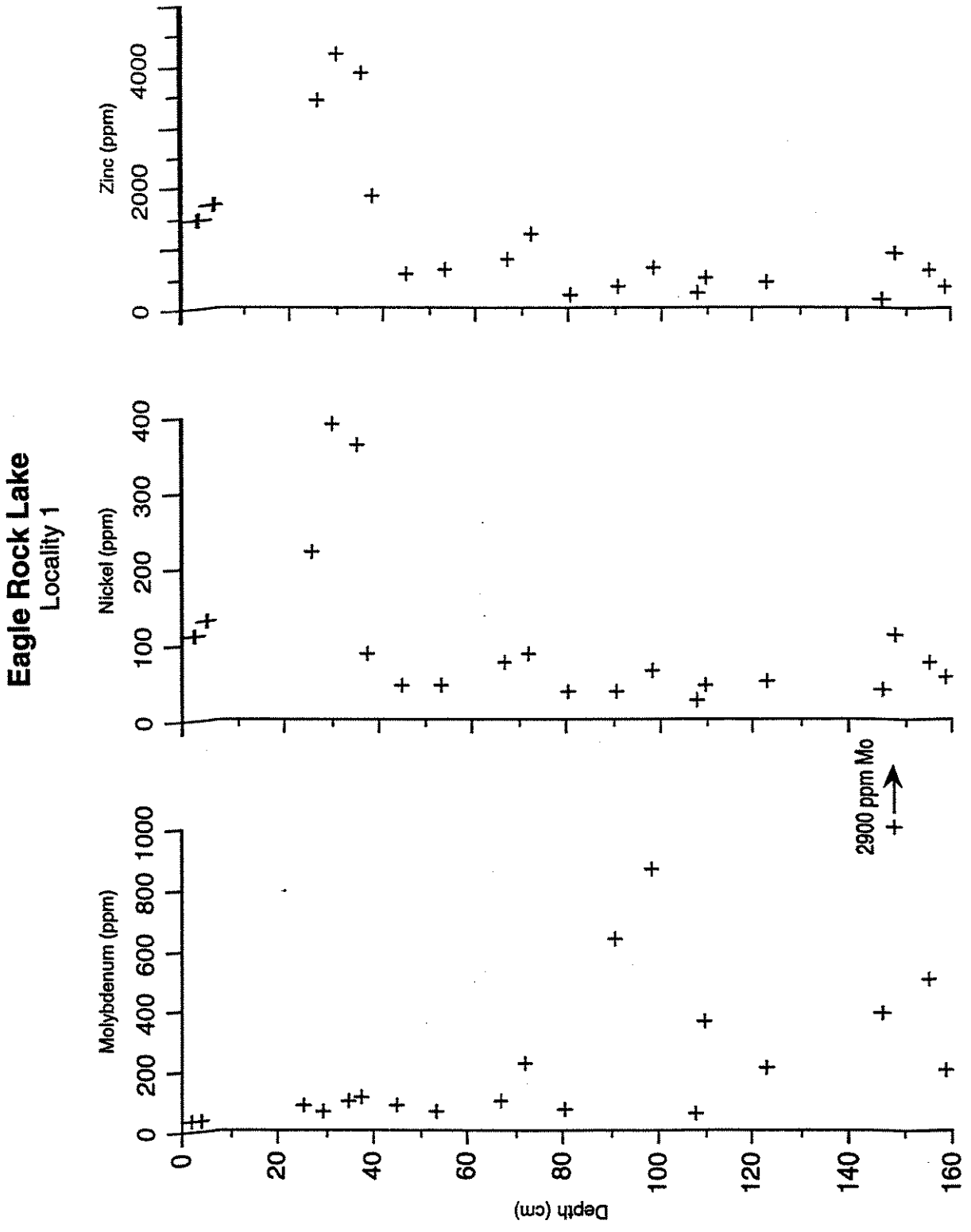

Figure A16, continued.

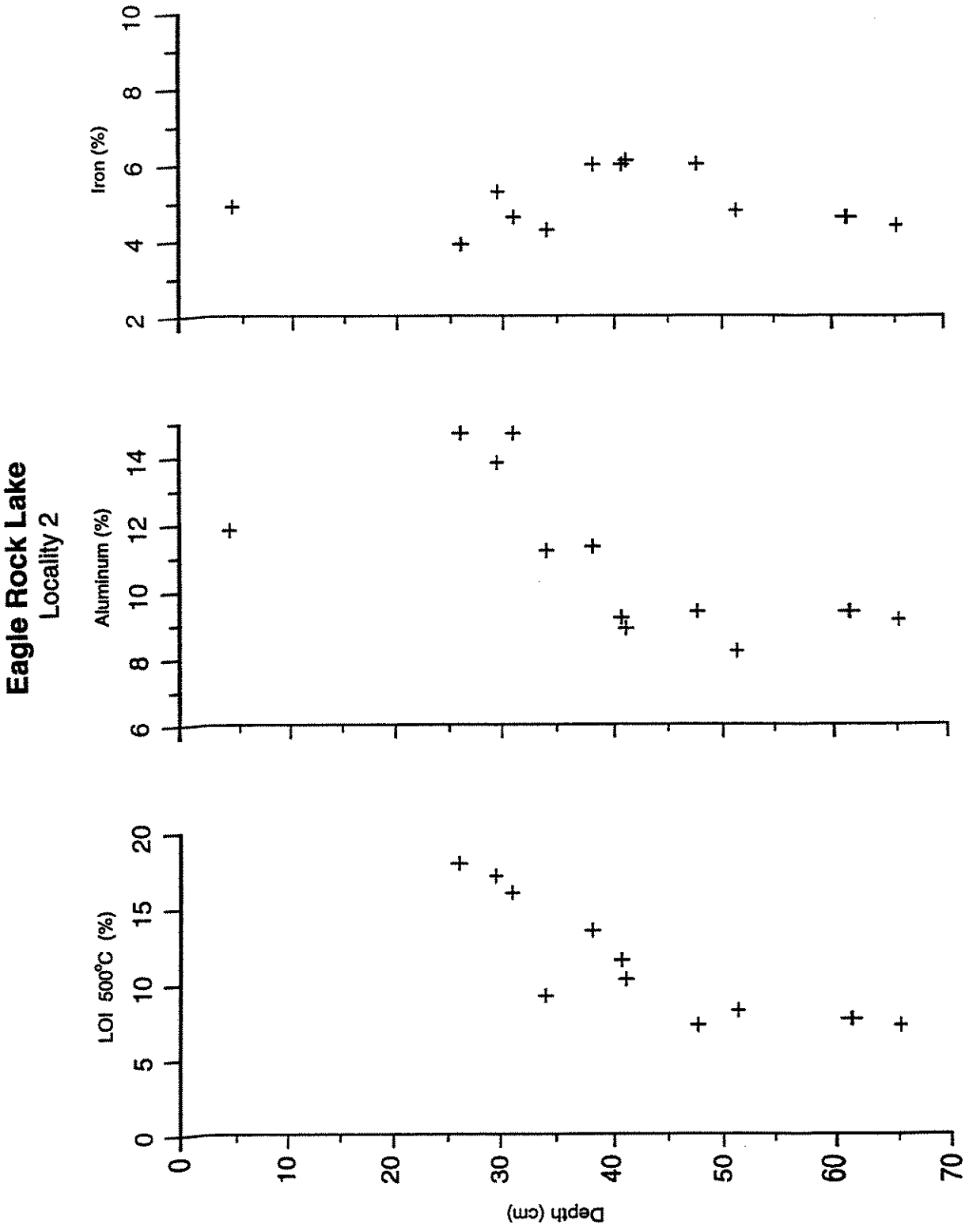

Figure A17. Concentration vs. depth, core ERL-C2.

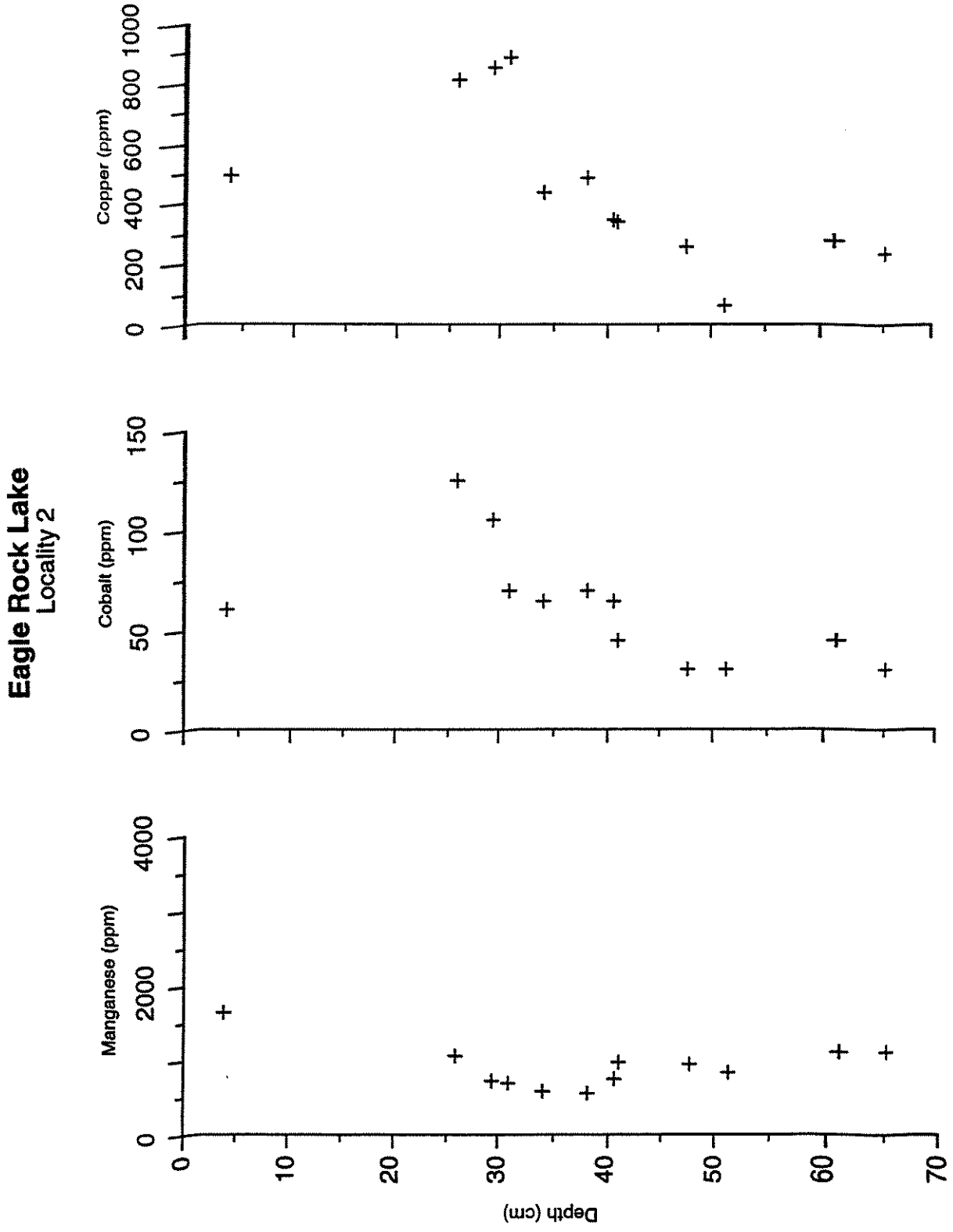

Figure A17, continued.

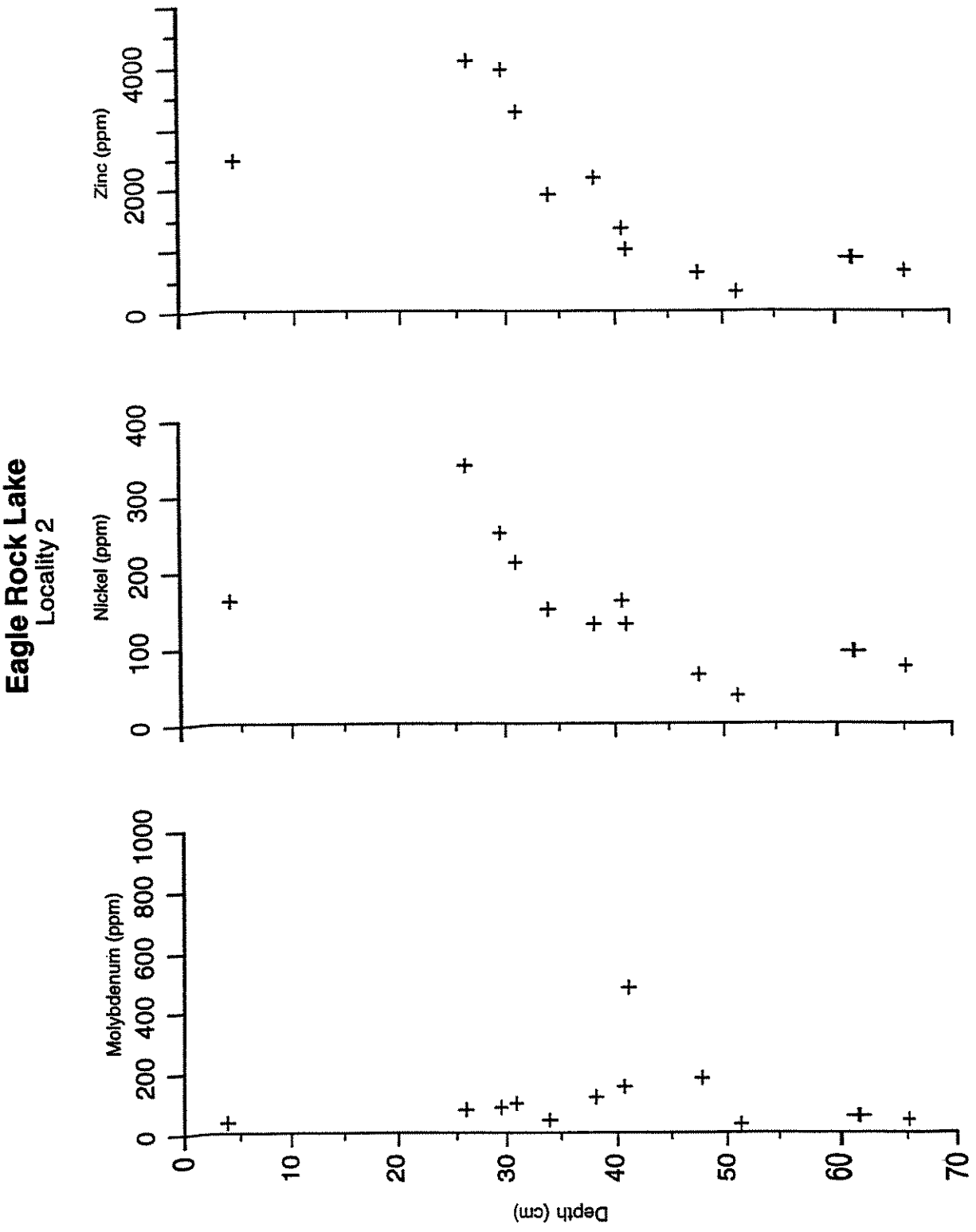

Figure A17, continued.

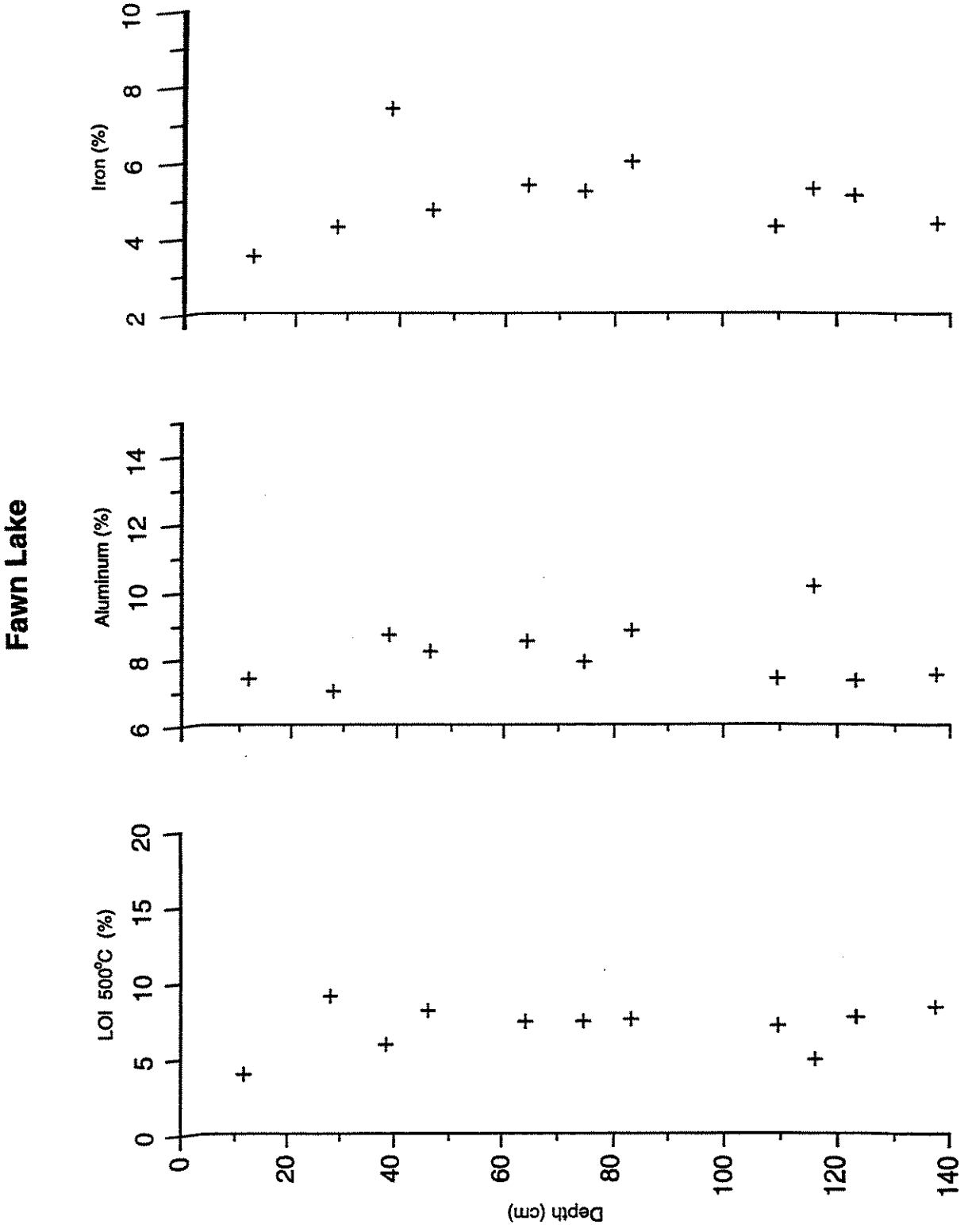

Figure A18. Concentration vs. depth, upper Fawn Lake core.

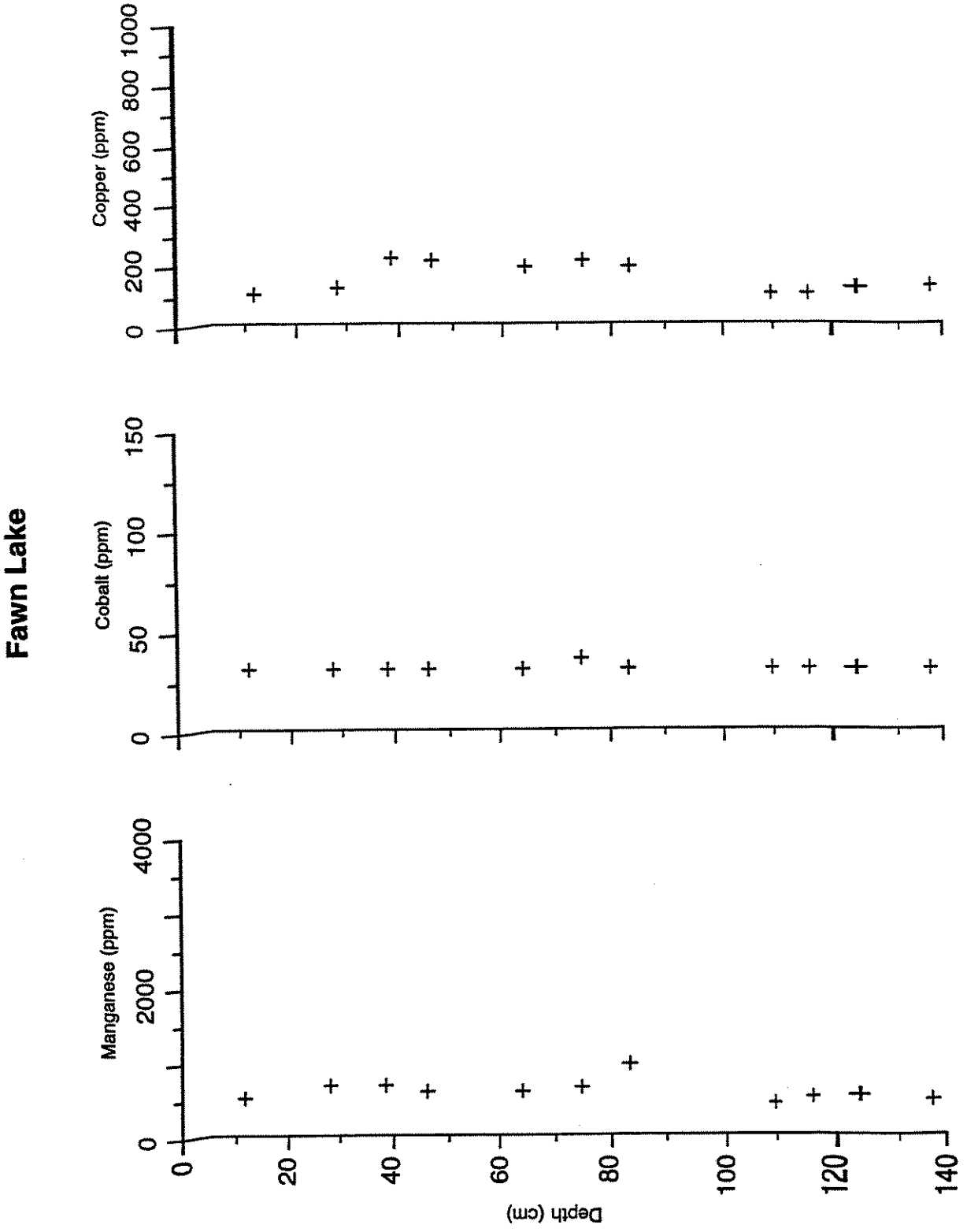

Figure A18, continued.

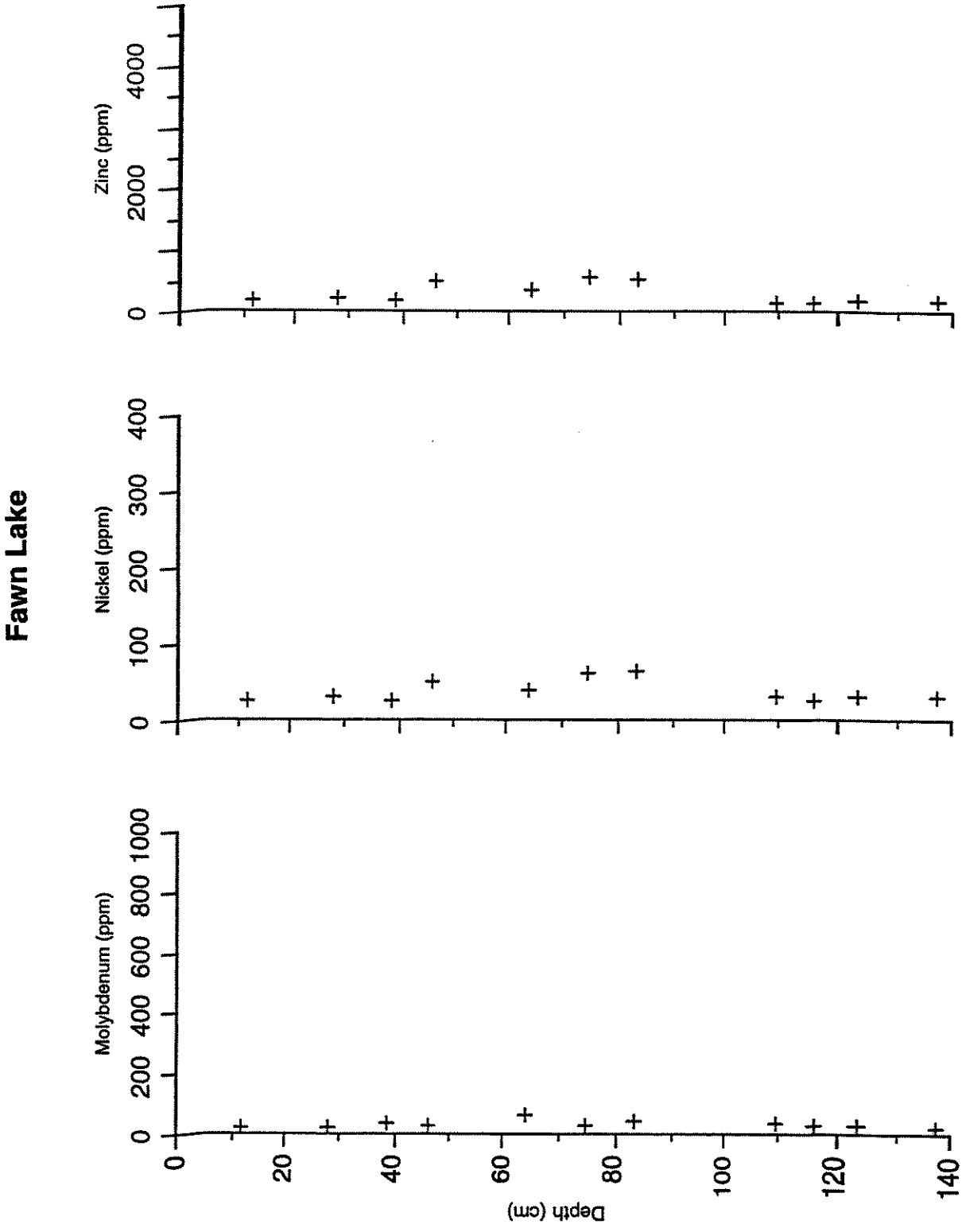

Figure A18, continued.

Table A9. Analytical results, tree-wood samples.

1989–1998 Wood.

(Bolded values are mean concentrations by locality)

Wood Type	Sample	Year	Concentration, PPM in dry wood sample Mn	Cu	Zn
Fir	RR-S10-TW-1	89-98	3.5	15	7.7
		n=1 ->	**3.5**	**15**	**7.7**
Fir	RR-03-TW-1	89-98	15	40	17
		n=1 ->	**15**	**40**	**17**
Fir	RR-02-TW-1	89-98	27	3.6	3.3
Pine	RR-02-TW-5	89-98	14	3.0	3.2
Pine	RR-02-TW-10	89-98	45	7.5	4.4
		n=3 ->	**29**	**5**	**4**
Pine	RR-S1-TW-1	89-93	45	3.9	6.9
"	"	94-98	40	3.5	6.2
"	"	94-98	39	2.5	5.0
		n=3 ->	**41**	**3**	**6**
Pine	RR-01-TW-1	89-93	46	5.6	5.1
"	"	94-98	39	3.2	4.7
Fir	RR-01-TW-5	89-93	25	4.0	3.9
"	"	94-98	20	4.4	3.3
		n=4 ->	**32**	**4**	**4**

Different Age Samples from Same Tree.

Wood Type	Sample	Year	Concentration, PPM in dry wood sample Mn	Cu	Zn
Pine	RR-02-TW-5	89-98	14	3.0	3.2
"	"	69-78	18	3.8	4.9
"	"	49-58	42	3.0	10
Pine	RR-S1-TW-1	94-98	40	3.0	5.6
"	"	89-93	45	3.9	6.9
"	"	64-68	62	2.2	11
"	"	54-58	70	3.7	12
Pine	RR-01-TW-1	94-98	39	3.2	4.7
"	"	89-93	46	5.6	5.1
"	"	79-83	89	2.6	7.3
"	"	69-73	78	4.5	11
Fir	RR-01-TW-5	94-98	20	4.4	3.3
"	"	89-93	25	4.0	3.9
"	"	49-58	8.5	<1	2.9

Pine Growing on Debris Fan at Locality 03.

Wood Type	Sample	Year	Concentration, PPM in dry wood sample Mn	Cu	Zn
Pine	RR-03-TW-12	39-98	24	<1	3.8
"	"	39-98	24	<1	3.3

Table A10. Hyporheic invertebrates collected in the Red River from 10 L of well water, March 1998 (N=number of wells; Ephemeroptera, Plecoptera, and Trichoptera (traditional indicator groups)--EPT--in bold; shaded panel=below mine).

	Localities			
Taxon	**S10, N=3**	**03, N=2**	**02, N=3**	**01, N=2**
Turbellaria	2			
Nematoda				
Oligochaeta	7	2		
Copepoda				
Ostracoda	2	28	8	
Amphipoda				
Stygobromus	3			
Acari			2	
Insecta				
Collembola	2			
Ephemeroptera				
Baetidae	3	3	1	
Heptageniidae				
Plecoptera				
Capniidae	3	7	3	
Chloroperidae			9	
Nemouridae	34			
Perlodidae				
Trichoptera				
Brachycentridae	2		6	
Lepidostomatidae			1	
Diptera				
Ceratopogonidae				
Chironomidae		10	7	
Dolichopodidae				
Empididae				
Tipulidae			4	
Other		3		2
Coleoptera				
Elmidae			1	
# of Taxa	9	6	10	1
# of individuals	58	53	42	2

Table A11. Hyporheic invertebrates collected in the Red River from 10 L of well water, April 1998 (N=number of wells; Ephemeroptera, Plecoptera, and Trichoptera (traditional indicator groups)--EPT--in bold; shaded panel=below mine).

	Localities					
Taxon	**S10, N=3**	**02, N=3**	**S3, N=3**	**S2, N=2**	**S1, N=2**	**01, N=2**
Turbellaria	1		1			
Nematoda	1					
Oligochaeta	19	2	39	6		1
Copepoda				1		2
Ostracoda	120	7	30	8		
Amphipoda						
Stygobromus	2					
Acari	1	1				
Insecta						
Collembola		1				
Ephemeroptera						
Baetidae	**27**	**2**		4		
Heptageniidae	**3**		**10**			
Plecoptera						
Capniidae	**2**		**1**			**1**
Chloroperidae	**2**	**68**	**7**	3		**4**
Nemouridae			**1**			
Perlodidae			**2**			
Trichoptera						
Brachycentridae		**2**				
Lepidostomatidae	**3**		**10**			
Diptera						
Ceratopogonidae		1		1		
Chironomidae	9	200	32	2		1
Dolichopodidae						
Empididae		1	3			
Tipulidae		2				
Other	1		1			
Coleoptera						
Elmidae	1	1	3			
# of Taxa	14	12	13	7	0	6
# of individuals	192	288	140	25	0	9

APPENDIX II

Sample Images

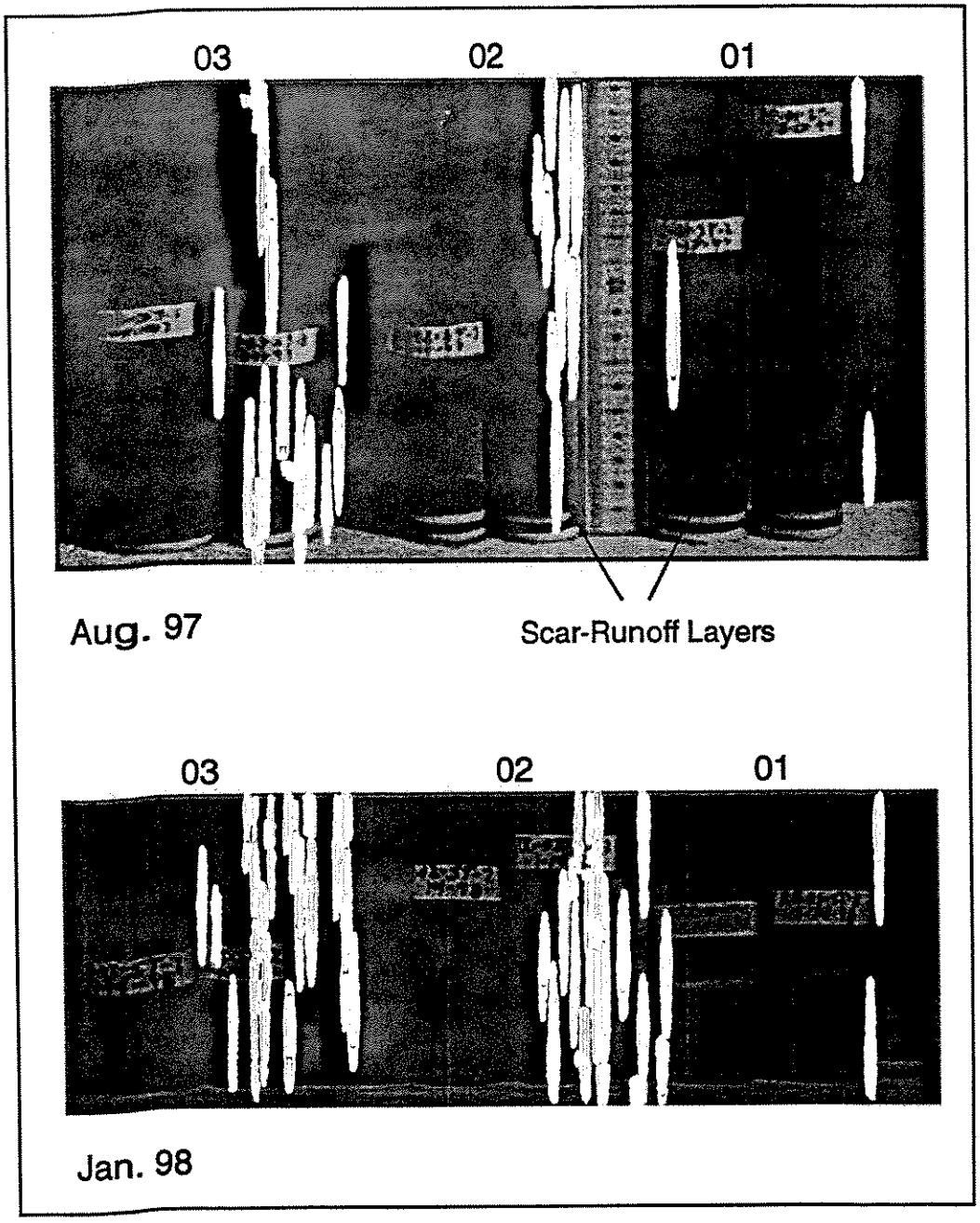

Figure A19. Stream sediment-trap samples collected August, 1997 (top) and January, 1998 (bottom) from sampling localities 01, 02, and 03 (Fig. 3). Light-colored layers in August samples are sediments derived from scar areas during storm-runoff event. Analyses of stream sediment-trap samples are presented in Table A3. Analyses of scar-runoff layers from August trap samples are presented in Table A8.

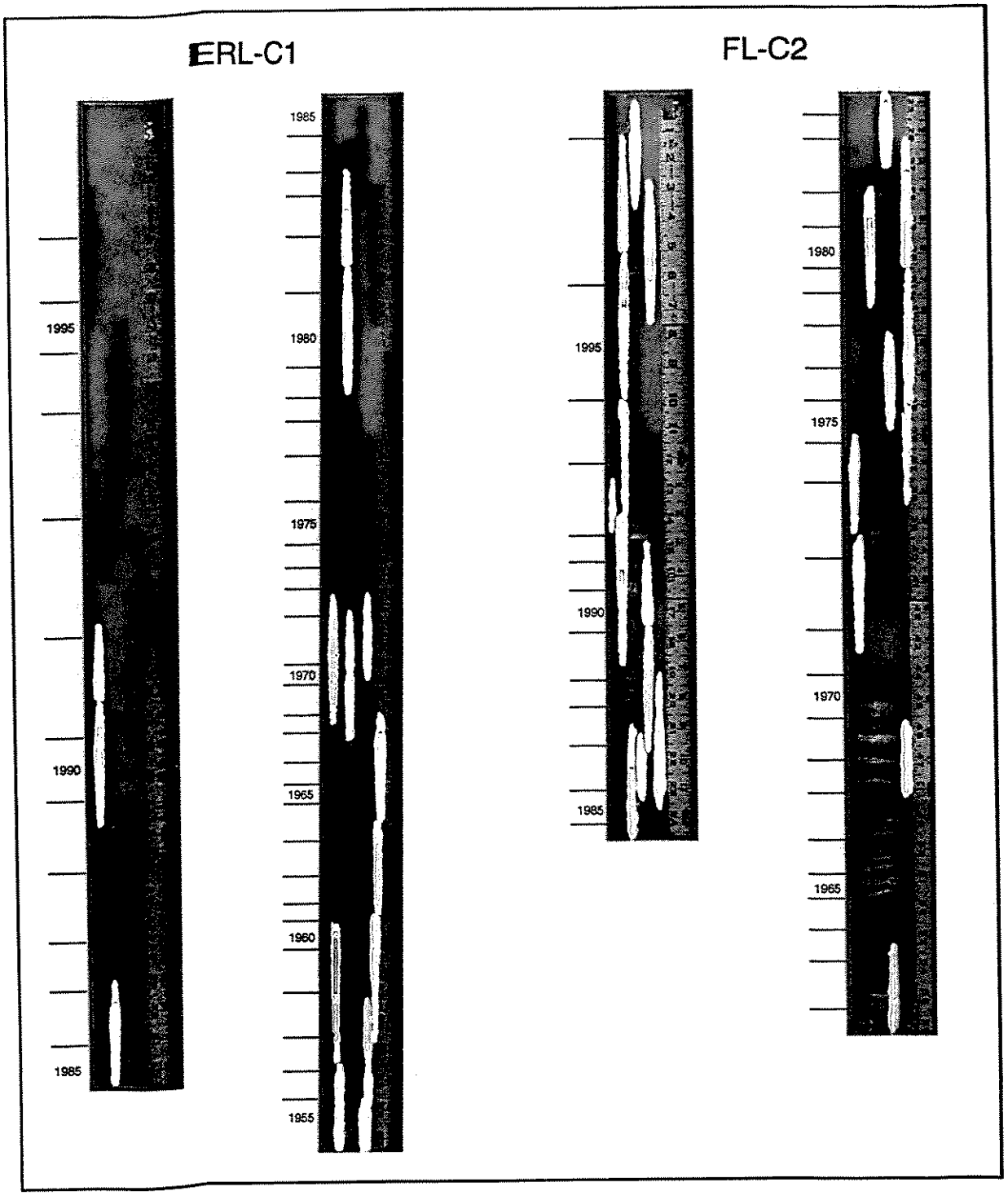

Figure A20. Photomosaic of sediment cores collected near inlets of Eagle Rock (ERL) and Fawn Lakes, showing seasonal layering due to runoff from scar areas. Interpreted approximate chronology based on seasonal layering as indicated. Geochemical profiles from the pond sequences (Table A6, Figs. A15-A18) represent sediment samples from dark layers in the cores. Analyses of scar-runoff layers are presented in Table A8; aluminum-enriched layers (from upper part of ERL sequence) in Table A7. Units on scale are inches.

APPENDIX III

Sampling Equipment

Figure A21. Description of stream sediment trap device.

Device

Sediment carried by streamflow is collected by a flow-resistant, non-metal sediment trap installed in the stream bed. The sediment trap has a removable sampling tube for multiple collections.

The sediment trap consists of a polycarbonate sampling tube which contains a nylon plug at the lower end, equipped with a neoprene O-ring, lubricated with Dow laboratory-grade silicone grease. A nylon honeycomb baffle is affixed within the upper end by a nylon screw.

The flow-resistant apparatus consists of 1/2- to 5/8-inch steel rebar driven into the stream bed and encased in 1/2-inch PVC pipe extending at least 4 inches into the stream bed. The top of the PVC shielding pipe is filled and sealed with RTV grade silicone sealant and capped. A PVC Schedule 40 housing tube is attached to the shielded rebar with nylon ties.

The sampling tube is installed in the housing tube and fixed with two nylon screws.

The device has no exposed metal surfaces. The sampling tube assembly (tube, baffle/ screws, nylon plug, O-ring) is acid washed prior to assembly and sealed in plastic wrap until deployment.

Sample Recovery

Cover top of sampling tube with plastic wrap, loosen nylon screws holding sampling tube in place, and remove from the housing tube. Wrap sampling tube in plastic wrap and pack vertically in ice chest. Allow contents of sampling tube to settle then decant as much water as feasible without losing sample. Re-wrap sampling tube in plastic wrap and pack in ice chest for transport to laboratory. Sediment is extruded in the laboratory by pushing on the O-ring plug at the bottom of the sampling tube.

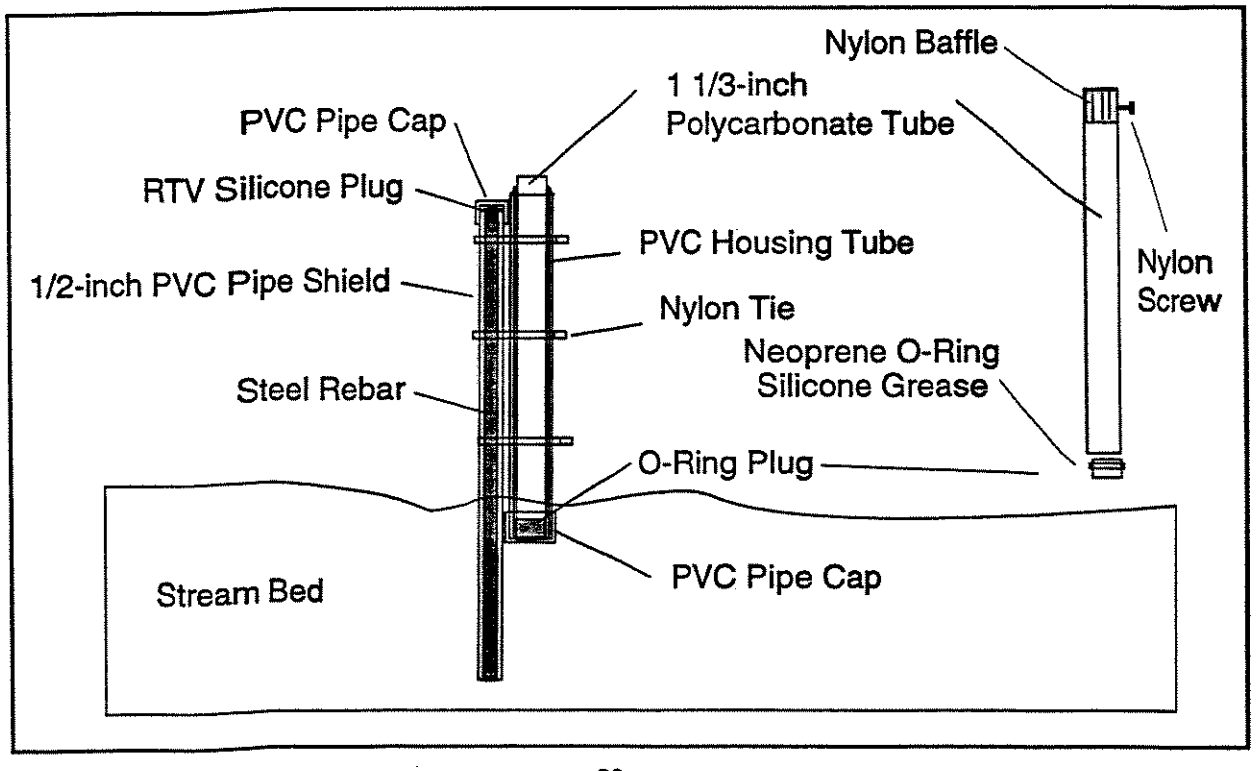

Figure A22. Description of pond sediment trap device.

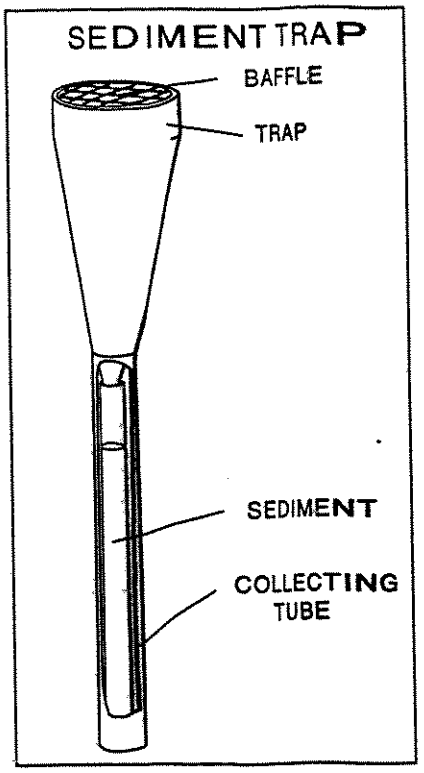

Device

The trapping system consists of a fiberglass or PVC cone or funnel equipped with a baffle in the large opening and a housing tube at the small opening which holds a polycarbonate collecting tube. Sediment and suspended matter (seston) in the water body settles through the baffle and is deflected into the collecting tube.

The trap opening is fitted with a nylon honeycomb baffle or an acrylic baffle. A trap-mounting bar, constructed of PVC pipe, is inserted through bushings set into the wall of the trap. The lower end of the trap funnel is affixed to a PVC threaded fitting. A flapper-type water-release valve is placed in the trap wall near the lower end of the funnel.

The PVC collecting-tube housing screws into the threaded fitting at the lower end of the trap. The polycarbonate collecting tube is closed at the lower end by a nylon plug which is equipped with an O-ring. The collecting tube sits within the collecting-tube housing and is connected to the funnel by a plastic tube adapter.

All trap construction materials are non-metallic (PVC, fiberglass, nylon, delrin, etc.). All parts that are exposed to accumulating sediment are acid washed before deployment.

Trap Deployment and Sample Recovery

Determine the depth of the trap site in advance. Secure mounting line to center hole of trap mounting bar. Attach collecting tube of appropriate length and diameter to the funnel using appropriate tube adapter. Attach collecting-tube housing, applying silicone grease to all threads. Lay out anchor, mooring-mounting bar and triangle, mooring line, recovery hook, and unsinkable buoy with tether-release loop for appropriate water depth. Lower apparatus into water body and locate position by photo-triangulation.

Recover device by affixing line to recovery hook. Upon recovery, remove collecting tube from collecting-tube housing and cover top of collecting tube with plastic wrap. Describe and photograph collecting tube shortly after recovery and before transport. Wrap collecting tube in plastic wrap and pack vertically in ice chest. Allow contents of collecting tube to settle then decant as much water as feasible without losing sample. Re-wrap collecting tube in plastic wrap and pack in ice chest for transport to laboratory. Sediment is extruded in the laboratory by pushing on the O-ring plug at the bottom of the collecting tube.

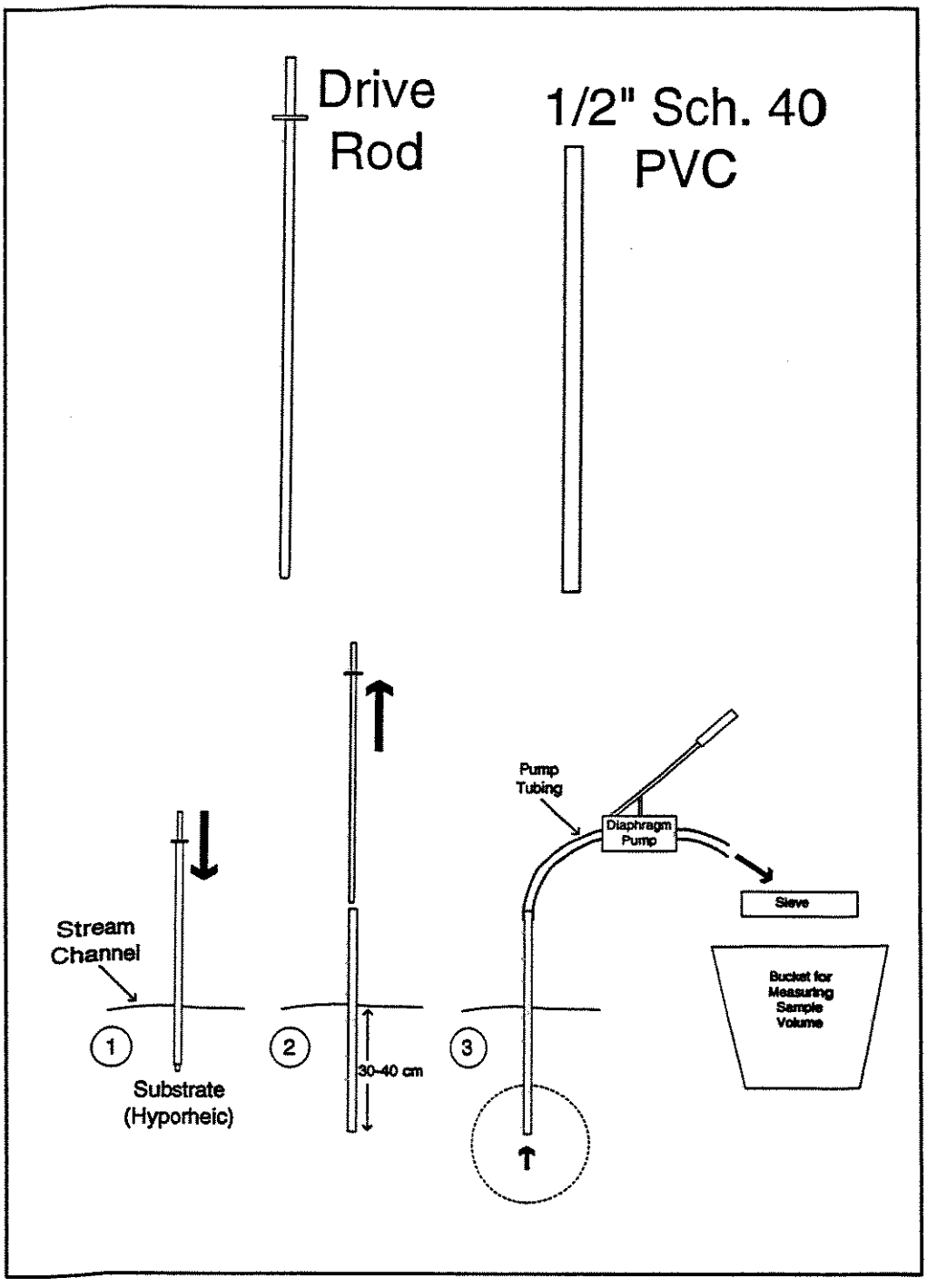

Figure A23. Lysimeter for collecting hyporheic samples. 1) PVC pipe is driven into substrate using an internal drive rod for strength and to keep pipe clear of debris, 2) drive rod is removed, and 3) diaphragm pump is used to collect sample. Sample is collected on a sieve and preserved in ethanol. Similar sample volumes are obtained at each locality by measuring amount of pumped material, allowing semi-quantitative comparison of taxon abundances between localities.